Biochemical studies and applications of sugar and polyamine metabolisms in gut microbes

Yuta Sugiyama

2020

TABLE OF CONTENTS

ABBREVIATIONS

AAT	Agmatine aminopropyltransferase
ADC	Arginine decarboxylase
ADI	Agmatine deiminase
AdoMetDC	*S*-Adenosylmethionine decarboxylase
AGM	Agmatine
AguD	Putrescine-agmatine antiporter
APAGM	Aminopropylagmatine
APAUH	Aminopropylagmatine ureohydrolase
Ara	Arabinose
ARG	Arginine
ASA	Aspartate-β-semialdehyde
ATP	Adenosine triphosphate
AUH	Agmatine ureohydrolase
*Bb*AfcA	1,2-α-L-Fucosidase from *Bifidobacterium bifidum* JCM1254
BHI	Brain-heart infusion
BLAST	Basic local alignment search tool
BlastP	Protein BLAST
BT2970	1,3-1,4-α-L-Fucosidase from *Bacteroides thetaiotaomicron* VPI-5482
CAD	Charged aerosol detector
CASDC	Carboxyspermidine decarboxylase
CASDH	Carboxyspermidine dehydrogenase
CSPD	Carboxyspermidine
dcSAM	Decarboxylated *S*-adenosylmethionine
dHex	Deoxyhexose
DMSO	Dimethylsulfoxide
DNA	Deoxyribonucleic acid
2'-FL	2'-Fucosyllactose
3-FL	3-Fucosyllactose
FRT	Flippase recognition target
Fru	Fructose
Fuc	Fucose
FucF	Fucopyranosyl fluoride
FUT	Fucosyltransferase
Gal	Galactose

GalN	Galactosamine
GalNAc	*N*-Acetylgalactosamine
GAM	Gifu anaerobic medium
GC	Gas chromatography
GH	Glycoside hydrolase
Glc	Glucose
GlcN	Glucosamine
GlcNAc	*N*-Acetylglucosamine
GNB	Galacto-*N*-biose
HEPES	4-(2-Hydroxyethyl)-1-piperazineethanesulfonic acid
Hex	Hexose
HexNAc	*N*-Acetylhexose
HMO	Human milk oligosaccharide
HPAEC	High-performance anion-exchange chromatography
HPLC	High-performance liquid chromatography
kan^{+}	Kanamycin resistant gene
Lac	Lactose
LacNAc	*N*-Acetyllactosamine
LB	Luria-Bertani broth
LDFT	Lactodifucotetraose
Le	Lewis
LNB	Lacto-*N*-biose I
LNFP	Lacto-*N*-fucopentaose
LNT	Lacto-*N*-tetraose
LN*n*T	Lacto-*N*-*neo*tetraose
MALDI-TOF MS	Matrix assisted laser desorption/ionization-time of flight mass spectrometry
MdtJI	Spermidine exporter from *Escherichia coli*
MES	2-(*N*-Morpholino) ethanesulfonic acid
MS	Mass spectrometry
MTA	5'-Deoxy-5'methylthioadenosine
NCP	*N*-Carbamoylputrescine
NCPAH	*N*-Carbamoylputrescine amidohydrolase
NMR	Nuclear magnetic resonance
OD	Optical density
ODC	Ornithine decarboxylase
ORN	Ornithine

PA	Pyridylaminated
PAD	Pulsed amperometric detector
PCR	Polymerase chain reaction
PCT	Putrescine carbamoyltransferase
PGM	Porcine gastric mucin
PlaP	Low-affinity putrescine importer
PNA	Peanut agglutinin
PNG-F	Peptide: *N*-glycanase-F
*p*NP	*p*-Nitrophenyl
PotABCD	ATP-binding cassette type spermidine preferential importer
PotE	Putrescine-ornithine antiporter
PotFGHI	ATP-binding cassette type putrescine specific importer
PuuP	High-affinity putrescine importer
Put (PUT)	Putrescine
Rha	Rhamnose
SAM	*S*-Adenosylmethionine
SD	Standard deviation
SDS-PAGE	Sodium dodecyl sulfate-polyacrylamide gel electrophoresis
Spd (SPD)	Spermidine
SPDsyn	Spermidine synthase
Spm	Spermine
TBS-T	Tris-buffered saline containing 0.05 % (*v*/*v*) Tween-20
t-BuOH	2-Methyl-2-propanol
TCA	Trichloroacetic acid
TLC	Thin layer chromatography
Tris	Tris (hydroxymethyl) aminomethane
UEA-I	*Ulex europaeus* agglutinin I
WT	Wild type
XLLG	Xyloglucan nonasaccharide
Xyl	Xylose

GENERAL INTRODUCTION

Over 2000 species (1) and approximately 40 trillion cells (2) of gut microbes colonize the human colon. Recent studies have revealed that gut microbes influence host health and physiology, and cause, for example, obesity (3), diabetes (4), and autism (5). Several studies have shown that host interacts with gut microbes. For example, mothers supply human milk oligosaccharides (HMOs) (6,7), which are the third most abundant solid component in breast milk and are not digestible by humans (8), to *Bifidobacterium* species which have beneficial effects on human (9,10). Gut microbes produce various bioactive metabolites, such as short-chain fatty acid (10), hydroxy fatty acid (11), aromatic amino acid derivatives (12) from dietary compounds. The physiological effects of gut microbes on the host are a result of host-gut microbe interactions. Hence, understanding the details of host-gut microbe interactions is key for controlling host health and developing a good symbiosis with gut microbes. However, the mechanism involved in host-gut microbe interactions are still unclear. The aim of this study was to construct a basis for understanding host-gut microbe interactions at the compound level. The author focused on glycans as the host-derived compounds and polyamines as the gut microbe-derived compounds in this study.

In CHAPTER I, the author focused on generating highly efficient 1,2-α-L-fucosynthase, which is useful for the enzymatic synthesis of H-antigen structure (Fucα1-2Gal, Fig. 1). H-antigens are observed on the non-reducing end of HMOs (7) and glycans of host secreted glycoproteins (13). H-antigen structure promotes the colonization of *Bifidobacterium* species (14,15) and prevents the host from pathogen infection (16-18). Hence, H-antigen is an important glycan structure responsible for host-gut microbe interactions. If H-antigen can be efficiently synthesized, it will be possible to provide useful tools to accelerate the elucidation of host-gut microbe interactions mediated by H-antigens. However, regio- and stereo-selective synthesis of H-antigen structure is difficult by chemical synthesis. Therefore, in SECTION I, the author focused on the enzymatic synthesis of H-antigen and generated a highly functional 1,2-α-L-fucosynthase *Bb*AfcA N423H mutant (*Bb*AfcA^{N423H}) from 1,2-α-L-fucosidase of *Bifidobacterium bifidum* (*Bb*AfcA) (19). In SECTION II, the author applied *Bb*AfcA^{N423H} for introducing the H-antigen structure on various glycoconjugates (glycolipid, *O*- and *N*-glycans of glycoproteins, and xyloglucan). H-antigen structure has been observed not only on oligosaccharide and *O*-glycans but also on glycolipids (20), *N*-glycans (21), and plant xyloglucans. Fucosyl ganglioside GM1, a glycolipid containing H-antigen structure, has been observed on the surface of intestinal epithelial cells in response to gut microbe colonization (20),

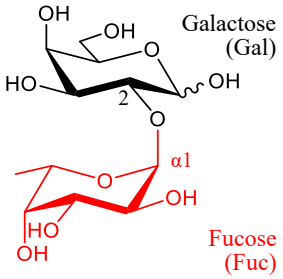

Fig. 1. Structure of H-antigen.

suggesting that fucosyl ganglioside GM1 contributes to the development of symbiosis between the host and gut microbes in the colon. Fucosyl xyloglucan nonasaccharide is a bioactive plant glycan that shows inhibition activity against auxin-stimulated stem growth (22). Therefore, the author enzymatically synthesized these H-antigen containing glycoconjugates using *Bb*AfcA^{N423H}.

In CHAPTER II, the author focused on the polyamine biosynthesis and transport ability of human gut microbes. Several hundred micromolar to a few millimolar concentrations of polyamines exist in the colonic lumen (23) and these polyamines are derived from gut microbes (24-26). These colonic luminal polyamines can affect host health, such as expanding lifespan, cognitive improvement (27), amelioration of inflammation (28), and vascular endothelial function improvement (29). Understanding the polyamine biosynthetic and transport abilities of the human dominant gut microbes which are the main source of colonic polyamines is important to maintain host health via the regulation of colonic polyamine levels. Therefore, in SECTION I, the author analyzed the biosynthetic and transport abilities of the polyamines (putrescine, spermidine, and spermine, Fig. 2) of the human dominant gut microbes that are culturable in Gifu anaerobic medium (30). Furthermore, the author presumed the presence of novel polyamine biosynthetic and transport proteins in the human dominant gut microbes based on the results of BlastP analysis combined with polyamine biosynthetic- and transport abilities. SECTION II focused on the biosynthetic and transport abilities of the polyamines (putrescine, spermidine, and spermine) of human indigenous *Bifidobacterium* species. Bifidobacteria are one of the typical human indigenous bacteria (31-33). Although there are many reports on the functionality of bifidobacteria as probiotics, the physiological analysis of bifidobacteria itself has not progressed and, to the best of my knowledge, there is only one report on the ability of biosynthesis and transport of polyamines (34). Therefore, the author evaluated the ability of biosynthesis and transport of polyamines (Fig. 2) for 13 species reported as human indigenous *Bifidobacterium* species (31-33). Furthermore, the possibility of the existence of novel polyamine biosynthesis and transport protein(s) was presumed by inferring and collating the analyzed results in the presence and absence of known polyamine biosynthetic and transport proteins. SECTION III focused on the putrescine exporter of *Escherichia coli*, which functions under a neutral pH environment. The colonic lumen is neutral pH (35). However, putrescine exporter that functions under a neutral pH environment has not been identified in gut microbes. The author observed putrescine excretion under a neutral pH environment in *E. coli*, a model gut microbe. The author performed genome-wide screening using the Keio collection (36) and discovered SapBCDF as a novel putrescine exporter in *E. coli*.

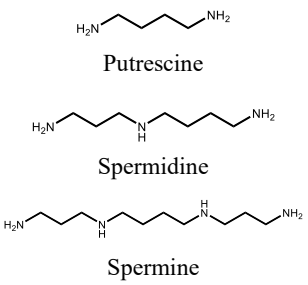

Fig. 2. Polyamine structures measured in this study.

REFERENCES

1. Almeida, A., Mitchell, A. L., Boland, M., Forster, S. C., Gloor, G. B., Tarkowska, A., Lawley, T. D., and Finn, R. D. (2019) A new genomic blueprint of the human gut microbiota. *Nature* **568**, 499-504
2. Sender, R., Fuchs, S., and Milo, R. (2016) Revised Estimates for the Number of Human and Bacteria Cells in the Body. *PLoS Biol* **14**, e1002533
3. Ridaura, V. K., Faith, J. J., Rey, F. E., Cheng, J., Duncan, A. E., Kau, A. L., Griffin, N. W., Lombard, V., Henrissat, B., Bain, J. R., Muehlbauer, M. J., Ilkayeva, O., Semenkovich, C. F., Funai, K., Hayashi, D. K., Lyle, B. J., Martini, M. C., Ursell, L. K., Clemente, J. C., Van Treuren, W., Walters, W. A., Knight, R., Newgard, C. B., Heath, A. C., and Gordon, J. I. (2013) Gut microbiota from twins discordant for obesity modulate metabolism in mice. *Science* **341**, 1241214
4. Pedersen, H. K., Gudmundsdottir, V., Nielsen, H. B., Hyotylainen, T., Nielsen, T., Jensen, B. A., Forslund, K., Hildebrand, F., Prifti, E., Falony, G., Le Chatelier, E., Levenez, F., Doré, J., Mattila, I., Plichta, D. R., Pöhö, P., Hellgren, L. I., Arumugam, M., Sunagawa, S., Vieira-Silva, S., Jørgensen, T., Holm, J. B., Trošt, K., Kristiansen, K., Brix, S., Raes, J., Wang, J., Hansen, T., Bork, P., Brunak, S., Oresic, M., Ehrlich, S. D., Pedersen, O., and Consortium, M. (2016) Human gut microbes impact host serum metabolome and insulin sensitivity. *Nature* **535**, 376-381
5. Sharon, G., Cruz, N. J., Kang, D. W., Gandal, M. J., Wang, B., Kim, Y. M., Zink, E. M., Casey, C. P., Taylor, B. C., Lane, C. J., Bramer, L. M., Isern, N. G., Hoyt, D. W., Noecker, C., Sweredoski, M. J., Moradian, A., Borenstein, E., Jansson, J. K., Knight, R., Metz, T. O., Lois, C., Geschwind, D. H., Krajmalnik-Brown, R., and Mazmanian, S. K. (2019) Human Gut Microbiota from Autism Spectrum Disorder Promote Behavioral Symptoms in Mice. *Cell* **177**, 1600-1618.e1617
6. Katayama, T. (2016) Host-derived glycans serve as selected nutrients for the gut microbe: human milk oligosaccharides and bifidobacteria. *Biosci Biotechnol Biochem* **80**, 621-632
7. Bode, L. (2012) Human milk oligosaccharides: every baby needs a sugar mama. *Glycobiology* **22**, 1147-1162
8. Brand-Miller, J. C., McVeagh, P., McNeil, Y., and Messer, M. (1998) Digestion of human milk oligosaccharides by healthy infants evaluated by the lactulose hydrogen breath test. *J Pediatr* **133**, 95-98
9. Sivan, A., Corrales, L., Hubert, N., Williams, J. B., Aquino-Michaels, K., Earley, Z. M., Benyamin, F. W., Lei, Y. M., Jabri, B., Alegre, M. L., Chang, E. B., and Gajewski, T. F. (2015) Commensal *Bifidobacterium* promotes antitumor immunity and facilitates anti-PD-

L1 efficacy. *Science* **350**, 1084-1089

10. Fukuda, S., Toh, H., Hase, K., Oshima, K., Nakanishi, Y., Yoshimura, K., Tobe, T., Clarke, J. M., Topping, D. L., Suzuki, T., Taylor, T. D., Itoh, K., Kikuchi, J., Morita, H., Hattori, M., and Ohno, H. (2011) Bifidobacteria can protect from enteropathogenic infection through production of acetate. *Nature* **469**, 543-547
11. Miyamoto, J., Igarashi, M., Watanabe, K., Karaki, S. I., Mukouyama, H., Kishino, S., Li, X., Ichimura, A., Irie, J., Sugimoto, Y., Mizutani, T., Sugawara, T., Miki, T., Ogawa, J., Drucker, D. J., Arita, M., Itoh, H., and Kimura, I. (2019) Gut microbiota confers host resistance to obesity by metabolizing dietary polyunsaturated fatty acids. *Nat Commun* **10**, 4007
12. Dodd, D., Spitzer, M. H., Van Treuren, W., Merrill, B. D., Hryckowian, A. J., Higginbottom, S. K., Le, A., Cowan, T. M., Nolan, G. P., Fischbach, M. A., and Sonnenburg, J. L. (2017) A gut bacterial pathway metabolizes aromatic amino acids into nine circulating metabolites. *Nature* **551**, 648-652
13. Hakomori, S. (1999) Antigen structure and genetic basis of histo-blood groups A, B and O: their changes associated with human cancer. *Biochim Biophys Acta* **1473**, 247-266
14. Korpela, K., Salonen, A., Hickman, B., Kunz, C., Sprenger, N., Kukkonen, K., Savilahti, E., Kuitunen, M., and de Vos, W. M. (2018) Fucosylated oligosaccharides in mother's milk alleviate the effects of caesarean birth on infant gut microbiota. *Sci Rep* **8**, 13757
15. Lewis, Z. T., Totten, S. M., Smilowitz, J. T., Popovic, M., Parker, E., Lemay, D. G., Van Tassell, M. L., Miller, M. J., Jin, Y. S., German, J. B., Lebrilla, C. B., and Mills, D. A. (2015) Maternal fucosyltransferase 2 status affects the gut bifidobacterial communities of breastfed infants. *Microbiome* **3**, 13
16. Pham, T. A., Clare, S., Goulding, D., Arasteh, J. M., Stares, M. D., Browne, H. P., Keane, J. A., Page, A. J., Kumasaka, N., Kane, L., Mottram, L., Harcourt, K., Hale, C., Arends, M. J., Gaffney, D. J., Dougan, G., Lawley, T. D., and Project, S. M. G. (2014) Epithelial IL-22RA1-mediated fucosylation promotes intestinal colonization resistance to an opportunistic pathogen. *Cell Host Microbe* **16**, 504-516
17. Goto, Y., Obata, T., Kunisawa, J., Sato, S., Ivanov, I. I., Lamichhane, A., Takeyama, N., Kamioka, M., Sakamoto, M., Matsuki, T., Setoyama, H., Imaoka, A., Uematsu, S., Akira, S., Domino, S. E., Kulig, P., Becher, B., Renauld, J. C., Sasakawa, C., Umesaki, Y., Benno, Y., and Kiyono, H. (2014) Innate lymphoid cells regulate intestinal epithelial cell glycosylation. *Science* **345**, 1254009
18. Pickard, J. M., Maurice, C. F., Kinnebrew, M. A., Abt, M. C., Schenten, D., Golovkina, T. V., Bogatyrev, S. R., Ismagilov, R. F., Pamer, E. G., Turnbaugh, P. J., and Chervonsky, A. V. (2014) Rapid fucosylation of intestinal epithelium sustains host-commensal symbiosis in sickness. *Nature* **514**, 638-641

19. Katayama, T., Sakuma, A., Kimura, T., Makimura, Y., Hiratake, J., Sakata, K., Yamanoi, T., Kumagai, H., and Yamamoto, K. (2004) Molecular cloning and characterization of *Bifidobacterium bifidum* 1,2-alpha-L-fucosidase (AfcA), a novel inverting glycosidase (glycoside hydrolase family 95). *J Bacteriol* **186**, 4885-4893
20. Umesaki, Y., Suzuki, A., Kasama, T., Tohyama, K., Mutai, M., and Yamakawa, T. (1981) Presence of asialo GM1 and glucosylceramide in the intestinal mucosa of mice and induction of fucosyl asialo GM1 by conventionalization of germ-free mice. *J Biochem* **90**, 1731-1738
21. Canis, K., McKinnon, T. A., Nowak, A., Haslam, S. M., Panico, M., Morris, H. R., Laffan, M. A., and Dell, A. (2012) Mapping the *N*-glycome of human von Willebrand factor. *Biochem J* **447**, 217-228
22. Augur, C., Yu, L., Sakai, K., Ogawa, T., Sinaÿ, P., Darvill, A. G., and Albersheim, P. (1992) Further studies of the ability of xyloglucan oligosaccharides to inhibit auxin-stimulated growth. *Plant Physiol* **99**, 180-185
23. Matsumoto, M., Kakizoe, K., and Benno, Y. (2007) Comparison of fecal microbiota and polyamine concentration in adult patients with intractable atopic dermatitis and healthy adults. *Microbiol Immunol* **51**, 37-46
24. Noack, J., Kleessen, B., Proll, J., Dongowski, G., and Blaut, M. (1998) Dietary guar gum and pectin stimulate intestinal microbial polyamine synthesis in rats. *J Nutr* **128**, 1385-1391
25. Noack, J., Dongowski, G., Hartmann, L., and Blaut, M. (2000) The human gut bacteria *Bacteroides thetaiotaomicron* and *Fusobacterium varium* produce putrescine and spermidine in cecum of pectin-fed gnotobiotic rats. *J Nutr* **130**, 1225-1231
26. Matsumoto, M., Kibe, R., Ooga, T., Aiba, Y., Kurihara, S., Sawaki, E., Koga, Y., and Benno, Y. (2012) Impact of intestinal microbiota on intestinal luminal metabolome. *Sci Rep* **2**, 233
27. Kibe, R., Kurihara, S., Sakai, Y., Suzuki, H., Ooga, T., Sawaki, E., Muramatsu, K., Nakamura, A., Yamashita, A., Kitada, Y., Kakeyama, M., Benno, Y., and Matsumoto, M. (2014) Upregulation of colonic luminal polyamines produced by intestinal microbiota delays senescence in mice. *Sci Rep* **4**, 4548
28. Matsumoto, M., Kurihara, S., Kibe, R., Ashida, H., and Benno, Y. (2011) Longevity in mice is promoted by probiotic-induced suppression of colonic senescence dependent on upregulation of gut bacterial polyamine production. *PLoS One* **6**, e23652
29. Matsumoto, M., Kitada, Y., and Naito, Y. (2019) Endothelial Function is improved by Inducing Microbial Polyamine Production in the Gut: A Randomized Placebo-Controlled Trial. *Nutrients* **11**
30. Gotoh, A., Nara, M., Sugiyama, Y., Sakanaka, M., Yachi, H., Kitakata, A., Nakagawa, A., Minami, H., Okuda, S., Katoh, T., Katayama, T., and Kurihara, S. (2017) Use of Gifu

Anaerobic Medium for culturing 32 dominant species of human gut microbes and its evaluation based on short-chain fatty acids fermentation profiles. *Biosci Biotechnol Biochem* **81**, 2009-2017

31. Bottacini, F., Ventura, M., van Sinderen, D., and O'Connell Motherway, M. (2014) Diversity, ecology and intestinal function of bifidobacteria. *Microb Cell Fact* **13 Suppl 1**, S4
32. Milani, C., Duranti, S., Lugli, G. A., Bottacini, F., Strati, F., Arioli, S., Foroni, E., Turroni, F., van Sinderen, D., and Ventura, M. (2013) Comparative genomics of B*ifidobacterium animalis* subsp. *lactis* reveals a strict monophyletic bifidobacterial taxon. *Appl Environ Microbiol* **79**, 4304-4315
33. Yatsunenko, T., Rey, F. E., Manary, M. J., Trehan, I., Dominguez-Bello, M. G., Contreras, M., Magris, M., Hidalgo, G., Baldassano, R. N., Anokhin, A. P., Heath, A. C., Warner, B., Reeder, J., Kuczynski, J., Caporaso, J. G., Lozupone, C. A., Lauber, C., Clemente, J. C., Knights, D., Knight, R., and Gordon, J. I. (2012) Human gut microbiome viewed across age and geography. *Nature* **486**, 222-227
34. Hamana, K. (1997) Polyamine Distribution Patterns in Gram-Positive Eubacteria : The Absence of Cellular Polyamine Synthesis. *Ann. Rep. Coo. Med. Care Technol. Gunma Univ.* **17**, 137-144
35. Ringel-Kulka, T., Choi, C. H., Temas, D., Kim, A., Maier, D. M., Scott, K., Galanko, J. A., and Ringel, Y. (2015) Altered Colonic Bacterial Fermentation as a Potential Pathophysiological Factor in Irritable Bowel Syndrome. *Am J Gastroenterol* **110**, 1339-1346
36. Baba, T., Ara, T., Hasegawa, M., Takai, Y., Okumura, Y., Baba, M., Datsenko, K. A., Tomita, M., Wanner, B. L., and Mori, H. (2006) Construction of *Escherichia coli* K-12 in-frame, single-gene knockout mutants: the Keio collection. *Mol Syst Biol* **2**, 2006.0008

CHAPTER I
Introduction of H-antigen structures on various glycoconjugates

SECTION I
Generation of highly functional 1,2-α-L-fucosynthase from 1,2-α-L-fucosidase of *Bifidobacterium bifidum*

Fucα1-2Gal disaccharide structures (H-antigens), which constitute histo-blood group antigens, are frequently found at the non-reducing ends of sugar chains of glycoconjugates including glycoproteins, glycolipids, and oligosaccharides (1). They play important roles in various biological processes and are sometimes used as the markers of embryogenesis and carcinogenesis (2,3). In humans, the structures are synthesized by fucosyltransferase (FUT) 1 and 2 (4,5). *FUT*1 is highly expressed in early erythroid and endothelial cells to synthesize the core of ABO blood group substances, while *FUT2* is abundantly expressed in secretory organs: trachea, salivary glands, small intestine, colon, and prostate (6). Interestingly, *FUT2* expression is known to be stimulated by the presence of gut microbes in mouse intestines (7-9). This was initially regarded as a host system to provide nutritional advantage for certain bacteria possessing 1,2-α-L-fucosidase, by specifically enabling them to degrade the intestinal glycans (7). However, recent study revealed that Fuc liberated from the intestinal glycans by such microbes can attenuate the virulence gene expression of enterohemorrhagic *Escherichia coli* (10). Pham *et al*. showed that administration of H-antigen-containing oligosaccharides to mice that are genetically deficient in intestinal fucosylation confers resistance to invasion by the opportunistic pathogen *Enterococcus faecalis* (11). H-antigen structures present in the gut ecosystem might therefore be important for host health. Moreover, increased risks of Crohn disease and type-1 diabetes have been reported in *FUT2*$^{-/-}$ individuals (non-secretors), in comparison with secretors (12,13).

H-antigen-containing sugars are supplied into intestines, not only by host individuals, but also by mothers during breast-feeding. Human milk oligosaccharides (HMOs), the third most abundant solid component in breast milk, are known to be highly fucosylated, provided that the mothers are secretors (14-16). HMOs are resistant to human digestive enzymes, and therefore reach the colon (17), where they are assumed to selectively stimulate the growth of bifidobacteria, microbes that exclusively possess HMOs-degrading enzymes (18-25). Fucosylated HMOs also serve as decoys for the receptor of *Campylobacter jejuni* in the intestine (26). 2'-Fucosyllactose (2'-FL: Fucα1-2Galβ1-4Glc), one of the most abundant HMOs, is shown to attenuate the lipopolysaccharide-induced inflammatory response of intestinal cells by downregulating CD14 expression (27). These results indicate that H-antigen-containing glycans are important for establishing the harmonious relationship between gut

microbes and the host, and also for preventing various gut-related disorders. Hence, glycoconjugates with H-antigens have great potential, not only as research tools, but also as therapeutic agents.

Enzymatic synthesis of H-antigen structure has been demonstrated by several groups using α-1,2-fucosyltransferases or α-fucosidase (in this case, transfucosylation). Drouillard *et al*. succeeded in constructing a recombinant *E. coli* strain that produces 2'-FL and lacto-*N*-fucopentaose IV (LNFP IV: Fucα1-2Galβ1-4GlcNAcβ1-3Galβ1-4Glc, type-2 H-antigen) at gram-per-liter levels, by introducing several glycosyltransferases including α-1,2-fucosyltransferase from *Helicobacter pylori* (28). Gram-scale synthesis of 2'-FL was also accomplished by Baumgärtner *et al*. by using an engineered *E. coli* (29). Zhao *et al*. synthesized 1 g of lacto-*N*-fucopentaose I (LNFP I: Fucα1-2Galβ1-3GlcNAcβ1-3Galβ1-4Glc, type-1 H-antigen) using one-pot enzyme system involving α-1,2-fucosyltransferase from *Thermosynechococcus elongates* and bifunctional fucokinase/GDP-Fuc pyrophosphorylase, starting from Fuc and lacto-*N*-tetraose (LNT: Galβ1-3GlcNAcβ1-3Galβ1-4Glc) (30). Vasiliu *et al*. employed human FUT2 to introduce α-(1→2)-linked Fuc residue at the non-reducing end of poly-*N*-acetyllactosamine (type-2 H-antigen) (31). Glycosyltransferases thus serve as valuable tools for synthesizing specific oligosaccharide with a defined structure, although they show strict acceptor specificity and therefore the types of oligosaccharides to be synthesized have been limited. Osanjo *et al*. described, using a mutant α-L-fucosidase (retaining enzyme) from *Thermotoga maritima*, the transfer of Fuc from *p*NP-α-L-fucoside to Galβ-*p*NP to form Fucα1-2Galβ-*p*NP with relatively high specificity (32). These results demonstrate the effectiveness of enzyme-based methods for targeted oligosaccharide synthesis.

Glycosynthase is a mutant glycosidase that is devoid of hydrolysis but is able to transfer glycosyl residue from a fluorine-activated sugar with opposite anomer; once the glycosidic bond is formed, the linkage can be free from hydrolysis (33). This methodology, which was developed based on the finding by Hehre *et al*. (34), was first applied to retaining glycosidases (35,36), and was recently extended to inverting enzymes (37-40). Previously Wada *et al*. succeeded in applying the technology to inverting 1,2-α-L-fucosidase from *Bifidobacterium bifidum* JCM1254 (*Bb*AfcA, glycoside hydrolase family [GH] 95). However, the reaction efficiency was too low for further use of the generated 1,2-α-L-fucosynthase in oligosaccharide synthesis (40). Nonetheless, the author pursued further exploration of the synthase because of high activity and specificity of wild-type *Bb*AfcA (*Bb*AfcA^{WT}) for all H-antigen-containing oligosaccharides and sugar chains of glycoproteins (H type-1, H type-2, H type-3, and H type-4 chains) (41,42). 1,2-α-L-Fucosidase adopts a unique reaction mechanism in which asparagine (Asn-423) activated by the neighboring aspartic acid (Asp-766) acts as a base residue (43,44) (Fig. 1). The attacking water molecule is suitably poised for nucleophilic attack by being supported by two asparagine residues (Asn-421 and Asn-423 [base]). Asn-421 makes a hydrogen bond with glutamic acid residue of Glu-566 (acid residue), which allows the side chain of Glu-566 to be properly oriented towards glycosidic oxygen. In the present study, the author first shows

a drastic improvement of the synthase reaction efficiency by introducing a series of mutations at the catalytic residues of *Bb*AfcA. The author then describes the detailed specificity analysis of the synthase reaction using various mono- and oligosaccharides, and show its capability to efficiently introduce H-antigen structures onto a glycoprotein. Finally, the author discusses a unique structural requirement for acceptors of the synthase reaction, which was unraveled from glycosynthase technology. My results show that this 1,2-α-L-fucosynthase serves as an alternative tool for introducing H-antigens on a variety of glycoconjugates.

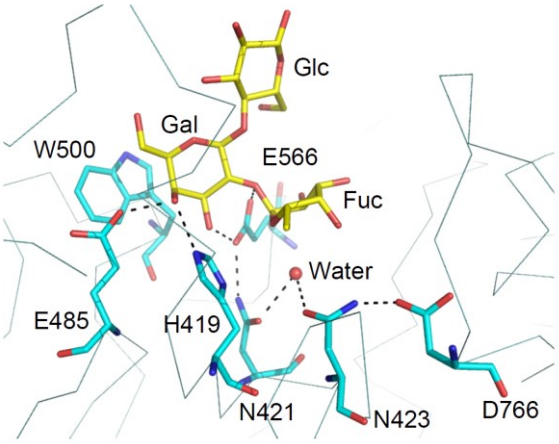

Fig. 1. Structure of the catalytic site of 1,2-α-L-fucosidase from *B. bifidum*. The catalytic residues (N421, N423, E566, and D766) and Gal-recognizing residues (H419, E485, W500, and E566) are shown by cyan sticks with the attacking water molecule depicted by a red sphere (PDB ID: 2EAC) (44). 2'-FL observed in the crystal structure of E566A mutant (PDB ID: 2EAD) is incorporated and shown in yellow. The hydrogen bond network is formed by the water, N421, N423, E566, and D766. The Gal residue of 2'-FL forms hydrogen bonds with the side chains of H419, E485, and E566, and is stacked by W500. The image was created by PyMol.

MATERIALS AND METHODS

Chemicals

Melibiose (Galα1-6Glc) and xylobiose (Xylβ1-4Xyl) were obtained from Tokyo Chemical Industry Co. Ltd. (Tokyo, Japan). 4-β-Galactobiose (Galβ1-4Gal), 6-β-galactobiose (Galβ1-6Gal), Lewis a trisaccharide (Le^a: Galβ1-3(Fucα1-4)GlcNAc), Lewis x trisaccharide (Le^x: Galβ1-4(Fucα1-3)GlcNAc), *N*-acetyllactosamine (LacNAc: Galβ1-4GlcNAc), 3-fucosyllacose (Galβ1-4(Fucα1-3)Glc), LNT, and LNFP I were obtained from Dextra Laboratories (Reading, UK), and Lewis b tetrasaccharide (Le^b: Fucα1-2Galβ1-3(Fucα1-4)GlcNAc) and Lewis y tetrasaccharide (Le^y: Fucα1-2Galβ1-4(Fucα1-3)GlcNAc) were acquired from Carbosynth (Compton, UK). 2'-FL and lacto-*N*-*neo*tetraose (LN*n*T: Galβ1-4GlcNAcβ1-3Galβ1-4Glc) were purchased from Sigma-Aldrich (St. Louis, MO, USA), and lactodifucotetraose (LDFT: Fucα1-2Galβ1-4(Fucα1-3)Glc) was purchased from Isosep (Tullinge, Sweden). Galacto-*N*-biose (GNB: Galβ1-3GalNAc), lacto-*N*-biose I (LNB: Galβ1-3GlcNAc), 3-β-galactobiose (Galβ1-3Gal), 3-β-galactosylglucose (Galβ1-3Glc), and β-fucosyl fluoride (β-FucF) were prepared, as described previously (40,45-47). Other reagents of analytical grade were obtained from various commercial sources.

Construction of 1,2-α-L-fucosidase mutants

QuikChange site-directed mutagenesis method (Stratagene, CA) was used for introducing amino acid replacements. pET23b-*BbafcA*, which carries the gene encoding the catalytic domain of *Bb*AfcA from *Bifidobacterium bifidum* JCM1254, was used as the template (42). The primers used are listed in Table 1. The entire sequence of the catalytic domain of *BbafcA* was sequenced to ensure that no base change other than those designed had occurred. The resulting plasmids were used to transform *Escherichia coli* BL21 Δ*lacZ* (DE3) (48).

Expression and purification of 1,2-α-L-fucosidase mutants

Expression of the recombinant proteins was carried out, as described previously (42). The enzymes were purified using Ni-nitrilotriacetic acid affinity chromatography according to the manufacturer's instruction (QIAGEN, Hilden, Germany), and dialyzed against 10 mM Tris-HCl buffer (pH 8.0) using Slide-A Lyzer G2 (Thermo Fisher Scientific, Waltham, MA, USA). When necessary, the proteins were further purified by Mono Q 5/50 GL (0−1 M NaCl in 20 mM Tris-HCl buffer, pH 8.0) (GE Healthcare Life Sciences, Buckinghamshire, UK) column chromatography. The purity of the proteins was examined by sodium dodecyl sulfate-polyacrylamide gel electrophoresis. Protein concentration was determined with the theoretical coefficient of 184,165 M^{-1} cm^{-1} at 280 nm.

Enzyme assay

Hydrolytic activity of 1,2-α-L-fucosidase mutants was measured using 2'-FL as a substrate (1 mM). The liberated Fuc was quantified by fucose dehydrogenase-linked assay, as described previously (42). The enzyme concentrations were 0.51 nM for wild-type (WT), 1.0 nM for N421D mutant, 10.2 nM for N423D mutant, 51 nM for N423Q mutant, and 102 nM for the other mutants.

Fucosynthase activity of various mutants was examined using β-FucF and Lac as the donor and acceptor substrates, respectively. The reaction was carried out at 30 ºC for 30 min in 100 mM sodium citrate buffer (pH5.0), containing 10 mM substrates and 4 μM enzyme. The reaction products were analyzed by a high-performance liquid chromatography (HPLC) system (Ultimate 3000, Thermo Fisher Scientific) equipped with Asahipak NH2P-50 4E column (4.6 × 250 mm, Showa Denko, Tokyo, Japan). Elution was carried out with 73 % acetonitrile at a flow rate of 1.0 mL/min, and was monitored using a charged aerosol detector (CAD) (Thermo Fisher Scientific). The amount of synthesized 2'-FL was determined based on the standard curve prepared from known concentrations of the compound. Optimal pH of the synthase reaction was determined by testing the enzyme in 100 mM citrate-NaOH buffer (pH 4.5–6.0), 2-morpholinoethanesulfonic acid buffer (pH 6.0–7.0), and 3-morpholinopropanesulfonic acid buffer (pH 7.0–8.0). Thermostability was examined by incubating the enzyme for 30 min at various temperatures in 100 mM citrate-NaOH buffer (pH 5.5 for N423H mutant and pH 5.0 for N423D/D766N mutant) prior to the assay.

Acceptor specificity of *Bb*AfcA^{N423H} was examined using various mono- and oligosaccharides. The reaction was carried out at 30 ºC for 30 min in 100 mM citrate-NaOH buffer (pH 5.5), containing 10 mM β-FucF and 10 mM acceptor, in the presence of 10 μM enzyme. The reaction was stopped by boiling for 3 min. The reaction mixtures were analyzed by thin-layer chromatography (TLC) and HPLC-CAD. The reaction efficiency was evaluated by determining the consumed amounts of acceptors. TLC analysis was carried out using silica gel 60 aluminum sheet (Merck, NJ). The plate was developed in a solvent system of 1-butanol/acetic acid/water (2/1/1), and the sugars were visualized by heating the plate after spraying with diphenylamine-aniline-phosphoric acid reagent (49). HPLC-CAD analysis was carried out using HILICpak VG-50 4E column (4.6 × 250 mm, Showa Denko) at 40 ºC. The elution was done with 73 % acetonitrile at a flow rate of 1.0 mL/min. When xylobiose was used as an acceptor, acetonitrile/methanol/water of 75/20/5 was used as an eluent.

Porcine gastric mucin (PGM) was also used as an acceptor substrate. Prior to the synthase reaction, the Fuc residues were removed from sugar chains of PGM. The defucosylation was carried out at 30 ºC for 48 h in 50 mM sodium phosphate buffer (pH 6.5) containing 2 mg/mL PGM, 1 mM dithiothreitol, and 10 μM 1,2-α-L-fucosidase WT (*Bb*AfcA^{WT}). After stopping the reaction by boiling, the reaction mixture was dialyzed against water and lyophilized to obtain defucosylated PGM. Fucosylation was carried out at 30 ºC for 30 min in the reaction mixture containing 50 mM citrate-NaOH buffer (pH 5.5), 1 mg/mL defucosylated PGM, 10 mM β-FucF, and 10 μM *Bb*AfcA^{N423H}. For

lectin blotting, the samples were taken from the mixtures, spotted on Immobilon-P membrane (Millipore, MA) that was pretreated with methanol. The membrane was incubated for 60 min with a blocking reagent: 2 % (*w*/*v*) bovine serum albumin in Tris-buffered saline with 0.05 % (*v*/*v*) Tween-20 (TBS-T). Biotin conjugated lectins (UEA-I and PNA, J-Oil Mills, Tokyo, Japan), dissolved in TBS-T (0.4 μg/mL), and horseradish peroxidase (HRP)-conjugated streptavidin (0.125 μg/mL) were then added. The membrane was further incubated for 60 min at room temperature. After washing the membrane with TBS-T, signals were detected using SuperSignal West Pico Chemiluminescent Substrate (Thermo Fischer Scientific) and LAS-3000 (Fujifilm, Tokyo, Japan).

Purification of the synthesized oligosaccharides

Several synthesized oligosaccharides (see RESULTS) were purified for subsequent instrumental analyses. The reaction mixtures (total volume of 750-4300 μL) were deionized with Amberlite MB-3 (Organo, Tokyo, Japan), lyophilized and subjected to HPLC equipped with Sugar-D column (20 × 250 mm, Nacalai Tesque, Kyoto, Japan). Elution was done under a constant flow (5.0 mL/min) of 72 % acetonitrile at 40 ºC, and monitored by refractive index detector (RID-10A, Shimadzu, Kyoto, Japan). The peak fractions were combined, concentrated, lyophilized, and further purified by using TSK-gel 80Ts (20 × 250 mm, Tosoh, Tokyo, Japan) column. Elution was carried out by water at a flow rate of 7.0 mL/min and monitored by RID-10A. The peak fractions were collected, lyophilized to dryness, and used for the instrumental analyses.

Nuclear magnetic resonance (NMR) spectroscopy

The NMR spectra 1D (^{1}H and ^{13}C) and 2D (^{1}H-^{1}H DQF-COSY, ^{1}H-^{1}H TOCSY, ^{1}H-^{13}C HSQC and ^{1}H-^{13}C HMBC) were taken in D_2O at 298K using Bruker Avance 800 or Avance 500 spectrometers (Bruker BioSpin, MA, USA) with 2-methyl-2-propanol as an internal standard (1.23 ppm for ^{1}H; 31.3 ppm for ^{13}C). Positions of the glycosyl linkages were assigned by the inter-ring cross peaks with the anomeric ^{1}H and ^{13}C signals that appeared in the HMBC spectra.

High–performance anion exchange chromatography (HPAEC)

HPAEC with pulsed amperometric detection (PAD) (Thermo Fisher Scientific) analysis was performed using Carbopac PA1 column (2 × 250 mm, Dionex, Sunnyvale, CA, USA) at 30 ºC. The elution was done with 16 mM NaOH at a flow rate of 0.25 mL/min.

Release of* O*-glycans from porcine gastric mucin

The *O*-linked glycans were released by reductive β-elimination, essentially as described previously (50). In brief, the lyophilized glycoprotein (100 μg) was resuspended in 500 μL of 100 mM sodium hydroxide containing 1 M sodium borohydride, and the mixture was incubated for 18 h at 45

ºC in a glass tube. The mixture was then neutralized with 10 % (*v*/*v*) acetic acid on ice, and desalted by a Dowex-50W-X8 (H^+ form, 100-200 mesh, Sigma-Aldrich) column. Oligosaccharide alditols were collected in the elution with 5 % acetic acid, and lyophilized. Borate was removed as an azeotrope with methanol, by adding 0.3 mL of 10 % acetic acid in methanol and drying under a nitrogen stream at 40 ºC. This step was repeated five times. The samples were reconstituted in 0.3 mL of 5 % acetic acid and loaded onto a pre-equilibrated Sep-pak C_{18} cartridges (Waters, Milford, MA, USA). The oligosaccharide alditols were recovered in flow-through and in washing with 2 mL of 5 % acetic acid, and were lyophilized for subsequent permethylation.

Permethylation of oligosaccharides and alditols

Permethylation was performed according to the method of Anumula and Taylor (51), to improve sensitivity and allow structure determination in MS analysis. The lyophilized oligosaccharides and *O*-glycan alditols were reconstituted in 200 µL of anhydrous dimethylsulfoxide (DMSO). Permethylation was carried out by mixing the sample vigorously for 5 min with 250 µL of base (sodium hydroxide in DMSO) and 150 µL of iodomethane. After adding 2 mL of 5 % acetic acid and 2 mL of dichloromethane, the permethylated samples were extracted in the organic phase, which was then dried under a nitrogen stream at 40 ºC. The samples were loaded onto pre-equilibrated Sep-pak C_{18} cartridges, washed with water and eluted with 85 % (*v*/*v*) acetonitrile. The eluted fractions were again dried under a nitrogen stream at 40 ºC.

Matrix-assisted laser desorption/ionization time-of-flight mass spectroscopy (MALDI-TOF MS) and MALDI-TOF/TOF MS analyses

Molecular masses of the permethylated samples were determined by MALDI-TOF MS in positive ion mode (Bruker UltrafleXtreme, Bruker Daltonics, MA, USA) with 2,5-dihydroxybenzoic acid as matrix. MALDI-TOF/TOF MS was also performed to obtain MS/MS spectra of the glycans of interest. The MS and MS/MS spectra were manually interpreted to deduce glycan structures. Theoretical masses were calculated using the software GlycoWorkbench 2.0 (52). Semi-quantitative estimation of relative glycan amounts is calculated based on signal intensity of MS spectra.

Table 1. 1,2-α-L-Fucosidase mutants used in this study and their hydrolytic activity towards 2'-FL.

Mutant	Primer[a] or reference	Hydrolytic activity (%)[b]	Mutant	Primer	Hydrolytic activity (%)
N421A[c]	Ref. (44)	nd[d]	L	cgttccagatcctgggcaacttcgg	nd
D	acttccacatggatgtgaacctcca	36	M	cgttccagatcatgggcaacttcgg	nd
E	acttccacatggaagtgaacctcca	nd	N	cgttccagatcaacggcaacttcgg	0.079
G[c]	Ref. (40)	nd	P	cgttccagatcccgggcaacttcgg	nd
H	acttccacatgcatgtgaacctcca	nd	Q	cgttccagatccagggcaacttcgg	nd
Q	acttccacatgcaggtgaacctcca	nd	R	cgttccagatccgtggcaacttcgg	nd
S	acttccacatgagcgtgaacctcca	0.018	S	cgttccagatcagcggcaacttcgg	nd
T	acttccacatgaccgtgaacctcca	nd	T	cgttccagatcaccggcaacttcgg	nd
V	acttccacatggtggtgaacctcca	nd	V	cgttccagatcgtgggcaacttcgg	nd
N423A	acatgaacgtggcgctccagatgaa	nd	W	cgttccagatctggggcaacttcgg	nd
C[c]	acatgaacgtgtgcctccagatgaa	nd	Y	cgttccagatctatggcaacttcgg	nd
D[c]	Ref. (44)	4.9	N423D/D766E	cgttccagatcgaaccgaacttcgg	0.17
E	acatgaacgtggaactccagatgaa	nd	/D766G	cgttccagatcggcggcaacttcgg	nd
G[c]	Ref. (40)	0.082	/D766H	cgttccagatccatggcaacttcgg	nd
H	acatgaacgtgcatctccagatgaa	nd	/D766N	cgttccagatcaacggcaacttcgg	0.012
Q	acatgaacgtgcagctccagatgaa	0.17	/D766Q	cgttccagatccagggcaacttcgg	nd
S	acatgaacgtgagcctccagatgaa	nd	/D766S	cgttccagatcagcggcaacttcgg	0.026
V	acatgaacgtggtgctccagatgaa	nd	/D766V	cgttccagatcgtgggcaacttcgg	nd
D766A[c]	Ref. (44)	0.064	N423H/D766E	cgttccagatcgaaccgaacttcgg	0.20
C	cgttccagatctgcggcaacttcgg	nd	/D766G	cgttccagatcggcggcaacttcgg	nd
E[c]	Ref. (44)	25	/D766H	cgttccagatccatggcaacttcgg	nd
F	cgttccagatctttggcaacttcgg	nd	/D766N	cgttccagatcaacggcaacttcgg	0.011
G[c]	Ref. (40)	0.021	/D766Q	cgttccagatccagggcaacttcgg	nd
H	cgttccagatccatggcaacttcgg	nd	/D766S	cgttccagatcagcggcaacttcgg	nd
I	cgttccagatcatcggcaacttcgg	nd	/D766V	cgttccagatcgtgggcaacttcgg	nd
K	cgttccagatcaaaggcaacttcgg	nd			

[a]; Those primers and their complementary strands were used for mutagenesis. [b]; Hydrolytic activity of wild-type enzyme was taken as 100 %. [c]; Those mutants were from Wada *et al*. (40) and Nagae *et al*. (44). [d]; not detected. Assays were performed in duplicate and the representative data are shown.

RESULTS

Isolation of an efficient 1,2-α-L-fucosynthase

As mentioned, the catalytic center of 1,2-α-L-fucosidase (*Bb*AfcA) comprises four residues Asn-421 (N421), Asn-423 (N423), Glu-566 (E566) and Asp-766 (D766) (Fig. 1). E566 acts as a general acid residue in hydrolysis, and should hence serve as a base residue in the synthesis reaction. Accordingly, the author first singly introduced amino acid replacements at N421, N423, and D766 sites. N421 was replaced with A, D, E, G, H, Q, S, T, and V, while N423 was replaced with A, C, D, E, G, H, Q, S, and V. D766 was replaced with other 19 amino acids (Table 1). The mutants showed drastically impaired hydrolytic activity towards 2'-FL, except for N421D, N423D, and D766E mutants that retained 36 %, 4.9 %, and 25 % activity of *Bb*AfcA^{WT}, respectively. Among these single mutants, N423H exhibited the highest fucosynthase activity when β-FucF and lactose (Lac) were used as the substrates (Fig. 2A). The synthase activity of the other mutant N423D was comparable with that of D766G mutant which was isolated in previous study (40). None of the N421 mutants exhibited synthase activity. The author then introduced amino acid replacements at D766 position in a N423D background or N423H background, i.e. N423D/D766E, N423D/D766G, N423D/D766H, N423D/D766N, N423D/D766Q, N423D/D766S, N423H/D766E, N423H/D766G, N423H/D766H, N423H/D766N, N423H/D766Q, N423H/D766S, and N423H/D766V double mutants were constructed (Table 1). Hydrolytic activity of these mutants was also extremely low. D766N substitution in N423D background led to a drastic increase in the synthase activity, while introduction of any additional replacement at D766 site resulted in a decrease of the synthase activity in N423H background (Fig. 2B and 2C). Consequently, the author chose N423H mutant (*Bb*AfcA^{N423H}) and N423D/D766N (*Bb*AfcA$^{N423D/D766N}$) mutants for further analysis.

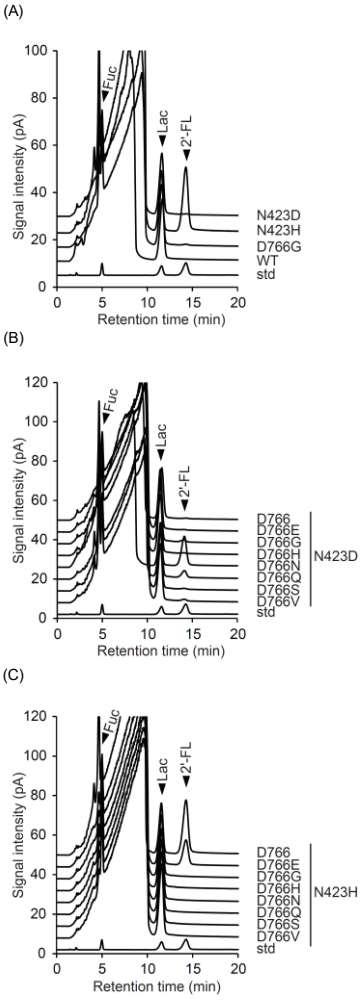

Fig. 2. Fucosynthase activity of 1,2-α-L-fucosidase variants. Amino acid replacements were introduced at the catalytic residues N421, N423, and D766 singly or in combination. The purified enzyme (4 μM) was added to the reaction mixture consisting of 100 mM sodium citrate (pH5.5), β-FucF (10 mM), and Lac (10 mM), and the mixture (50 μl) was incubated at 30°C for 30 min. The reaction products were analyzed by HPLC-CAD.
(A) The fucosynthase activity detected for N423D and N423H mutants was compared with that of D766G, the synthase isolated by Wada *et. al.* (40).
(B) The synthase activity of D766 mutants with N423D background.
(C) The synthase activity of D766 mutants with N423H background. The peaks of Fuc, Lac, and 2'-FL are indicated by arrowheads. Assays were repeated at least twice with essentially the same results, and the data for a representative experiment are shown.

The *Bb*AfcA^{N423H} mutant showed the highest activity at pH 5.5, while the *Bb*AfcA$^{N423D/D766N}$ mutant had the highest activity at pH 5.0. The synthase activity of both mutants was significantly higher than that of the D766G mutant that was obtained in previous study (40) (Fig. 3A). Regardless of the enzyme used, the synthase reaction reached a plateau within 30 min, and the proportional relationship between the product amounts (2'-FL) and the enzyme concentrations was observed only at the initial stage of the reaction (< 3 min) (Fig. 3A). This is due to the short half-life (20 min) of β-FucF in an aqueous solution at 30 ºC (22). The yield against the added β-FucF and Lac (actual yield/theoretical yield) was slightly higher for *Bb*AfcA^{N423H} (88−100 %) than that for *Bb*AfcA$^{N423D/D766N}$ (83−94 %) at any substrate concentration. The synthase reaction catalyzed by *Bb*AfcA$^{N423D/D766N}$ appeared to be more sensitive to high concentration of acceptor (Lac), compared with the one catalyzed by *Bb*AfcA^{N423H} (Fig. 3B). The yield decreased to 60 % for *Bb*AfcA$^{N423D/D766N}$, while it remained 80 % for N423H mutant in the presence of 100 mM Lac. *Bb*AfcA^{N423H} retained 90 % activity after 30 min incubation at 55 ºC, whereas *Bb*AfcA$^{N423D/D766N}$ lost activity when incubated at 40 ºC for 30 min (Fig. 4). The author therefore selected the *Bb*AfcA^{N423H} for further characterization since it was the most efficient 1,2-α-L-fucosynthase.

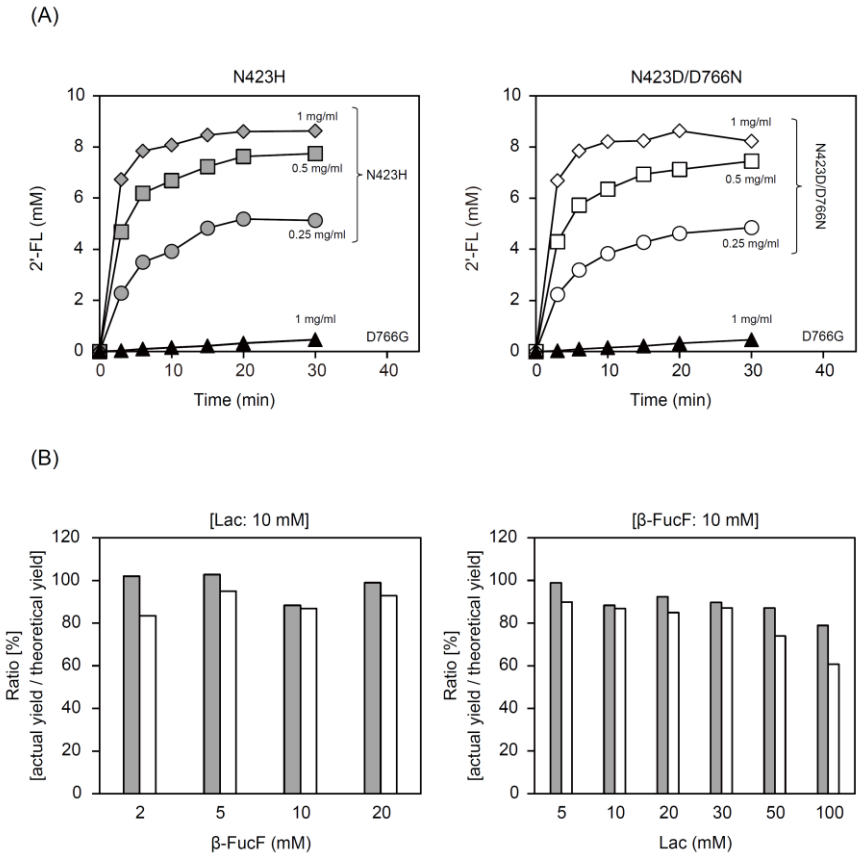

Fig. 3. Time course (A) and efficiency (B) of the fucosynthase reaction catalyzed by *Bb*AfcA^{N423H}, *Bb*AfcA$^{N423D/D766N}$, and D766G mutants.
(A) The reaction (50 μL) was carried out at 30 ºC in the presence of 10 mM β-FucF, and Lac, and the samples were taken at the indicated times. The enzyme concentrations were varied as indicated.
(B) The reaction was carried out at 30 ºC for 30 min in 100 mM sodium citrate buffer (pH 5.5 for *Bb*AfcA^{N423H} (gray bars) or pH5.0 for *Bb*AfcA$^{N423D/D766N}$ (white bars)) containing various concentrations of the substrates in the presence of 10 μM enzymes. The concentrations of β-FucF (left) and Lac (right) were varied. The reaction efficiency (%) was deduced by dividing the actual yield with the theoretical yield of the reaction. Assays were repeated at least twice with essentially the same results, and the data for a representative experiment are shown.

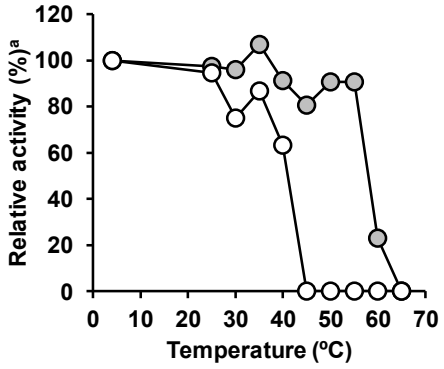

Fig. 4. Thermostability of *Bb*AfcA^{N423H} and *Bb*AfcA$^{N423D/D766N}$.
Each variant was incubated for 30 min at the indicated temperatures in 10 mM Tris-HCl buffer (pH 8.0). After the incubation, the fucosynthase reaction was performed. The reaction (25 μL) was carried out at 30 ºC in the presence of 2 μM variant, 10 mM β-FucF, and Lac for 15 min in 100 mM sodium citrate buffer (pH 5.5 for *Bb*AfcA^{N423H} [gray circles] or pH5.0 for *Bb*AfcA$^{N423D/D766N}$ [white circles]). [a] The value obtained at 4 ºC as 100 %.

Acceptor specificity of Bb*AfcA^{N423H}*

The author examined the acceptor specificity of the *Bb*AfcA^{N423H} using various mono- and oligosaccharides at 10 mM, listed in Table 2. β-FucF was used at the same concentration. The activity was assessed by determining the amounts of acceptors consumed in the reactions. Among the twelve monosaccharides, Gal was consumed most efficiently (83 %) in the reaction. A new spot and a peak appeared in the thin-layer chromatography (TLC) and high–performance anion exchange chromatography with pulsed amperometric detection (HPAEC-PAD) analysis, respectively (Fig. 5A). L-Ara, which forms a pyranose ring in water (53), also served as a good acceptor with 48 % being consumed. Glc and Xyl acted as poor substrates with 8.4 % and 7.2 % being utilized, and faint spots and small peaks were detected in the TLC and HPAEC-PAD analysis, respectively (Fig. 5B, 5C, and 5D). L-Rha was also slightly

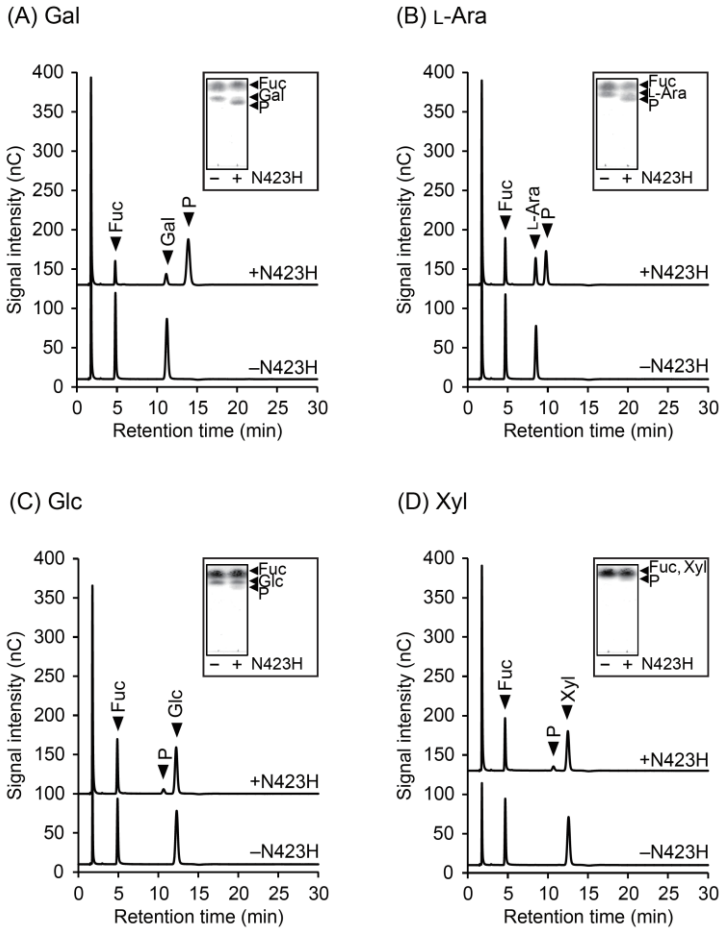

Fig. 5. Acceptor specif icity of 1,2-α-L-fucosynthase *Bb*AfcA^{N423H} towards monosaccharides.
The reactions were carried out at 30 ºC for 30 min in 100 mM sodium citrate buffer (pH5.5) containing β-FucF (10 mM), various monosaccharides (10 mM), and 10 μM enzyme. The mixtures were analyzed by TLC (inset) and HPAEC-PAD. The chromatograms o btained for (A) Gal, (B) L-Ara, (C) Glc, and (D) Xyl as acceptors are shown. The peaks of Fuc, acceptor, and product (P) are indicated by arrowheads. Assays were repeated at least twice with essentially the same results, and the data for a representative experiment are shown. See also Table 2.

consumed in the synthase reaction (Table 2). Regio-specificity of these synthase reactions is described in later sections. Neither of L-Fuc, Fru, GalN, GalNAc, GlcN, GlcNAc, nor Man was used as an acceptor (Table 2).

3-β-Galactobiose, Lac, and 6-β-galactobiose were most effectively (>85 %) fucosylated among the tested disaccharides (Table 2). Melibiose, galacto-*N*-biose (GNB), 3-β-galactosylglucose, lacto-*N*-biose I (LNB), 4-β-galactobiose, lactulose, and *N*-acetyllactosamine (LacNAc) were also effectively recognized by the enzyme as acceptors, with 45 % to 79 % substrates consumption in the reactions (Table 2, Fig. 6A, 6B and 6C). As for the di-glucosides, maltose, isomaltose, cellobiose, and gentiobiose served as poor substrates (2.6 % to 22 % being consumed), while trehalose, laminaribiose and sucrose were not utilized in the reactions. Addition of xylobiose in the reaction resulted in 33 % of its consumption, along with appearance of a new peak at the retention time of 9.5 min (Table 2, Fig. 6D). The chemical structure of the fucosylated xylobiose was determined by instrumental analyses, which is described later.

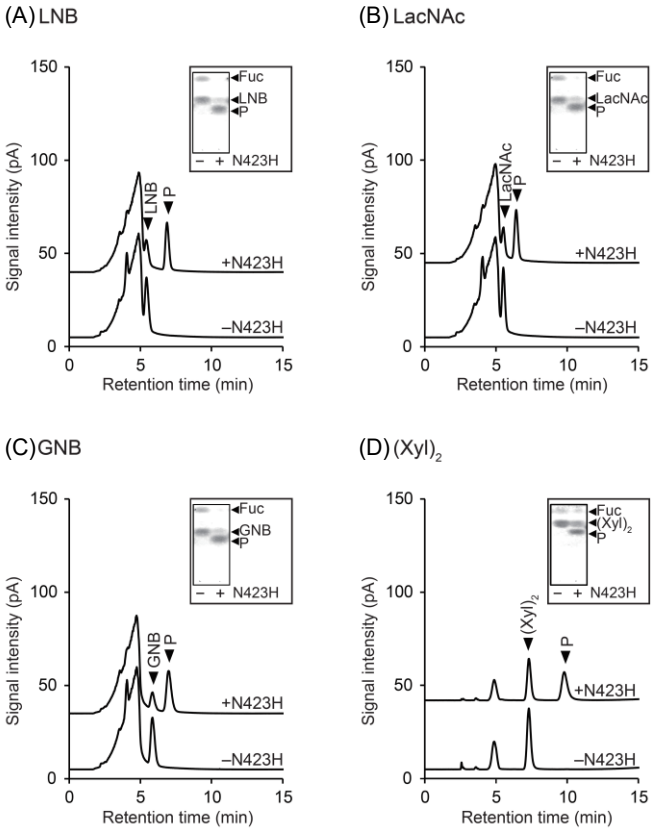

Fig. 6. Acceptor specificity of 1,2-α-L-fucosynthase *Bb*AfcA^{N423H} towards disaccharides.

The reactions were carried out as described in Figure 3 legend, except for disaccharides being included. The reaction products were analyzed by TLC (inset) and HPLC-CAD, and the chromatograms obtained for (A) LNB, (B) LacNAc, (C) GNB, and (D) xylobiose as acceptors are shown. Note that elution conditions were different between (A-C) and (D) (see *MATERIALS AND METHODS*). The peaks of acceptor and product (P) are indicated by arrowheads. Assays were repeated at least three times with essentially the same results, and the data for a representative experiment are shown. See also Table 2.

3-Fucosyllactose (3-FL) was found to be a good acceptor for the synthase reaction, as 82 % of the substrate was consumed (Table 2). A peak that shows the same retention time as that of standard lactodifucotetraose (LDFT: Fucα1-2Galβ1-4(Fucα1-3)Glc) appeared in the high-performance liquid chromatography with a charged aerosol detection (HPLC-CAD) analysis (Fig. 7A). The *Bb*AfcA^{N423H} appeared to produce Le^{b} and Le^{y} tetrasaccharides from Le^{a} and Le^{x} trisaccharides with yields of 43 % and 62 %, respectively (Table 2, Fig. 7B and 7C). A peak corresponding to LNFP I appeared when LNT was used as the acceptor (Fig. 8A). The reaction efficiency was 75 % (Table 2). Use of LN*n*T as the acceptor resulted in 59 % of the substrate consumption, and a peak with a retention time of 15 min appeared in the HPLC-CAD analysis (Table 2 and Fig. 8B). The structures of these products are described later.

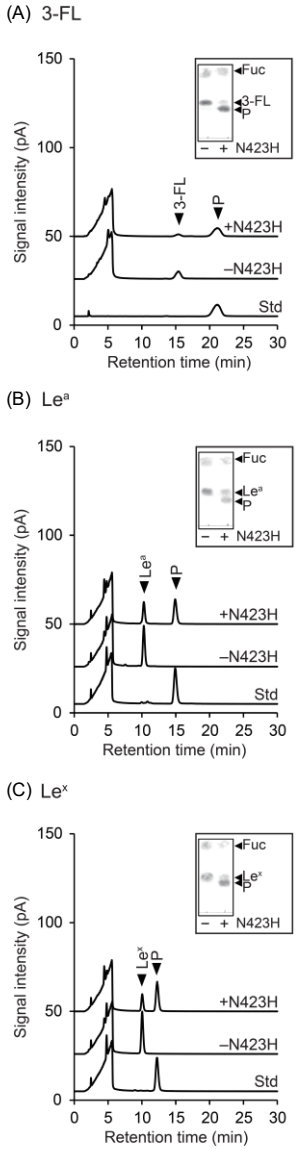

Fig. 7. Acceptor specificity of 1,2-α-L-fucosynthase *Bb*AfcA^{N423H} towards trisaccharides.

The reactions were carried out as described in Fig. 5 legend, except for trisaccharides being included. The reaction products were analyzed by TLC (inset) and HPLC-CAD, and the chromatograms obtained for (A) 3-FL (B) Le^{a}, and (C) Le^{x} as acceptors are shown. The peaks of acceptor and product (P) are indicated by arrowheads. Assays were repeated at least three times with essentially the same results, and the data for a representative experiment are shown. See also Table 2.

Standard (Std):
(A) LDFT
(B) Le^{b} tetrasaccharide
(C) Le^{y} tetrasaccharide

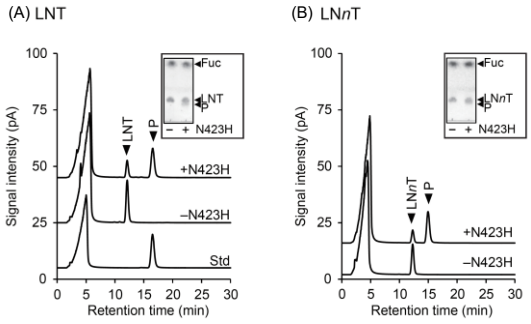

Fig. 8. Acceptor specificity of 1,2-α-L-fucosynthase *Bb*AfcA^{N423H} towards oligosaccharides.

The reactions were carried out at 30 ºC for 30 min in 100 mM sodium citrate buffer (pH5.5) containing β-FucF (10 mM), acceptors (10 mM), and 10 μM enzyme. The mixtures were analyzed by TLC (inset) and HPLC-CAD. The chromatograms obtained for (A) LNT and (B) LN*n*T as acceptors are shown. The peaks of acceptor and product (P) are indicated by arrowheads. Assays were repeated at least three times with essentially the same results, and the data for a representative experiment are shown. See also Table 2.

Table 2. Acceptor specificity of 1,2-α-L-fucosynthase *Bb*AfcA^{N423H}.

Acceptor		Product	Yield[c] (%)
Name	Structure	Deduced[a] or determined[b] structure	
Monosaccharides			
L-Arabinose		Fucα1-2Ara[a]	48
L-Fucose			0
Fructose			0
Galactose		Fucα1-2Gal[a]	83
Galactosamine			0
N-Acetylgalactosamine			0
Glucose		Fucα1-3Glc[a]	8.4
Glucosamine			0
N-Acetylglucosamine			0
Mannose			0
L-Rhamnose		Fucα1-4Rha[a]	2.3
Xylose		Fucα1-3Xyl[a]	7.2
Disaccharides			
Trehalose	Glcα1-1αGlc		0
Sucrose	Glcα1-2βFru		0
Maltose	Glcα1-4Glc	Glcα1-4(Fucα1-3)Glc[a]	2.6
Isomaltose	Glcα1-6Glc	Glcα1-6(Fucα1-3)Glc[a]	22
Laminaribiose	Glcβ1-3Glc		0
Cellobiose	Glcβ1-4Glc	Glcβ1-4(Fucα1-3)Glc[a]	5.6
Gentiobiose	Glcβ1-6Glc	Glcβ1-6(Fucα1-3)Glc[a]	22
Melibiose	Galα1-6Glc	Fucα1-2Galα1-6Glc[a]	45
3-β-Galactobiose	Galβ1-3Gal	Fucα1-2Galβ1-3Gal[a]	86
Galacto-*N*-biose	Galβ1-3GalNAc	Fucα1-2Galβ1-3GalNAc[b]	57
3-β-Galactosylglucose	Galβ1-3Glc	Fucα1-2Galβ1-3Glc[a]	79

Table 2. *Continued.*

Acceptor		Product	Yield[c] (%)
Name	Structure	Deduced[a] or determined[b] structure	
Lacto-*N*-biose I	Galβ1-3GlcNAc	Fucα1-2Galβ1-3GlcNAc[a]	68
4-β-Galactobiose	Galβ1-4Gal	Fucα1-2Galβ1-4Gal[a]	63
Lactulose	Galβ1-4Fru	Fucα1-2Galβ1-4Fru[a]	72
Lactose	Galβ1-4Glc	Fucα1-2Galβ1-4Glc[b]	86
N-Acetyllactosamine	Galβ1-4GlcNAc	Fucα1-2Galβ1-4GlcNAc[a]	67
6-β-Galactobiose	Galβ1-6Gal	Fucα1-2 Galβ1-6Gal[a]	85
Xylobiose	Xylβ1-4Xyl	Xylβ1-4(Fucα1-3)Xyl[b]	33
Tri-, and tetrasaccharides			
3-FL	Galβ1-4(Fucα1-3)Glc	Fucα1-2Galβ1-4(Fucα1-3)Glc[a]	82
Lewis a trisaccharide	Galβ1-3(Fucα1-4)GlcNAc	Fucα1-2Galβ1-3(Fucα1-4)GlcNAc[a]	43
Lewis x trisaccharide	Galβ1-4(Fucα1-3)GlcNAc	Fucα1-2Galβ1-4(Fucα1-3)GlcNAc[a]	62
LNT	Galβ1-3GlcNAcβ1-3Galβ1-4Glc	Fucα1-2Galβ1-3GlcNAcβ1-3Galβ1-4Glc[b]	75
LN*n*T	Galβ1-4GlcNAcβ1-3Galβ1-4Glc	Fucα1-2Galβ1-4GlcNAcβ1-3Galβ1-4Glc[b]	59

[a]; The linkages were deduced based on Fig. 17 and/or HPLC profile (Figs. 7 and 8).

[b]; The structures were determined by NMR and MS analysis.

[c]; Yield was deduced from the consumed amount of the acceptor.

Assays were performed in duplicate or in triplicate and the data for a representative experiment are shown.

Instrumental analyses of the synthesized oligosaccharides

To determine the acceptor specificity of the synthase reaction, the author purified the synthesized oligosaccharides by preparative HPLC from the reaction mixtures that contained GNB, xylobiose, LNT, and LN*n*T as acceptors. The purified products were then analyzed by MALDI-TOF MS (Fig. 9) and NMR (Figs. 10-13). Table 3 shows the signals in 1D and 2D NMR spectra obtained for the products synthesized from β-FucF and xylobiose. Fuc was found to be introduced at O3 position of the reducing-end Xyl residue of xylobiose to form 3-fucosylxylobiose (Xylβ1-4(Fucα1-3)Xyl). The molecular ion peak corresponding to 3-fucosylxylobiose ($[M+Na]^+$, calculated, 563.2; observed, 563.3) was detected in MALDI-TOF MS analysis after permethylation. When GNB, LNT, and LN*n*T were used as acceptors, Fuc was found to be attached with the non-reducing Gal residue via α-(1→2)-linkage to form 2'-fucosyl GNB (H type-3 and 4 chains), LNFP I (Fucα1-2Galβ1-3GlcNAcβ1-3Galβ1-4Glc, H type-1 chain), and Lacto-*N*-fucopentaose IV (LNFP IV: Fucα1-2Galβ1-4GlcNAcβ1-3Galβ1-4Glc, H type-2 chain), respectively. GalNAc residue in 2'-fucosyl GNB was present in both pyranose and furanose forms (53). Molecular ion peaks of the sodium adducts of 2'-fucosyl GNB (calculated, 692.3; observed, 692.4), LNFP I (calculated, 1100.5; observed, 1100.7), and LNFP IV (calculated, 1100.5; observed, 1100.7) were detected in MALDI-TOF MS analysis, confirming one Fuc residue being attached to each acceptor (Fig. 8). The amounts of the purified products and their recovery rates were 11.4 mg and 50 %mol for 2'-fucosyl GNB, 0.4 mg and 4 %mol for 3-fucosylxylobiose, 2.0 mg and 30 %mol for LNFP I, and 2.7 mg and 41 %mol for LNFP IV.

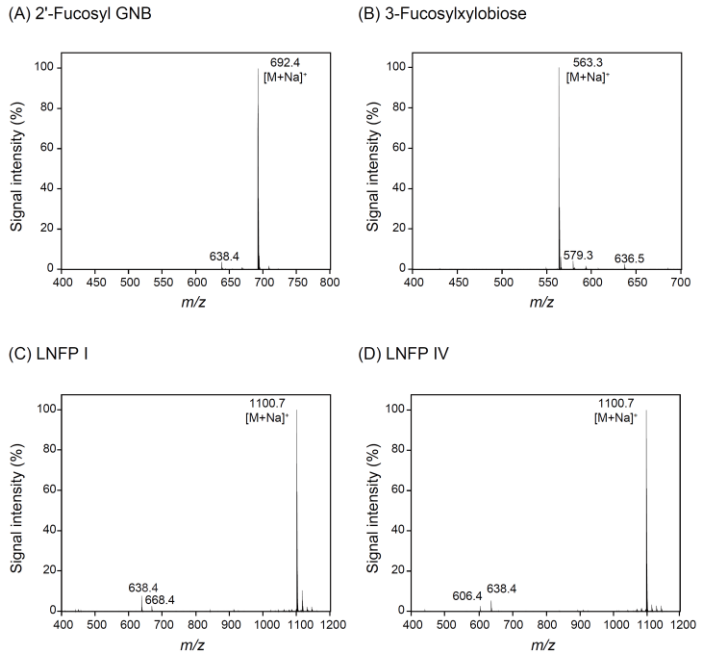

Fig. 9. MS analysis of the synthesized oligosaccharides.

The synthase reactions were carried out in the presence of (A) GNB, (B) xylobiose, (C) LNT, and (D) LN*n*T as acceptors. The products were purified as described under Material and Methods and analyzed by MALDI-TOF MS after permethylation.

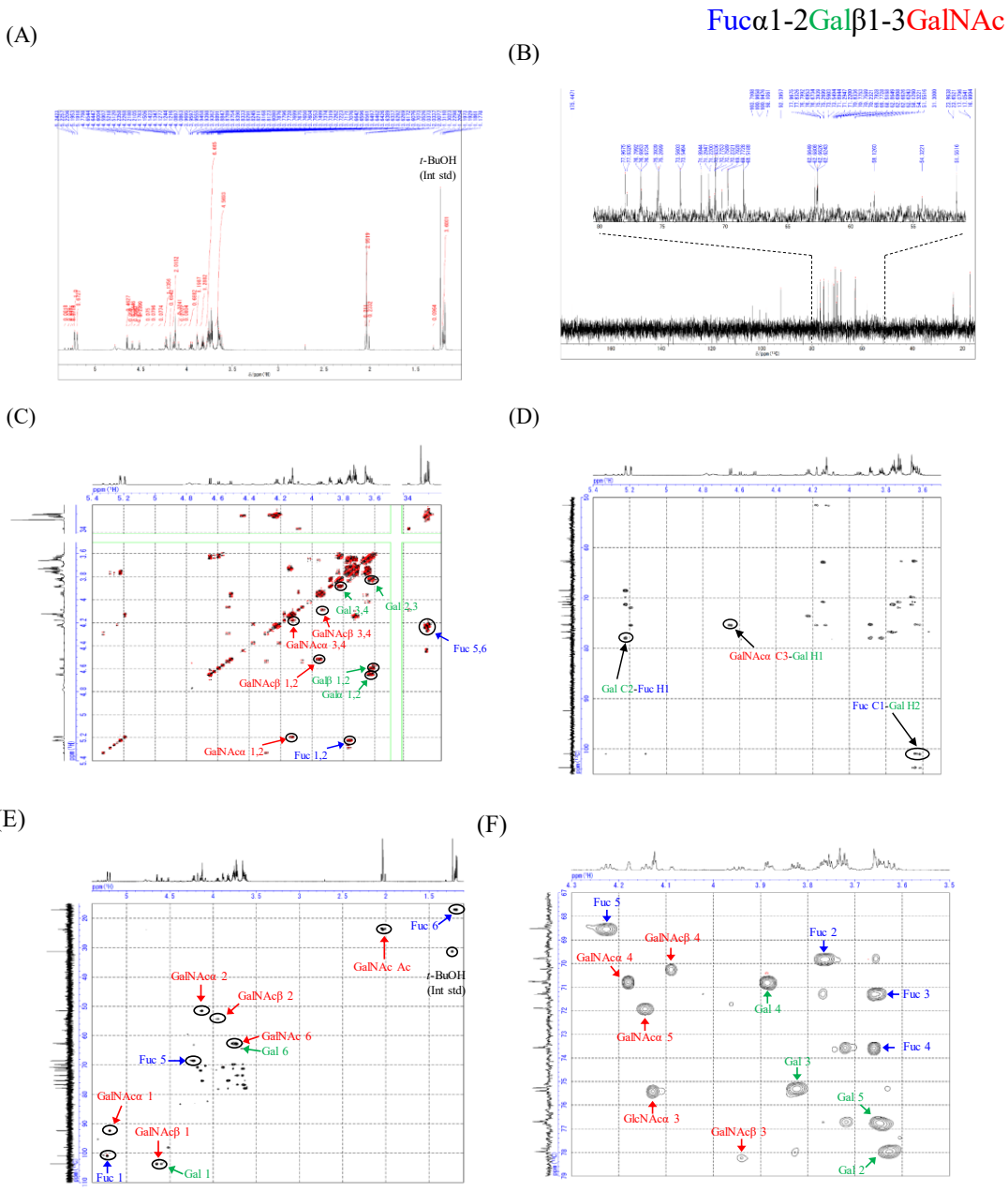

Fig. 10. NMR spectra of the purified trisaccharide product from GNB and β-FucF.

(A) ^{1}H-NMR
(B) ^{13}C-NMR
(C) DQF-COSY
(D) HMBC
(E) HSQC
(F) Enlarged HSQC

The spectra were measured in D_2O using 2-methyl-2-propanol (*t*-BuOH) as the internal standard.

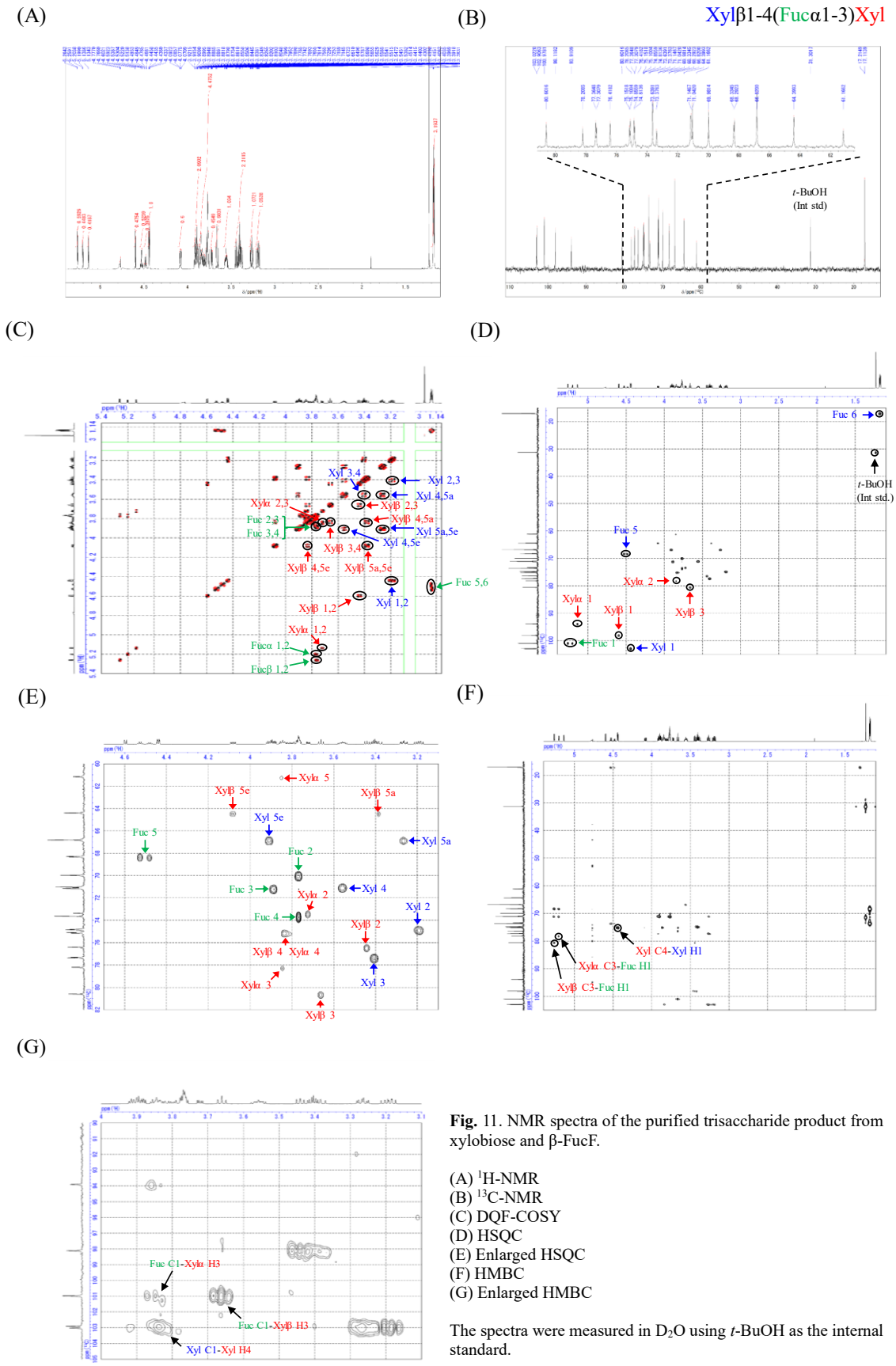

Fig. 11. NMR spectra of the purified trisaccharide product from xylobiose and β-FucF.

(A) ^{1}H-NMR
(B) ^{13}C-NMR
(C) DQF-COSY
(D) HSQC
(E) Enlarged HSQC
(F) HMBC
(G) Enlarged HMBC

The spectra were measured in D_2O using *t*-BuOH as the internal standard.

Table 3. ^{1}H- and ^{13}C-NMR data obtained for the product synthesized from β-FucF and xylobiose by *Bb*AfcA^{N423H}.

		α-anomer				β-anomer			
		^{1}H			^{13}C	^{1}H			^{13}C
Residue	Position	δ (ppm)	Pattern	*J* (Hz)	δ (ppm)	δ (ppm)	Pattern	*J* (Hz)	δ (ppm)
Xyl (reducing end)	1	5.14	d	3.4 ($J_{1,2}$)	93.9	4.60	d	7.8 ($J_{1,2}$)	98.1
	2	3.72	dd	3.4 ($J_{1,2}$), 8.6 ($J_{2,3}$)	73.4	3.44	dd	7.9 ($J_{1,2}$), 8.9 ($J_{2,3}$)	76.4
	3	3.85	m		78.2	3.66	t	9.1 ($J_{2,3}$, $J_{3,4}$)	80.6
	4	3.83	m		75.2	3.84	m		75.1
	5_{ax}	3.85	m		61.2	3.38	dd	10.5 ($J_{4,5eq}$), 11.7 ($J_{5ax,5eq}$)	64.4
	5_{eq}	3.85	m			4.08	dd	5.3 ($J_{4,5eq}$), 11.9 ($J_{5ax,5eq}$)	
Xyl (non-reducing end)	1	4.44	d	7.8 ($J_{1,2}$)	103.0	4.44	d	7.8 ($J_{1,2}$)	102.9
	2	3.20	dd	8.0 ($J_{1,2}$), 9.4 ($J_{2,3}$)	74.8	3.18	dd	8.0 ($J_{1,2}$), 9.4 ($J_{2,3}$)	74.9
	3	3.41	t	9.3 ($J_{2,3}$, $J_{3,4}$)	77.3	3.40	t	9.3 ($J_{2,3}$, $J_{3,4}$)	77.4
	4	3.56	m		71.0	3.56	m		41.0
	5_{ax}	3.27	t	11.2 ($J_{4,5ax}$, $J_{5ax,5eq}$)	66.8	3.26	t	11.2 ($J_{4,5ax}$, $J_{5ax,5eq}$)	66.8
	5_{eq}	3.91	m			3.91	m		
Fuc	1	5.20	d	3.9 ($J_{1,2}$)	101.0	5.26	d	4.0 ($J_{1,2}$)	101.0
	2	3.76	m		70.0	3.77	m		70.0
	3	3.89	m		71.1	3.89	m		71.1
	4	3.77	m		73.6	3.77	m		73.6
	5	4.48	q	6.7 ($J_{5,6}$)	68.3	4.53	q	6.6 ($J_{5,6}$)	68.3
	6	1.18	d	6.6 ($J_{5,6}$)	17.1	1.17	d	6.6 ($J_{5,6}$)	17.1

The spectra were obtained in D_2O at 298K with *t*-BuOH as an internal standard using Bruker Avance800 (for ^{1}H) and Avance500 (for ^{13}C). See also Fig. 11.

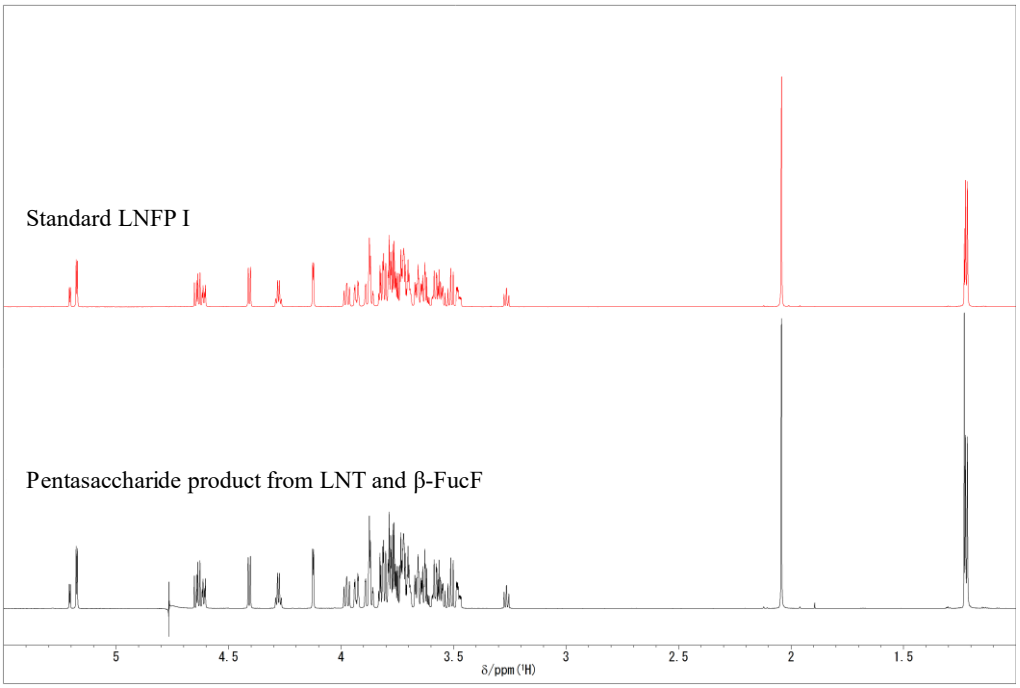

Fig. 12. ^{1}H-NMR analysis of standard LNFP I (upper panel) and the purified pentasaccharide product from LNT and β-FucF (lower panel).
The spectra was measured in D_2O using *t*-BuOH as the internal standard.

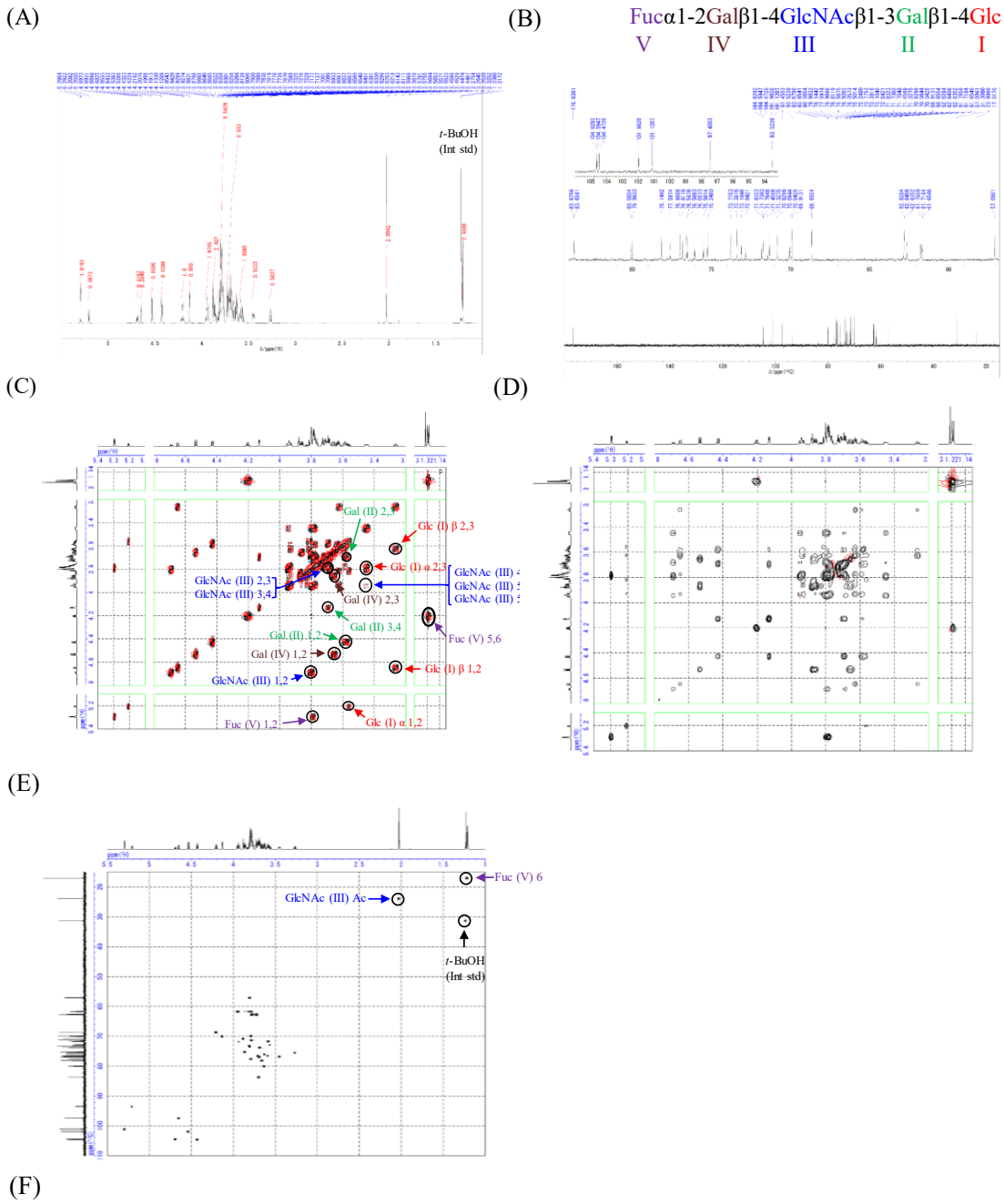

Fig. 13. NMR spectra of the purified pentasaccharide product from LN*n*T and β-FucF.
(A) ^{1}H-NMR
(B) ^{13}C-NMR
(C) DQF-COSY
(D) TOCSY
(E) HSQC
(F) HMBC
The spectra was measured in D_2O using *t*-BuOH as the internal standard.

Glycoprotein as an acceptor substrate

The author examined whether the 1,2-α-L-fucosynthase acts on glycan chains of glycoproteins. Porcine gastric mucin (PGM) was used for this purpose, as this glycoprotein is known to naturally possess H-antigen structures at the non-reducing ends of its *O*-linked glycans. Fig. 14 shows the results of lectin blotting using UEA-I and PNA for detecting H- (left) and T-antigens (right), respectively. Treatment of PGM with *Bb*AfcA^{WT} resulted in loss of signals for H-antigens (lanes 1 and 2), and unmasked T-antigen structures, which were otherwise less detectable, appeared instead (lanes 5 and 6). Incubation of defucosylated PGM with β-FucF in the presence of *Bb*AfcA^{N423H} rendered the glycoprotein UEA-I-positive (lane 3), while this did not occur in the absence of the enzyme (lane 4). The products were also stained by PNA although the signal intensity was slightly weaker than that obtained for the substrate (defucosylated PGM) and the control reaction without the enzyme (lanes 6, 7 and 8).

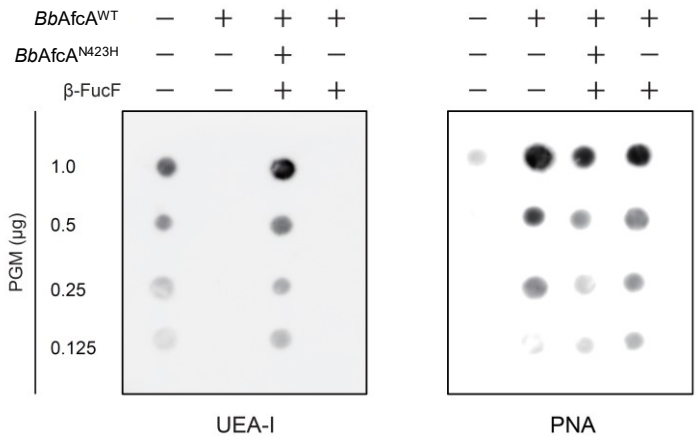

Fig. 14. 1,2-α-L-Fucosynthase activity towards glycoproteins. Porcine gastric mucin (PGM) was used for examining its availability as an acceptor substrate.

Lectin blotting of non-treated PGM (lane 1 and 5), 1,2-α-L-fucosidase WT (*Bb*AfcA^{WT})-treated PGM (lane 2 and 6), defucosylated PGM incubated with *Bb*AfcA^{N423H} and β-FucF (lane 3 and 7), and defucosylated PGM incubated with β-FucF in the absence of enzyme (lane 4 and 8). The samples were spotted on PVDF membrane in varying amounts (0.125 to 1.0 μg), and the membrane was blotted with UEA-I and PNA for detecting H- and T-antigens, respectively. The reactions and lectin-blotting were repeated twice with essentially the same results and the data for a representative experiment are shown.

O-Glycans were then released from the proteins, permethylated, and subjected to MALDI-TOF MS (Fig. 15A) and MALDI-TOF/TOF MS (Fig. 15B) analysis. Each of *O*-glycan structures was assigned, based on the diagnostic fragment ions in MS/MS spectra, two examples being shown in Fig. 15B. Relative contents of the selected peaks were expressed in terms of percentage of the total signal intensity detected for each of the samples (permethylated alditols released from PGM, *Bb*AfcA^{WT}-treated PGM, or *Bb*AfcA^{WT}/*Bb*AfcA^{N423H}-treated PGM), and compared (Fig. 16). Treatment of PGM with *Bb*AfcA^{WT} significantly decreased the relative content of the glycan chain with *m/z* of 708.4 (probably, Fucα1-2Galβ1-3GalNAc-itol), and increased the relative content of the glycan chain with *m/z* of 534.3 (Galβ1-3GalNAc-itol, white bars versus light gray bars in Fig. 16A). After the synthase

reaction, the relative content of deoxyhexose-containing glycan (*m/z* of 708.4) recovered to a level comparable with that of non-treated PGM (white bars vs. dark gray bars). Likewise, the relative contents of the glycan chains with *m/z* of 1157.7 (dHex1Hex2HexNAc2-itol) and 1331.8 (dHex2Hex2HexNAc2-itol) decreased significantly on treating PGM with *Bb*AfcA^{WT}, with a concomitant increase in the contents of deoxyhexose-free glycan with *m/z* of 983.6 (Hex2HexNAc-itol) (Fig. 16B). After the synthase reaction, the relative content of Hex2HexNAc2-itol signal (*m/z* 983.6) decreased, while the contents of deoxyhexose-containing glycans with *m/z* of 1157.7 and 1331.8 increased. The same tendency was observed between the glycan chains with *m/z* of 1228.7 (Hex2HexNAc3-itol), 1402.8 (dHex1Hex2HexNAc3-itol), and 1576.9 (dHex2Hex2HexNAc3-itol) (Fig. 16C) and between *m/z* of 2127.2 (Hex4HexNAc5-itol) and 2475.4 (dHex2Hex4HexNAc5-itol) (Figure 16E). In contrast, the content of the glycan chain with *m/z* of 1269.8, which should possess HexNAc residues at the non-reducing ends and lack dHex residue (probably GlcNAcβ1-3(GlcNAcβ1-3Galβ1-3/4GlcNAcβ1-6)GalNAc-itol) (54), was not influenced by the treatment with *Bb*AfcA^{WT} or

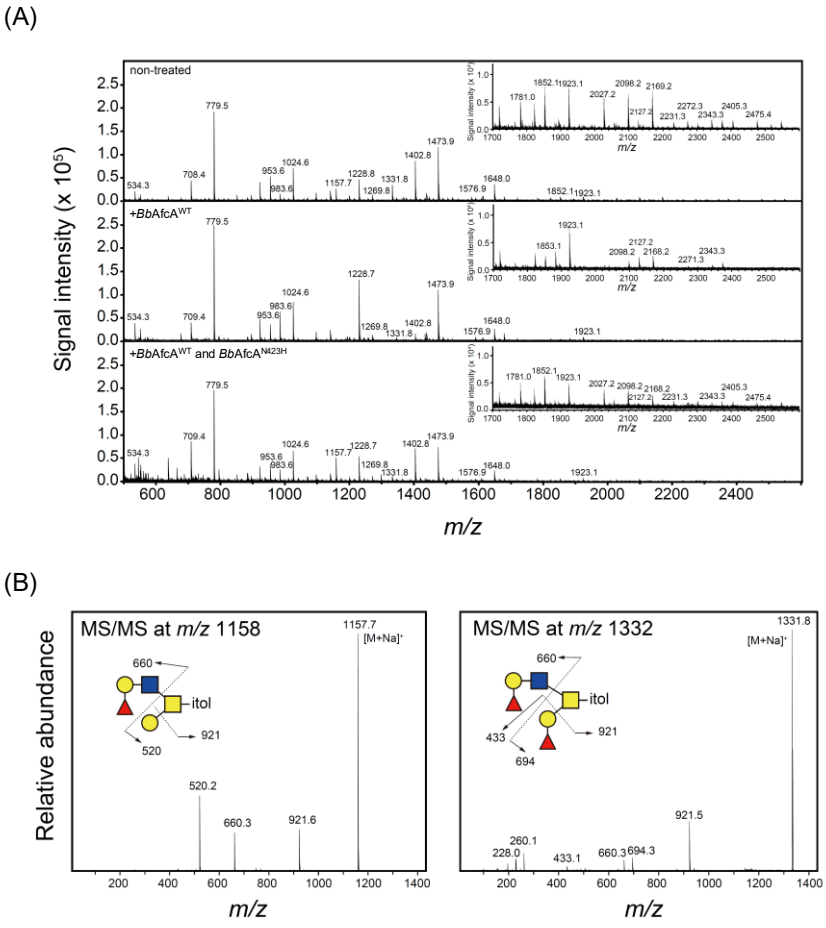

Fig. 15. 1,2-α-L-Fucosynthase activity towards glycoproteins. Porcine gastric mucin (PGM) was used for examining its availability as an acceptor substrate.

(A) MALDI-TOF MS analysis of permethylated *O*-glycan alditols. *O*-Glycans were released by reductive β-elimination from non-treated PGM (upper panel), *Bb*AfcA^{WT}-treated PGM (middle panel) or *Bb*AfcA^{WT}/ *Bb*AfcA^{N423H}-treated PGM (lower panel). Intensity of the selected peaks was compared between the samples as shown in Fig. 16.

(B) Representatives of MALDI-TOF/TOF MS spectra of MS peaks detected in the sample released from *Bb*AfcA^{WT}/*Bb*AfcA^{N423H}-treated PGM. Glycan structures of *m/z* 1158 (left panel) and *m/z* 1332 (right panel) were deduced from the patterns of diagnostic MS/MS fragment ions, and were drawn by cartoons with the symbols as follows: yellow square, GalNAc; yellow circle, Gal; blue square, GlcNAc; red triangle, L-Fuc.

*Bb*AfcA^{N423H} enzyme (Fig. 16D).

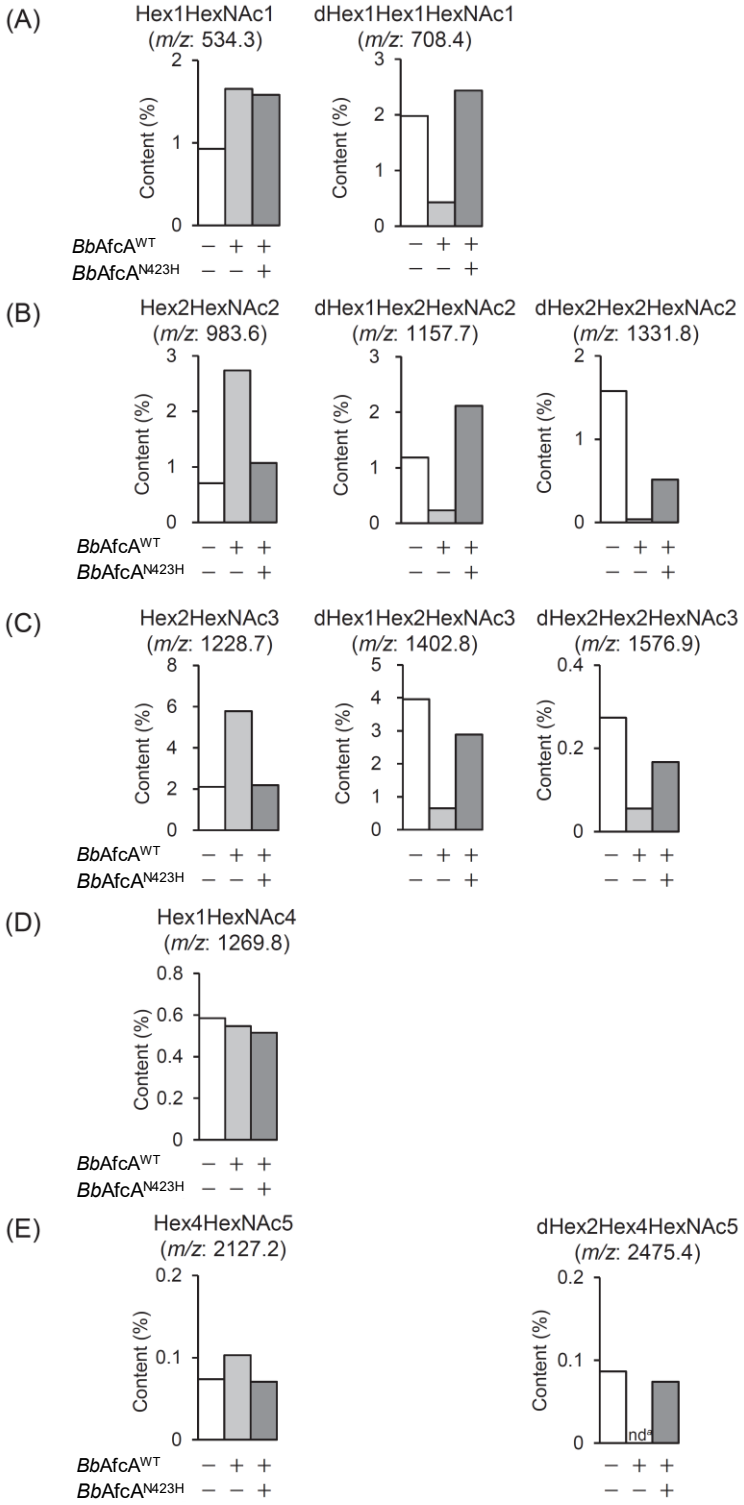

Fig. 16. Comparison of the relative contents of the selected glycans between the non-treated PGM (white bars), *Bb*AfcA^{WT}-treated PGM (light gray bars), and *Bb*AfcA^{WT}/*Bb*AfcA^{N423H}-treated (dark gray bars) PGM.

The relative contents of glycan alditols were estimated by dividing each of the signal intensity with the total signal intensity of the respective samples, and were expressed in terms of percentage (%). Sugar composition was deduced based on the precursor ion mass as a sodium adduct in MS spectra and the diagnostic fragment ions in MS/MS spectra. See also the legend of Figure 15.

[a]; not detected.

DISCUSSION

Acceptor specificity

In the previous study on AfcA D766G synthase, Wada *et al*. only used Lac as an acceptor to demonstrate its synthetic ability and regio-specificity (40). This is primarily due to the very low conversion ratio of the synthase (less than 6 % against added β-FucF), which rendered product purification laborious. In the present study, by virtue of the high catalytic efficiency of the *Bb*AfcA^{N423H}, the author succeeded in examining its acceptor specificity, i.e. (+) subsite structure, in more detail. The results revealed a unique feature of this enzyme. In addition to monosaccharide Gal and Gal-containing oligosaccharides at the non-reducing ends, the synthase recognized monosaccharides L-Ara, Glc, L-Rha, and Xyl and disaccharides maltose, isomaltose, cellobiose, gentiobiose, and xylobiose as acceptors. The ability of the synthase to recognize L-Ara was expected, because O4 of the sugar adopts an axial conformation in the $^4C_1$ pyranose form (53) (Fig. 17A and 17B). The synthesized product therefore should be Fucα1-2Ara. The lower yield than Gal could result from the lack of C6-hydroxymethyl group that otherwise participates in a stacking interaction with W500 of AfcA (44) (Fig. 1). The capability of the synthase to recognize L-Rha was also not surprising because its C2- (axial), C3- (equatorial), C4 (equatorial)-hydroxyl groups, and endocyclic oxygen overlap with C4-, C3-, C2-OHs, and endocyclic oxygen of Gal, respectively, when the $_1C^4$ ring of the sugar is inverted (Fig. 17C). It is therefore likely that the product is Fucα1-4Rha.

The finding that this synthase accepts gluco-series sugars was unexpected. The author then isolated the product synthesized from β-FucF and xylobiose, and identified it as 3-fucosylxylobiose (Xylβ1-4(Fucα1-3)Xyl). The results strongly suggest that the synthase can recognize the α-anomeric conformation of Xyl or Glc as an acceptor (Fig. 17D and 17E). The O1 (axial), O2 (equatorial), and O3 (equatorial) of the reducing-end Xyl residue of α-anomer of xylobiose structurally corresponds to O4 (axial), O3 (equatorial), and O2 (equatorial) of Gal. AfcA recognizes Gal at subsite (+1) by four hydrogen bonds with O2/O3/O4 atoms and by a stacking interaction with C6 hydroxymethyl group of the sugar, and its catalytic pocket appears to widely open towards the reducing end, although the catalytic pocket has (+2) subsite (44) (Fig. 1). Consequently, at the (+) subsite, the synthase accepted oligosaccharide carrying α-Glc at reducing end, despite the Glc being linked with an additional Glc via α/β-linkages at O4 and O6 positions to form maltose/cellobiose or isomaltose/gentiobiose (Fig. 17F-17I). Diglucosides with (1→3)-linkage such as laminaribiose did not serve as an acceptor because the O3 position of the reducing-end Glc is occupied. The synthase failed to recognize α-GalNAc and α-GlcNAc, although its C3 hydroxyl group is equatorial. Taken together, the structural requirement for acceptors by 1,2-α-L-fucosynthase was assumed to be a six-membered ring with chair conformation carrying one axial OH continued with two consecutive equatorial OHs (Fig. 17K). This finding agrees with the mode of Gal recognition by *Bb*AfcA in the crystal structure as mentioned above.

The results also provide a rationale behind the minor hydrolytic activity of *Bb*AfcA on α-(1→3)-fucosyl linkage in 3-FL (Galβ1-4(Fucα1-3)Glc) and lacto-*N*-fucopentaose V (Galβ1-3GlcNAcβ1-3Galβ1-4(Fucα1-3)Glc), but not in lacto-*N*-fucopentaose III (Galβ1-4(Fucα1-3)GlcNAcβ1-3Galβ1-4Glc) (Fig. 17J) (42). Interestingly, in Lac, the C6 hydroxymethyl group of Gal residue is present in close proximity to C3 OH of Glc residue, which should hinder the enzyme access to 3-FL. The significant difference observed in the synthase activity between cellobiose (5.6 %) and xylobiose (33 %) as acceptors may also result from this steric perturbation caused by the bulky hydroxymethyl group extended from the non-reducing end sugar.

The synthase appeared to specifically introduce Fuc residues into the non-reducing end Gal residues via α-(1→2)-linkages when GNB, LNT, and LN*n*T were used as acceptors. The product purity was estimated to be more than 95 %, from NMR spectroscopy. The author did not determine the chemical structures of the other products synthesized from Gal-containing sugars, but they could have terminal H-antigen structures. Some of the products eluted at the same retention times as those of the expected authentic compounds in HPLC analysis (e.g. LDFT and $Le^{b/y}$) (Fig. 7). The synthase reaction thus essentially occurred only at the non-reducing end Gal even though the saccharides used bear Glc or Gal residue at the reducing-end, which also fulfills the structural requirement for this synthase as shown in Fig. 17K. No peaks indicating the presence of by-products were detected in the HPLC profile for the reaction mixtures containing melibiose, 3-β-galactobiose, 3-β-galactosylglucose, 4-β-galactobiose, and 6-β-galactobiose as acceptors (data not shown).

The ability of the synthase to introduce Fucα1-2Gal linkages into intact glycoprotein is also worth mentioning. The abundance of H-antigen structures on the sugar chains was apparently comparable between non-treated PGM and *Bb*AfcA^{WT}/*Bb*AfcA^{N423H}-treated (defucosylated, then fucosylated) PGM, as revealed by MS analysis and lectin blotting using UEA-I (Figs. 14 and 15). Detection of T-antigen by PNA for the *Bb*AfcA^{WT}/*Bb*AfcA^{N423H}-treated PGM, but not for untreated PGM, probably resulted from denaturation of the glycoprotein by repeated boiling during sample preparation in the presence of a reducing agent (dithiothreitol). The lectin thus might become accessible to sugar chains more easily in the case of *Bb*AfcA^{WT}/*Bb*AfcA^{N423H}-treated PGM. The efficient action of the synthase on PGM, a large-sized and densely glycosylated protein, strongly suggests its use as a powerful tool to introduce H-antigen into apparently all glycoconjugates, including glycolipids and possibly sugar chains of intact cell surfaces.

Generation of glycosynthase from inverting enzymes

In 1979, Hehre *et al*. found that inverting β-amylase hydrolyzes β-maltosyl fluoride into β-maltose and hydrogen fluoride in two steps; transfer of maltose from β-maltosyl fluoride to a second molecule to yield β-maltotetraosyl fluoride and hydrogen fluoride, then rapid hydrolysis to form β-maltose and β-maltosyl fluoride (34). The reaction, later named Hehre-resynthesis hydrolysis, is a

prerequisite to convert inverting GHs into glycosynthases (37,40). Accordingly, efficient synthase mutants would be obtained if the introduced amino acid replacement decreases hydrolytic activity while retaining fluorine ion-releasing activity from donor substrates (37,55). In the case of typical inverting GHs that utilize a pair of carboxylic residues as acid and base catalysts and a non-acidic residue as an attacking water-holder, such conversion can occur simply by replacing the water holder with a neutral residue while a base residue remains intact. Examples include GH8 reducing-end xylose-releasing exo-oligoxylanase (37) and GH19 chitinase (56). However, several inverting GHs adopt non-canonical reaction mechanisms (38,57), which lack a generalized strategy to convert them to glycosynthases (37,40). 1,2-α-L-Fucosidase used in this study adopts a unique reaction mechanism as mentioned (Fig. 1). Among the fifty-one *Bb*AfcA mutants examined, two mutants *Bb*AfcA^{N423H} and *Bb*AfcA$^{N423D/D766N}$, both containing a base replacement, showed high synthase activity, while the water holder mutants (N421 mutants) showed no activity. Loss of hydrolytic activity of these mutants was expected, but the retention of fluorine-releasing activity by the two mutants (*Bb*AfcA^{N423H} and *Bb*AfcA$^{N423D/D766N}$) is unclear. Protonated imidazole or protonated carboxylic acid at residue 423 might be important during the catalytic cycle. Amino acid replacement at residue 421 might cause dislocation of the side-chain of E566 due to the loss of a hydrogen-bond between them. Creation of efficient glycosynthases from inverting GHs with atypical reaction mechanisms thus likely requires an empirical approach.

Due to the instability of β-FucF in water at 30 ºC, the author did not determine the kinetic parameters of the 1,2-α-L-fucosynthase reaction. However, assuming that the reaction catalyzed by *Bb*AfcA^{N423H} proceeded linearly during the first three minutes (Fig. 3A), the specific activity of the mutant for H-antigen synthesis is estimated to be 5 s^{-1}. This value is considerably higher than those of α-1,2-fucosyltransferases (1−20 min^{-1}) and thus exceeds the H-antigen introducing activity of currently available enzymes (28,30). Periodic feeding of β-FucF or conducting the reaction at a low temperature (< 4 ºC) is necessary to scale up the synthesis of the H-antigen-containing glycans by 1,2-α-L-fucosynthase.

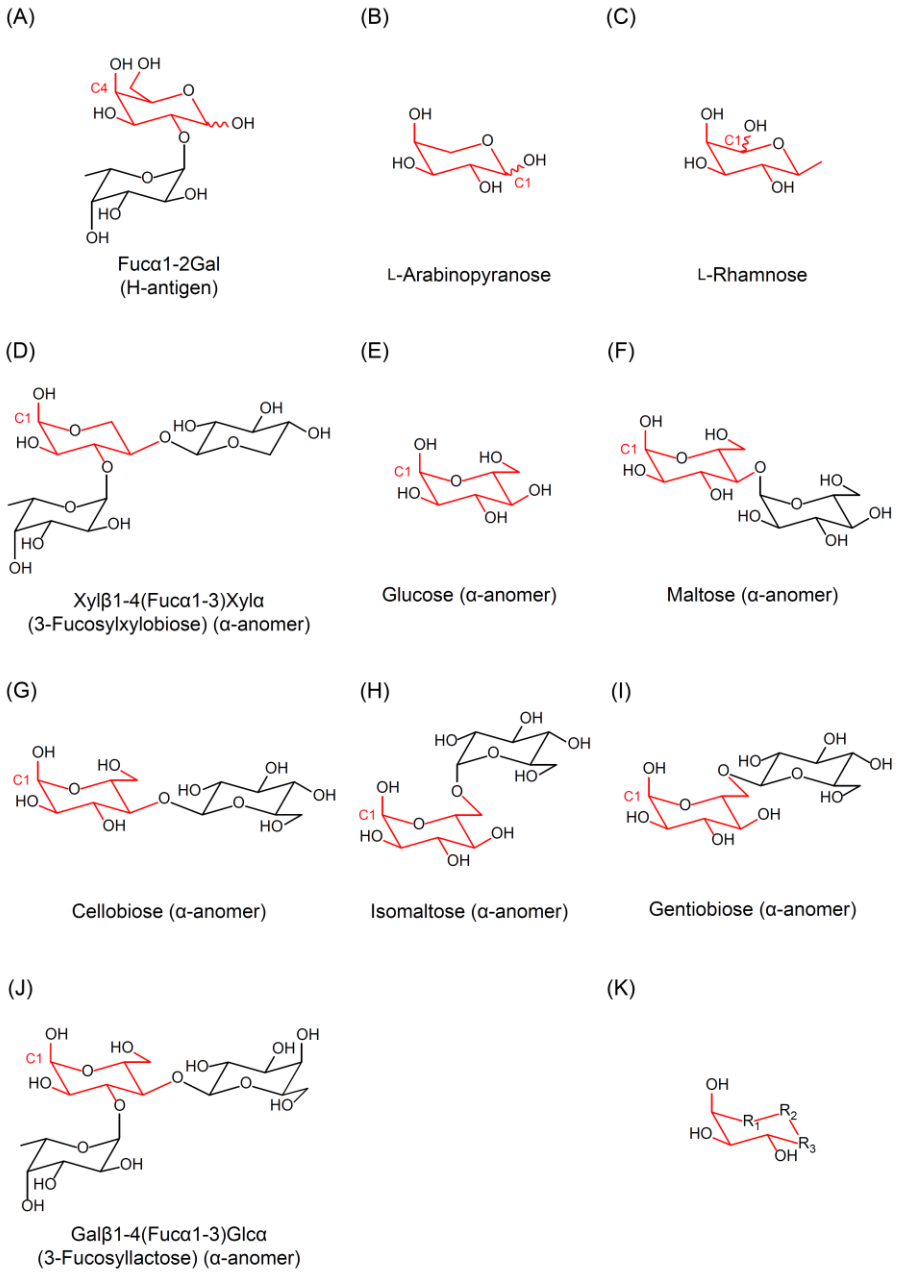

Fig. 17. Structural representation demonstrating substrate specificity of 1,2-α-L-fucosidase/fucosynthase reaction.

Structures of (A) H-antigen, (B) L-arabinopyranose, (C) L-rhamnose, (D) α-anomer of 3-fucosylxylobiose, (E) α-anomer of glucose, (F) α-anomer of maltose, (G) α-anomer of cellobiose, (H) α-anomer of isomaltose, (I) α-anomer of gentiobiose, and (J) α-anomer of 3-fucosyllactose are shown. (K) Structural requirement for acceptor molecules of the 1,2-α-L-fucosynthase reaction

REFERENCES

1. Hakomori, S. (1999) Antigen structure and genetic basis of histo-blood groups A, B and O: their changes associated with human cancer. *Biochim Biophys Acta* **1473**, 247-266
2. Heimburg-Molinaro, J., Lum, M., Vijay, G., Jain, M., Almogren, A., and Rittenhouse-Olson, K. (2011) Cancer vaccines and carbohydrate epitopes. *Vaccine* **29**, 8802-8826
3. Tateno, H., Matsushima, A., Hiemori, K., Onuma, Y., Ito, Y., Hasehira, K., Nishimura, K., Ohtaka, M., Takayasu, S., Nakanishi, M., Ikehara, Y., Ohnuma, K., Chan, T., Toyoda, M., Akutsu, H., Umezawa, A., Asashima, M., and Hirabayashi, J. (2013) Podocalyxin is a glycoprotein ligand of the human pluripotent stem cell-specific probe rBC2LCN. *Stem Cells Transl Med* **2**, 265-273
4. Mollicone, R., Candelier, J. J., Reguigne, I., Couillin, P., Fletcher, A., and Oriol, R. (1994) Molecular genetics of alpha-L-fucosyltransferase genes (H, Se, Le, FUT4, FUT5 and FUT6). *Transfus Clin Biol* **1**, 91-97
5. Rouquier, S., Lowe, J. B., Kelly, R. J., Fertitta, A. L., Lennon, G. G., and Giorgi, D. (1995) Molecular cloning of a human genomic region containing the H blood group alpha(1,2)fucosyltransferase gene and two H locus-related DNA restriction fragments. Isolation of a candidate for the human Secretor blood group locus. *J Biol Chem* **270**, 4632-4639
6. Su, A. I., Wiltshire, T., Batalov, S., Lapp, H., Ching, K. A., Block, D., Zhang, J., Soden, R., Hayakawa, M., Kreiman, G., Cooke, M. P., Walker, J. R., and Hogenesch, J. B. (2004) A gene atlas of the mouse and human protein-encoding transcriptomes. *Proc Natl Acad Sci U S A* **101**, 6062-6067
7. Bry, L., Falk, P. G., Midtvedt, T., and Gordon, J. I. (1996) A model of host-microbial interactions in an open mammalian ecosystem. *Science* **273**, 1380-1383
8. Goto, Y., Obata, T., Kunisawa, J., Sato, S., Ivanov, I. I., Lamichhane, A., Takeyama, N., Kamioka, M., Sakamoto, M., Matsuki, T., Setoyama, H., Imaoka, A., Uematsu, S., Akira, S., Domino, S. E., Kulig, P., Becher, B., Renauld, J. C., Sasakawa, C., Umesaki, Y., Benno, Y., and Kiyono, H. (2014) Innate lymphoid cells regulate intestinal epithelial cell glycosylation. *Science* **345**, 1254009
9. Pickard, J. M., Maurice, C. F., Kinnebrew, M. A., Abt, M. C., Schenten, D., Golovkina, T. V., Bogatyrev, S. R., Ismagilov, R. F., Pamer, E. G., Turnbaugh, P. J., and Chervonsky, A. V. (2014) Rapid fucosylation of intestinal epithelium sustains host-commensal symbiosis in sickness. *Nature* **514**, 638-641
10. Pacheco, A. R., Curtis, M. M., Ritchie, J. M., Munera, D., Waldor, M. K., Moreira, C. G., and Sperandio, V. (2012) Fucose sensing regulates bacterial intestinal colonization. *Nature*

492, 113-117

11. Pham, T. A., Clare, S., Goulding, D., Arasteh, J. M., Stares, M. D., Browne, H. P., Keane, J. A., Page, A. J., Kumasaka, N., Kane, L., Mottram, L., Harcourt, K., Hale, C., Arends, M. J., Gaffney, D. J., Dougan, G., Lawley, T. D., and Project, S. M. G. (2014) Epithelial IL-22RA1-mediated fucosylation promotes intestinal colonization resistance to an opportunistic pathogen. *Cell Host Microbe* **16**, 504-516
12. McGovern, D. P., Jones, M. R., Taylor, K. D., Marciante, K., Yan, X., Dubinsky, M., Ippoliti, A., Vasiliauskas, E., Berel, D., Derkowski, C., Dutridge, D., Fleshner, P., Shih, D. Q., Melmed, G., Mengesha, E., King, L., Pressman, S., Haritunians, T., Guo, X., Targan, S. R., Rotter, J. I., and Consortium, I. I. G. (2010) Fucosyltransferase 2 (FUT2) non-secretor status is associated with Crohn's disease. *Hum Mol Genet* **19**, 3468-3476
13. Smyth, D. J., Cooper, J. D., Howson, J. M., Clarke, P., Downes, K., Mistry, T., Stevens, H., Walker, N. M., and Todd, J. A. (2011) FUT2 nonsecretor status links type 1 diabetes susceptibility and resistance to infection. *Diabetes* **60**, 3081-3084
14. Kobata, A. (2010) Structures and application of oligosaccharides in human milk. *Proc Jpn Acad Ser B Phys Biol Sci* **86**, 731-747
15. Kunz, C., Rudloff, S., Baier, W., Klein, N., and Strobel, S. (2000) Oligosaccharides in human milk: structural, functional, and metabolic aspects. *Annu Rev Nutr* **20**, 699-722
16. Urashima, T., Asakuma, S., Leo, F., Fukuda, K., Messer, M., and Oftedal, O. T. (2012) The predominance of type I oligosaccharides is a feature specific to human breast milk. *Adv Nutr* **3**, 473S-482S
17. Brand-Miller, J. C., McVeagh, P., McNeil, Y., and Messer, M. (1998) Digestion of human milk oligosaccharides by healthy infants evaluated by the lactulose hydrogen breath test. *J Pediatr* **133**, 95-98
18. Asakuma, S., Hatakeyama, E., Urashima, T., Yoshida, E., Katayama, T., Yamamoto, K., Kumagai, H., Ashida, H., Hirose, J., and Kitaoka, M. (2011) Physiology of consumption of human milk oligosaccharides by infant gut-associated bifidobacteria. *J Biol Chem* **286**, 34583-34592
19. Katayama, T. (2016) Host-derived glycans serve as selected nutrients for the gut microbe: human milk oligosaccharides and bifidobacteria. *Biosci Biotechnol Biochem* **80**, 621-632
20. Kitaoka, M., Tian, J., and Nishimoto, M. (2005) Novel putative galactose operon involving lacto-*N*-biose phosphorylase in *Bifidobacterium longum*. *Appl Environ Microbiol* **71**, 3158-3162
21. Lewis, Z. T., Totten, S. M., Smilowitz, J. T., Popovic, M., Parker, E., Lemay, D. G., Van Tassell, M. L., Miller, M. J., Jin, Y. S., German, J. B., Lebrilla, C. B., and Mills, D. A. (2015) Maternal fucosyltransferase 2 status affects the gut bifidobacterial communities of

breastfed infants. *Microbiome* **3**, 13

22. Sakurama, H., Fushinobu, S., Hidaka, M., Yoshida, E., Honda, Y., Ashida, H., Kitaoka, M., Kumagai, H., Yamamoto, K., and Katayama, T. (2012) 1,3-1,4-α-L-fucosynthase that specifically introduces Lewis a/x antigens into type-1/2 chains. *J Biol Chem* **287**, 16709-16719
23. Sakurama, H., Kiyohara, M., Wada, J., Honda, Y., Yamaguchi, M., Fukiya, S., Yokota, A., Ashida, H., Kumagai, H., Kitaoka, M., Yamamoto, K., and Katayama, T. (2013) Lacto-*N*-biosidase encoded by a novel gene of *Bifidobacterium longum* subspecies *longum* shows unique substrate specificity and requires a designated chaperone for its active expression. *J Biol Chem* **288**, 25194-25206
24. Sela, D. A., Chapman, J., Adeuya, A., Kim, J. H., Chen, F., Whitehead, T. R., Lapidus, A., Rokhsar, D. S., Lebrilla, C. B., German, J. B., Price, N. P., Richardson, P. M., and Mills, D. A. (2008) The genome sequence of *Bifidobacterium longum* subsp. *infantis* reveals adaptations for milk utilization within the infant microbiome. *Proc Natl Acad Sci U S A* **105**, 18964-18969
25. Wada, J., Ando, T., Kiyohara, M., Ashida, H., Kitaoka, M., Yamaguchi, M., Kumagai, H., Katayama, T., and Yamamoto, K. (2008) *Bifidobacterium bifidum* lacto-*N*-biosidase, a critical enzyme for the degradation of human milk oligosaccharides with a type 1 structure. *Appl Environ Microbiol* **74**, 3996-4004
26. Ruiz-Palacios, G. M., Cervantes, L. E., Ramos, P., Chavez-Munguia, B., and Newburg, D. S. (2003) *Campylobacter jejuni* binds intestinal H(O) antigen (Fuc alpha 1, 2Gal beta 1, 4GlcNAc), and fucosyloligosaccharides of human milk inhibit its binding and infection. *J Biol Chem* **278**, 14112-14120
27. He, Y., Liu, S., Kling, D. E., Leone, S., Lawlor, N. T., Huang, Y., Feinberg, S. B., Hill, D. R., and Newburg, D. S. (2016) The human milk oligosaccharide 2'-fucosyllactose modulates CD14 expression in human enterocytes, thereby attenuating LPS-induced inflammation. *Gut* **65**, 33-46
28. Drouillard, S., Driguez, H., and Samain, E. (2006) Large-scale synthesis of H-antigen oligosaccharides by expressing *Helicobacter pylori* alpha1,2-fucosyltransferase in metabolically engineered *Escherichia coli* cells. *Angew Chem Int Ed Engl* **45**, 1778-1780
29. Baumgärtner, F., Seitz, L., Sprenger, G. A., and Albermann, C. (2013) Construction of *Escherichia coli* strains with chromosomally integrated expression cassettes for the synthesis of 2'-fucosyllactose. *Microb Cell Fact* **12**, 40
30. Zhao, C., Wu, Y., Yu, H., Shah, I. M., Li, Y., Zeng, J., Liu, B., Mills, D. A., and Chen, X. (2016) The one-pot multienzyme (OPME) synthesis of human blood group H antigens and a human milk oligosaccharide (HMOS) with highly active *Thermosynechococcus elongates*

α1-2-fucosyltransferase. *Chem Commun (Camb)* **52**, 3899-3902

31. Vasiliu, D., Razi, N., Zhang, Y., Jacobsen, N., Allin, K., Liu, X., Hoffmann, J., Bohorov, O., and Blixt, O. (2006) Large-scale chemoenzymatic synthesis of blood group and tumor-associated poly-*N*-acetyllactosamine antigens. *Carbohydr Res* **341**, 1447-1457
32. Osanjo, G., Dion, M., Drone, J., Solleux, C., Tran, V., Rabiller, C., and Tellier, C. (2007) Directed evolution of the alpha-L-fucosidase from *Thermotoga maritima* into an alpha-L-transfucosidase. *Biochemistry* **46**, 1022-1033
33. Shaikh, F. A., and Withers, S. G. (2008) Teaching old enzymes new tricks: engineering and evolution of glycosidases and glycosyl transferases for improved glycoside synthesis. *Biochem Cell Biol* **86**, 169-177
34. Hehre, E. J., Brewer, C. F., and Genghof, D. S. (1979) Scope and mechanism of carbohydrase action. Hydrolytic and nonhydrolytic actions of beta-amylase on alpha- and beta-maltosyl fluoride. *J Biol Chem* **254**, 5942-5950
35. Malet, C., and Planas, A. (1998) From beta-glucanase to beta-glucansynthase: glycosyl transfer to alpha-glycosyl fluorides catalyzed by a mutant endoglucanase lacking its catalytic nucleophile. *FEBS Lett* **440**, 208-212
36. Mackenzie, L. F., Wang, Q., J., R. A., Warren, and Withers, S. G. (1998) Glycosynthases: Mutant Glycosidases for Oligosaccharide Synthesis. *J. Am. Chem. Soc.* **120**, 5583-5584
37. Honda, Y., and Kitaoka, M. (2006) The first glycosynthase derived from an inverting glycoside hydrolase. *J Biol Chem* **281**, 1426-1431
38. Honda, Y., Arai, S., Suzuki, K., Kitaoka, M., and Fushinobu, S. (2016) The crystal structure of an inverting glycoside hydrolase family 9 exo-β-D-glucosaminidase and the design of glycosynthase. *Biochem J* **473**, 463-472
39. Ohnuma, T., Dozen, S., Honda, Y., Kitaoka, M., and Fukamizo, T. (2016) A glycosynthase derived from an inverting chitinase with an extended binding cleft. *J Biochem* **160**, 93-100
40. Wada, J., Honda, Y., Nagae, M., Kato, R., Wakatsuki, S., Katayama, T., Taniguchi, H., Kumagai, H., Kitaoka, M., and Yamamoto, K. (2008) 1,2-alpha-l-Fucosynthase: a glycosynthase derived from an inverting alpha-glycosidase with an unusual reaction mechanism. *FEBS Lett* **582**, 3739-3743
41. Gotoh, A., Katoh, T., Sugiyama, Y., Kurihara, S., Honda, Y., Sakurama, H., Kambe, T., Ashida, H., Kitaoka, M., Yamamoto, K., and Katayama, T. (2015) Novel substrate specificities of two lacto-*N*-biosidases towards β-linked galacto-*N*-biose-containing oligosaccharides of globo H, Gb5, and GA1. *Carbohydr Res* **408**, 18-24
42. Katayama, T., Sakuma, A., Kimura, T., Makimura, Y., Hiratake, J., Sakata, K., Yamanoi, T., Kumagai, H., and Yamamoto, K. (2004) Molecular cloning and characterization of *Bifidobacterium bifidum* 1,2-alpha-L-fucosidase (AfcA), a novel inverting glycosidase

(glycoside hydrolase family 95). *J Bacteriol* **186**, 4885-4893

43. Liu, J., Zheng, M., Zhang, C., and Xu, D. (2013) "Amide resonance" in the catalysis of 1,2-α-L-fucosidase from *Bifidobacterium bifidum*. *J Phys Chem B* **117**, 10080-10092
44. Nagae, M., Tsuchiya, A., Katayama, T., Yamamoto, K., Wakatsuki, S., and Kato, R. (2007) Structural basis of the catalytic reaction mechanism of novel 1,2-alpha-L-fucosidase from *Bifidobacterium bifidum*. *J Biol Chem* **282**, 18497-18509
45. Nakajima, M., Nishimoto, M., and Kitaoka, M. (2010) Practical preparation of D-galactosyl-beta1→4-L-rhamnose employing the combined action of phosphorylases. *Biosci Biotechnol Biochem* **74**, 1652-1655
46. Nishimoto, M., and Kitaoka, M. (2007) Practical preparation of lacto-*N*-biose I, a candidate for the bifidus factor in human milk. *Biosci Biotechnol Biochem* **71**, 2101-2104
47. Nishimoto, M., and Kitaoka, M. (2009) One-pot enzymatic production of beta-D-galactopyranosyl-(1→3)-2-acetamido-2-deoxy-D-galactose (galacto-*N*-biose) from sucrose and 2-acetamido-2-deoxy-D-galactose (*N*-acetylgalactosamine). *Carbohydr Res* **344**, 2573-2576
48. Ashida, H., Miyake, A., Kiyohara, M., Wada, J., Yoshida, E., Kumagai, H., Katayama, T., and Yamamoto, K. (2009) Two distinct alpha-L-fucosidases from *Bifidobacterium bifidum* are essential for the utilization of fucosylated milk oligosaccharides and glycoconjugates. *Glycobiology* **19**, 1010-1017
49. Anderson, K., Li, S. C., and Li, Y. T. (2000) Diphenylamine-aniline-phosphoric acid reagent, a versatile spray reagent for revealing glycoconjugates on thin-layer chromatography plates. *Anal Biochem* **287**, 337-339
50. Aoki, K., Porterfield, M., Lee, S. S., Dong, B., Nguyen, K., McGlamry, K. H., and Tiemeyer, M. (2008) The diversity of *O*-linked glycans expressed during *Drosophila melanogaster* development reflects stage- and tissue-specific requirements for cell signaling. *J Biol Chem* **283**, 30385-30400
51. Anumula, K. R., and Taylor, P. B. (1992) A comprehensive procedure for preparation of partially methylated alditol acetates from glycoprotein carbohydrates. *Anal Biochem* **203**, 101-108
52. Ceroni, A., Maass, K., Geyer, H., Geyer, R., Dell, A., and Haslam, S. M. (2008) GlycoWorkbench: a tool for the computer-assisted annotation of mass spectra of glycans. *J Proteome Res* **7**, 1650-1659
53. Angyal, S., and Pickles, V. (1972) Equilibria between pyranoses and furanoses. II. Aldoses. *Aust J Chem* **25**, 1695-1710
54. Karlsson, N. G., Herrmann, A., Karlsson, H., Johansson, M. E., Carlstedt, I., and Hansson, G. C. (1997) The glycosylation of rat intestinal Muc2 mucin varies between rat strains and

the small and large intestine. A study of *O*-linked oligosaccharides by a mass spectrometric approach. *J Biol Chem* **272**, 27025-27034

55. Hidaka, M., Fushinobu, S., Honda, Y., Wakagi, T., Shoun, H., and Kitaoka, M. (2010) Structural explanation for the acquisition of glycosynthase activity. *J Biochem* **147**, 237-244
56. Ohnuma, T., Fukuda, T., Dozen, S., Honda, Y., Kitaoka, M., and Fukamizo, T. (2012) A glycosynthase derived from an inverting GH19 chitinase from the moss *Bryum coronatum*. *Biochem J* **444**, 437-443
57. Helland, R., Larsen, R. L., Finstad, S., Kyomuhendo, P., and Larsen, A. N. (2009) Crystal structures of g-type lysozyme from Atlantic cod shed new light on substrate binding and the catalytic mechanism. *Cell Mol Life Sci* **66**, 2585-2598

SUMMARY

Fucα1-2Gal linkages, or H-antigens, constitute histo-blood group antigens and are involved in various physiological processes. In addition, recent studies have shown that the H-antigen-containing glycans play an important role, not only in establishing harmonious relationship between gut microbes and the host, but also in preventing gut dysbiosis-related diseases. Therefore, development of an efficient method for introducing Fuc residue at Gal residue at the non-reducing end of glycans via α-(1→2) linkage is desired for research as well as medicinal purposes. In this study, the author succeeded in derivatizing inverting 1,2-α-L-fucosidase (*Bb*AfcA) into a highly functional 1,2-α-L-fucosynthase (*Bb*AfcA^{N423H}). The synthase specifically synthesized H type 1-, type 2-, type 3- and type 4-chain containing oligosaccharides with yields of 57–75 % based on acceptor depletion. The synthase was also able to specifically introduce Fuc residues into Lewis a/x antigens to produce Lewis b/y antigens, with yields of 43 % and 62 %, respectively. In addition, the enzyme efficiently introduced H-antigens into sugar chains of porcine gastric mucins, as revealed by lectin blotting and mass spectroscopy analysis of the sugars. Detailed acceptor specificity analysis using various mono- and oligosaccharides unraveled unique substrate recognition feature of this synthase at the subsite (+1), which can be explained by previous x-ray crystallographic study of *Bb*AfcA by Nagae *et al.* (*J Biol Chem* **282**, 18497-18509). These results show that the synthase developed in this study could serve as an alternative to other H-antigen synthesis methods involving α-1,2-fucosyltransferases and retaining α-fucosidase.

SECTION II

Introduction of H-antigen structures on various glycoconjugates using highly functional 1,2-α-L-fucosynthase

H-antigens have been known as key structures in providing beneficial effects, such as prevention of pathogenic infection and for the establishment of symbiosis between host and gut microbiota as prebiotics (1-5). For instance, mothers supply babies with 2'-fucosyllactose (2'-FL) as well as other fucosylated human milk oligosaccharides (HMOs) in their breast milk (6,7). It is also known that in higher plants, α1,2-fucosylation regulates seedling growth (8,9). Thus, introduction of fucosyl residue into various compounds is of particular interest not only because of their prebiotic and pharmaceutical benefits but also because it can aid in elucidating the molecular mechanisms underlying fucosylation-mediated cellular responses observed in various organisms.

In SECTION I of CHAPTER I, the author developed a highly functional 1,2-α-L-fucosynthase (*Bb*AfcA^{N423H}), synthesizing 2'-FL with a considerably higher yield (88 % yield against β-fucosyl fluoride [β-FucF]). The *Bb*AfcA^{N423H} had a broad acceptor specificity and could transfer fucosyl residues onto various oligosaccharides and *O*-glycans in mucin glycoproteins (Table 2 and Fig. 16 in SECTION I of CHAPTER I). This 1,2-α-L-fucosynthase made it more feasible to introduce H-antigens onto various glycoconjugates, which were conventionally difficult to obtain from biological samples.

In this SECTION, the author explored additional application for the *Bb*AfcA^{N423H} with acceptor molecules, other than those described in SECTION I of CHAPTER I. The *Bb*AfcA^{N423H} could synthesize a wide range of glycoconjugates, including α1,2- L-fucosylated *N*- and *O*-glycans of fetuin glycoprotein, fucosyl GM1 glycolipid, and fucosyl xyloglucan nonasaccharide. These results demonstrated extensive robustness and broader application of this fucosynthase-based technique in functional glycomics.

MATERIALS AND METHODS

Chemicals

Fetuin, asialofetuin, and ganglioside GM1 were purchased from Sigma-Aldrich (St. Louis, MO, USA). Peptide:*N*-glycanase F (PNGase F) and sialidase obtained from *Vibrio cholerae* were purchased from Roche (Mannheim, Germany). Xyloglucan nonasaccharide (XLLG) was obtained from Tokyo Chemical Industry Co., Ltd. (Tokyo, Japan). Pyridylaminated (PA-) sugar chains (asialo bi- and tri-antennary complex-type *N*-glycan) were purchased from TaKaRa Bio Inc. (Kusatsu, Japan). β-FucF was prepared as previously described (10). Recombinant 1,3-1,4-α-L-fucosidase obtained from *Bacteroides thetaiotaomicron* VPI-5482 (BT_2970) was expressed and purified as described previously (11). Recombinant 1,2-α-L-fucosidase wild-type (*Bb*AfcA^{WT}) and 1,2-α-L-fucosynthase *Bb*AfcA^{N423H} were prepared as described previously (SECTION I of CHAPTER I).

Fucosynthase reaction with ganglioside GM1 and analysis of the reaction product

Ganglioside GM1 (50 μg) was reconstituted in 2 μL of dimethylsulfoxide (DMSO). The fucosynthase reaction was performed as follows: 50 μL of 100 mM sodium citrate buffer (pH 5.5) containing 1 mg/mL ganglioside GM1, 10 mM β-FucF, and 10 μM *Bb*AfcA^{N423H} was incubated at 30 °C for 60 min. The reaction mixture was analyzed by thin-layer chromatography (TLC) using silica gel 60 aluminum sheet (Merck, Darmstadt, Germany). The TLC plate was developed with a solvent system of chloroform-methanol-0.2 % calcium chloride (60/35/8, *v*/*v*/*v*). The gangliosides were visualized by heating the plate after spraying diphenylamine-aniline-phosphoric acid reagent (13). For mass spectrometry (MS) analysis, the gangliosides were purified by using a Sep-Pak C_{18} cartridge column (Waters, Milford, MA, USA) as follows: the enzyme was removed by acetone precipitation, and the supernatant was evaporated by centrifugal concentration to dryness and reconstituted in 50 % methanol. The samples were loaded onto the Sep-Pak C_{18} column pre-equilibrated with distilled water. Bound materials, including the gangliosides, were eluted by chloroform-methanol (2:1, *v*/*v*) solution, dried under a nitrogen stream, and subjected to matrix-assisted laser desorption/ionization-time of flight MS (MALDI-TOF/MS) analysis as described below.

Fucosynthase reaction with XLLG and analysis of the reaction product

The reaction was carried out as follows: 100 μL of 100 mM sodium citrate buffer (pH 5.5) containing 10 mM or 2 mM XLLG, 10 mM β-FucF, and 10 μM *Bb*AfcA^{N423H} was incubated at 30 °C for 30 min. The reaction mixture was analyzed by high-performance anion exchange chromatography with pulsed amperometric detection (HPAEC-PAD) (Thermo Fisher Scientific, Waltham, MA, USA). CarboPac PA1 column (2 × 250 mm, Dionex, Sunnyvale, CA, USA) was used at 30 °C, and the elution was carried out in 125 mM sodium hydroxide with a linear gradient of 0–330 mM sodium acetate for

20 min at a flow rate of 0.25 mL/min.

Fucosylation of glycoprotein

Prior to the fucosynthase reaction, the residual sialic acid residues of asialofetuin samples were removed by treatment with sialidase obtained from *Vibrio cholerae*. Fucosynthase reaction was then carried out as follows: 250 μL of 100 mM sodium citrate buffer (pH 5.5) with 1 mg/mL glycoprotein, 10 mM β-FucF, and 10 μM *Bb*AfcA^{N423H} was incubated at 30 °C for 60 min. Reaction was stopped by boiling, and the reaction mixture was dialyzed against 10 mM Tris-HCl buffer (pH 8.0) and then subjected to glycan analyses, as described below.

Fucosynthase reaction with PA-sugar chains and analysis of the reaction product

The reaction was carried out as follows: 60 μL of 100 mM sodium citrate buffer (pH 5.5) containing 2 μM PA-sugar chains, 100 μM β-FucF, and 10 μM *Bb*AfcA^{N423H} was incubated at 30 °C for 60 min. The reaction mixture was analyzed by high-performance liquid chromatography (HPLC). The HPLC was carried out using Waters e2695 separation module with TSKgel amide-80 column (4.6 × 250 mm; Tosoh, Tokyo, Japan) at 40 °C. The elution was carried out with solvent A (acetonitrile/500 mM acetic acid-triethylamine containing 10 % acetonitrile (pH7.3) = 75/15) and solvent B (acetonitrile/500 mM acetic acid-triethylamine containing 10 % acetonitrile (pH7.3) = 40/50) by a following gradient program: the solvent B was linearly increasing from 0 % to 100 % in 100 min and kept at 100 % for 20 min at a flow rate of 1 mL/min. The eluate was monitored by fluorescence of excitation at 310 nm and emission at 380 nm using a Waters 2475 Multi-wavelength Fluorescence Detector.

Lectin blot

For lectin blotting, asialofetuin samples (2 μg) were separated by sodium dodecyl sulfate-polyacrylamide gel electrophoresis (SDS-PAGE), and then transferred onto Immobilon-P membrane (Millipore, MA). The membrane was incubated for 60 min with blocking reagent; 2% (*w*/*v*) bovine serum albumin in Tris-buffered saline containing 0.05 % (*v*/*v*) Tween-20 (TBS-T). The membrane was then incubated with biotin-conjugated lectins, *Ulex europaeus* agglutinin I (UEA-I; J-Oil Mills, Tokyo, Japan) or Peanut agglutinin (PNA; J-Oil Mills) (0.4 μg/mL) and horseradish peroxidase-conjugated streptavidin (0.125 μg/mL) in blocking reagent for 60 min. The membrane was washed with TBS-T and the signals were visualized using SuperSignal West Pico Chemiluminescent Substrate (Thermo Fisher Scientific) and Luminescent Image Analyzer LAS-3000 (Fujifilm, Tokyo, Japan).

Release and separation of* N-*glycan from glycoproteins

N-Glycans were released from glycoproteins by PNGase F. To maximize the efficiency of PNGase F treatment, the protein was digested to glycopeptides by trypsin in advance. The protein sample was lyophilized, reconstituted in 200 μL of 100 mM Tris-HCl buffer (pH 8.2) containing 10 mM $CaCl_2$, and then incubated with 5 μL of 20 mg/mL trypsin at 37 °C for 15.5 h. After incubation, the sample was centrifuged at 15,000 rpm, 4 °C, for 10 min, and the supernatant was collected. Residual pellet was resuspended in water, centrifuged again, and the supernatant was collected. Both the supernatants were combined and dried by centrifugal concentration. The dried tryptic peptide was reconstituted in 300 μL of 5 % (*v*/*v*) acetic acid, loaded onto a Sep-Pak C_{18} cartridge column pre-equilibrated with 5 % acetic acid, and followed by washing with 5 % acetic acid. Bound materials containing glycopeptides were eluted in 20 % iso-propanol in 5 % acetic acid and 40 % iso-propanol in 5 % acetic acid. To release *N*-glycans from glycopeptides, the eluate was dried by a centrifugal concentrator and reconstituted in 27 μL of distilled water and 20 μL of 100 mM sodium phosphate buffer (pH 7.5), and then 3 μL of PNGase F was added. The solution was incubated at 37 °C for 16 h and then dried. The sample was dissolved in 300 μL of 5 % acetic acid, and loaded on a pre-equilibrated Sep-Pak C_{18} column. *N*-glycans released from glycopeptides were collected in a wash fraction with 5 % acetic acid, and then lyophilized and subjected to glycan permethylation, followed by MS analysis. Glycan permethylation was performed as described in SECTION I of CHAPTER I.

Preparation of* O-*glycan samples

Following the separation of *N*-glycan released from glycoproteins on Sep-Pak C_{18} cartridge columns as described above, the residual glycopeptides containing *O*-glycans were collected by elution with 20 % and 40 % iso-propanol/5 % acetic acid solutions, and they were used for a subsequent *O*-glycan analysis. To release the *O*-glycan from glycopeptides, reductive β-elimination was performed. Glycopeptides (80–100 μg) were reconstituted in 500 μL of 100 mM sodium hydroxide containing 1 M sodium borohydride, and the mixture was incubated at 45 °C for 18 h. After incubation, the mixtures were placed on ice and then 10 % (*v*/*v*) acetic acid was added to neutralize the reaction mixtures. The samples then underwent desalting on a Dowex-50W-X8 (H^+ form, 100–200 m, Sigma-Aldrich) column and the pass-through and wash fractions with 5 % acetic acid were collected and lyophilized. Residual borate was removed as an azeotrope with methanol by 0.3 mL of 10 % acetic acid in methanol, and dried under a nitrogen stream at 40 °C. To remove borate completely, this step was repeated five times. The released oligosaccharide alditols were dissolved in 0.3 mL of 5 % acetic acid, and purified by a Sep-Pak C_{18} cartridge column. The flow-through fraction containing the released oligosaccharide alditols was lyophilized and subjected to glycan permethylation, followed by MS analysis.

MALDI-TOF MS analysis

Molecular masses of glycan samples were analyzed by the UltrafleXtreme instrumentation for MALDI-TOF MS (Bruker Daltonics, Billerica, MA, USA) in the positive ion mode for permethylated glycans, and in the negative ion mode for ganglioside GM1 and its derivatives. 2,5-Dihydroxybenzoic acid was used as a matrix. MALDI-TOF/TOF MS was also performed to obtain MS/MS spectra of the glycan precursor ion peaks of interest. Theoretical masses were calculated using the software GlycoWorkbench 2.0 (14).

Determination of glycosidic linkage of fucosynthase reaction products

Positional assignment of the glycosidic linkages of the fucosyl residues introduced by the fucosynthase reaction were performed by treatments with regio-specific enzymes, *e.g.* 1,2-α-L-fucosidase (*Bb*AfcA^{WT}) and 1,3-1,4-α-L-fucosidase (BT_2970). 1,2-α-L-Fucosidase treatment was performed at 37 °C in 150 μL of 100 mM sodium phosphate buffer (pH 6.5) containing 1 μM *Bb*AfcA^{WT}, and 0.5 mg/mL fucosynthase-products as substrates. BT2970 treatment was performed at 37 °C in 150 μL of 100 mM 2-morpholinoethanesulfonic acid (MES) buffer containing 1.8 μM BT_2970, and 0.5 mg/ml fucosynthase-products as substrates. After the treatments, the samples were analyzed by MALDI-TOF MS and MALDI-TOF/TOF MS, as described earlier.

RESULTS AND DISCUSSION

Fucosylation of N- *and* O-*glycans on asialofetuin*

To examine whether *Bb*AfcA^{N423H} can add fucosyl residues onto *N*-glycans in glycoproteins, the author first tested fucosylation of *N*-glycans on a model glycoprotein, asialofetuin, obtained from fetal bovine serum. Fetuin is a 48-kDa α-globulin protein with three complex-type *N*-glycans and three *O*-glycans on its polypeptide (15). After the sialidase treatment and fucosynthase reaction, lectin blot analyses were performed using the two lectins: UEA-I (lanes 1-4) and PNA (lanes 5-8) to detect Fuc residue and Galβ1-3GalNAc structure of *O*-glycans, respectively (Fig. 1). The UEA-I signal was detected only after treatment with *Bb*AfcA^{N423H} (lane 3), and the signal was almost eliminated following PNGase F-treatment (lane 4). These results indicated that fucosyl residues were predominantly attached on *N*-glycans of asialofetuin. Meanwhile, PNA signal intensities appeared to be slightly decreased on *Bb*AfcA^{N423H} treatment (compared between lanes 5–6 and 7–8), probably due to capping by fucosylation of Galβ1-3GalNAc structure. Although UEA-I signal was not detected for the reaction product treated with PNGase-F (lane 4), these results implied that *Bb*AfcA^{N423H} also added fucose onto the *O*-glycans of asialofetuin.

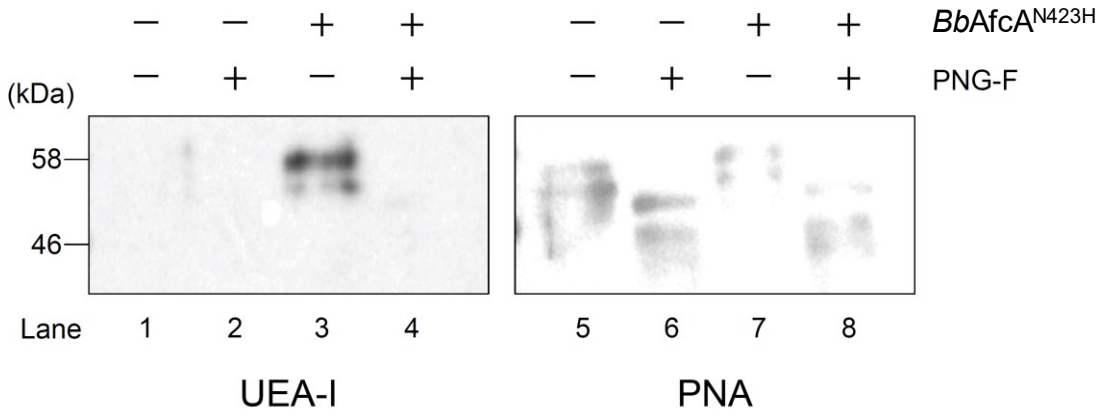

Fig. 1. Lectin blot analysis of the *Bb*AfcA^{N423H} -treated asialofetuin.
Aisalofetuin was treated with *Bb*AfcA^{N423H} and PNGase F (PNG-F), followed by lectin blot analysis with UEA-I (lanes 1–4) and PNA (lanes 5–8) lectins.

Subsequent MALDI-TOF MS analyses of the released glycans confirmed the observations of the lectin blots. The MS spectrum of the permethylated *N*-glycans from non-treated asialofetuin (Fig. 2A) showed that the protein was modified by a tri-antennary complex-type (*m/z* 2520.4) as a major *N*-glycan species, followed by a bi-antennary complex-type (*m/z* 2071.2), and sialidase-resistant monosialo-tri-antennary complex-type (*m/z* 2881.6). On the other hand, the MS spectrum of *Bb*AfcA^{N423H}-treated asialofetuin indicated a significant increase in a glycan ion signal at *m/z* 2694.5 and the appearance of signals at *m/z* 2245.2, *m/z* 2868.1 and *m/z* 3055.6 (Fig. 2B). The masses of these increased peaks corresponded to those with mono- (174 mass increase) or di- (348 mass increase)

deoxyhexose(s) of the original peaks at *m/z* 2071.2, *m/z* 2520.4 and *m/z* 2881.6, and indeed, the MS/MS spectrum of the peak at *m/z* 2694 exhibited a fragmentation pattern corresponding to monofucosylated tri-antennary complex-type *N*-glycan (Fig. 2E). Furthermore, the fragment ions at *m/z* 433 and *m/z* 2284 indicated the presence of a terminal deoxyhexose-hexose moiety, suggesting fucosylation on the Gal residues. Treatments with linkage-specific α-L-fucosidases (Figs. 2C and 2D) revealed that those fucosyl residues were, as expected, introduced by α-(1→2) linkage, but not by α-(1→3/4) linkage. Taken together, the *Bb*AfcA^{N423H} could synthesize Fucα1-2Gal structures on *N*-glycans of glycoproteins.

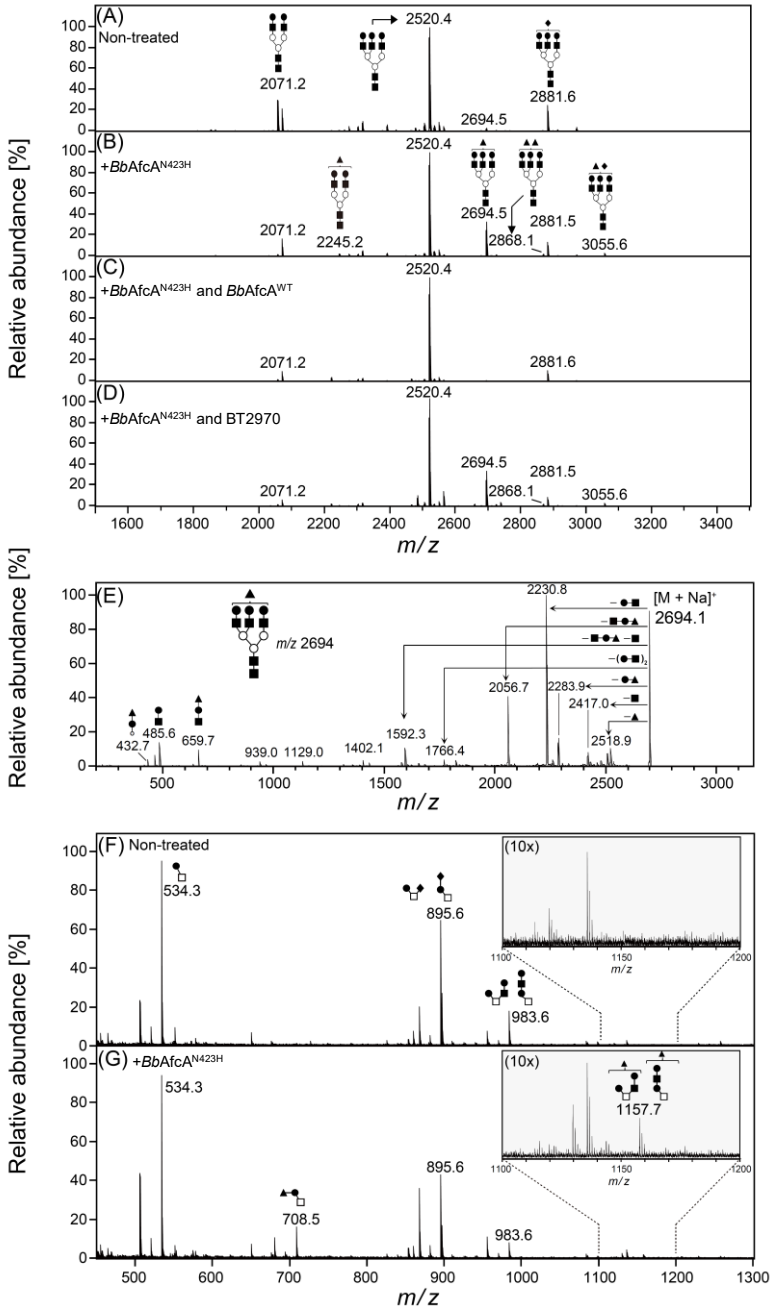

Fig. 2. MALDI-TOF MS analysis of the permethylated *N*- and *O*-glycans released from asialofetuin treated with *Bb*AfcA^{N423H}.

(A–D) Complete MS profiles of *N*-glycans that were released by PNGase F from asialofetuin samples treated with no enzyme (A), *Bb*AfcA^{N423H} (B), *Bb*AfcA^{N423H} followed by a 1,2-α-L-fucosidase *Bb*AfcA wild-type (*Bb*AfcA^{WT}) (C), and *Bb*AfcA^{N423H} followed by 1,3-1,4-α-L-fucosidase (BT_2970) (D). Released *N*-glycans were subsequently permethylated and analyzed by MALDI-TOF MS. (E) Fragmentation pattern of an MS/MS spectrum of a peak at *m/z* 2694 in the complete MS spectrum in (A) corresponded to mono-fucosylated *N*-glycan. Complete MS profiles of *O*-glycan released from non-treated asialofetuin (F) and *Bb*AfcA^{N423H} -treated asialofetuin (G). Estimated glycan structures were depicted in the figures with symbols as follows: filled diamond, *N*-acetylneuraminic acid; filled circle, galactose; filled square, *N*-acetylglucosamine; filled triangle, L-fucose; open circle, mannose; open square, *N*-acetylgalactosamine.

The efficiencies of the introduction of fucose onto the asialo-bi-antennary, asialo-, and monosialo-tri-antennary complex-type *N*-glycans on asialofetuin were calculated to be 9 %, 26 %, and 20 %, respectively, based on the MS signal ion intensities. Occurrence of fucosylation seemed to be varied among the glycan species. Therefore, the author examined the specificity of the synthase for PA-labeled bi-, and tri-antennary complex-type *N*-glycans. Normal-phase HPLC analysis of the *Bb*AfcA^{N423H}-treated PA-sugar chains showed newly generated two and three peaks in bi-, and tri-antennary, respectively, in addition to the original PA-sugar chains (Fig. 3A and 3B), indicating the addition of one to three fucose. The fucosylation efficiency reached 80 % and 81 % in bi- and tri-antennary complex-type *N*-glycans, respectively, based on the consumption of the substrates. These results indicated that *Bb*AfcA^{N423H} used the free bi-, and tri-antennary complex-type *N*-glycans at a similar rate as the acceptor. Therefore, the varied occurrence of fucosylation on asialofetuin was possibly due to the difference in the accessibility of the enzyme to the each glycan species. The presence of H-antigens on *N*-glycans has been demonstrated in human von Willebrand factor (16).

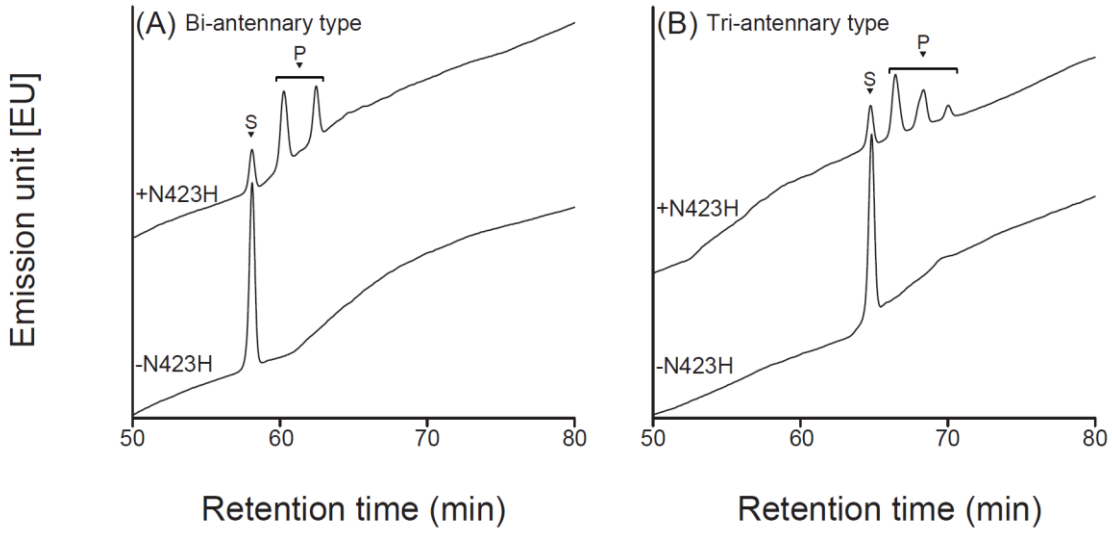

Fig. 3. Fucosynthase reaction using PA-sugar chains as acceptors.

The reaction was carried out for PA-sugar chains of asialo-bi-antennary (A) and asialo-tri-antennary (B) complex-type *N*-glycans with (+) and without (−) *Bb*AfcA^{N423H} (N423H). HPLC analyses of the reaction products were performed as described in materials and methods. The part of chromatograms is shown. The peaks of substrate (S) and products (P) are indicated by arrowheads.

Fucosylation of *O*-glycans on asialofetuin was also evidenced by MALDI-TOF MS analysis. After the treatment of *Bb*AfcA^{N423H}, some new signals corresponding to the masses of fucosylated *O*-glycan alditols (sodium adducts) were observed, i.e., *m/z* 708.5 for $Fuc_1Gal_1GalNAc$-itol, and *m/z* 1157.7 for $Fuc_1Gal_2GlcNAc_1GalNAc$-itol (Figs. 2F and 2G). This result may explain the slight decrease in PNA signals in the lectin blot data.

Bb*AfcA*^{N423H} *adds fucose onto sialylated* N-*glycan*

In the MS/MS spectrum of a signal at *m/z* 3055.6 found in *Bb*AfcA^{N423H}-treated asialofetuin *N*-glycans, a fragment peak at *m/z* 1022 $[M + Na]^+$ corresponding to the mass of $NeuAc_1dHex_1Hex_1HexNAc_1$ was observed. This fact allowed us to assume that this synthase could add Fuc residues onto sialylated *N*-glycans. To verify this possibility, the author carried out fucosynthase reaction with fetuin as an acceptor. As shown in Fig. 4A, fully sialylated complex-type *N*-glycans; disialo-biantennary (*m/z* 2793.4) and trisialo- (*m/z* 3603.8), and tetrasialo- (*m/z* 3966.0) triantennary, were detected as major glycans in a control fetuin sample. In *Bb*AfcA^{N423H}-treated fetuin sample (Fig. 4B), there were peaks corresponding to the fully sialylated *N*-glycans with monofucosylation (*m/z* 2967.5, *m/z* 3778.9 and 4140.1, respectively). These peaks disappeared upon treatment with *Bb*AfcA^{WT}, but not on treatment with BT_2970, confirming that α1,2-fucosyl residues were introduced (Figs. 4C and 4D). These results demonstrated that α1,2-fucosylation occurred on the sialylated branches of *N*-glycans. The MS-based fucosylation efficiency for disialo-biantennary, disialo-, trisialo- and tetrasialo-triantennary complex-type *N*-glycans were 12 %, 11 %, 15 %, and 11 %, respectively. It should be noted that in the *Bb*AfcA crystal structure complexed with 2′-FL, O6 of the Gal residue is exposed to the solvent (12). Accordingly, *Bb*AfcA has a sufficient space to accommodate NeuAcα2-6Gal structures present at the non-reducing ends of *N*-glycans.

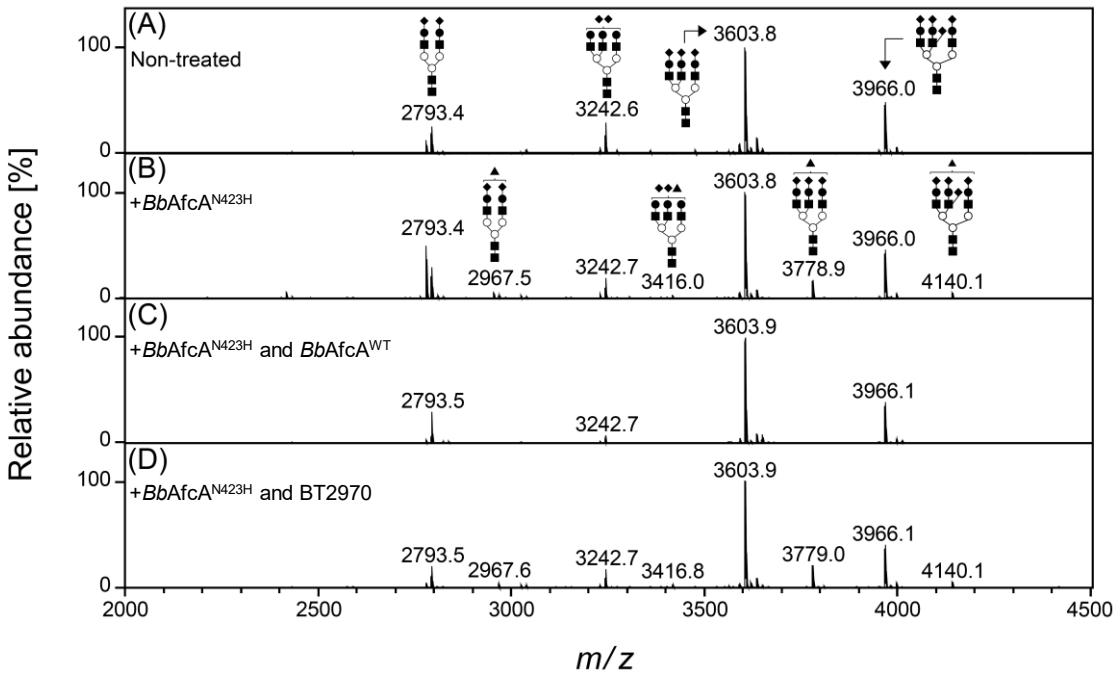

Fig. 4. MALDI-TOF MS spectra of permethylated *N*-glycans released from enzyme-treated fetuin.

Complete MS profiles of *N*-glycans that were released by PNGase F from fetuin samples treated with no enzyme (A), fucosynthase *Bb*Afc^{N423H} (B), *Bb*AfcA^{N423H} followed by a 1,2-α-L-fucosidase *Bb*AfcA wild-type (*Bb*AfcA^{WT}) (C), and *Bb*AfcA^{N423H} followed by 1,3-1,4-α-L-fucosidase (BT_2970) (D). Estimated *N*-glycan structures based on their mass values were depicted as described in Fig. 2.

Synthesis of fucosyl GM1 glycolipid

The author next examined whether this fucosynthase was able to transfer Fuc residues on to glycolipids. GM1 ganglioside (Fig. 5A) was chosen, since fucosyl GM1 was shown to be expressed in the mammalian digestive tract during the weaning period (17) and was also reported as a potential marker of small-cell lung cancer and hepatocellular carcinoma (18). Fucosynthase reaction was performed with GM1 obtained from bovine brain, and the reaction mixture was resolved by TLC analysis. A new spot of the product was observed beneath the GM1 spot (Fig. 5B). Further MS analysis revealed that in addition to GM1 peaks at *m/z* 1544.7 and *m/z* 1572.8, new peaks at *m/z* 1690.8 and *m/z* 1718.8 appeared, masses of which are estimated to be that of monofucosylated GM1 gangliosides (Figs. 5C and 5D). These peaks were eliminated on treatment with *Bb*AfcA^{WT}, confirming α1,2-fucosylation on GM1 ganglioside (Fig. 5E).

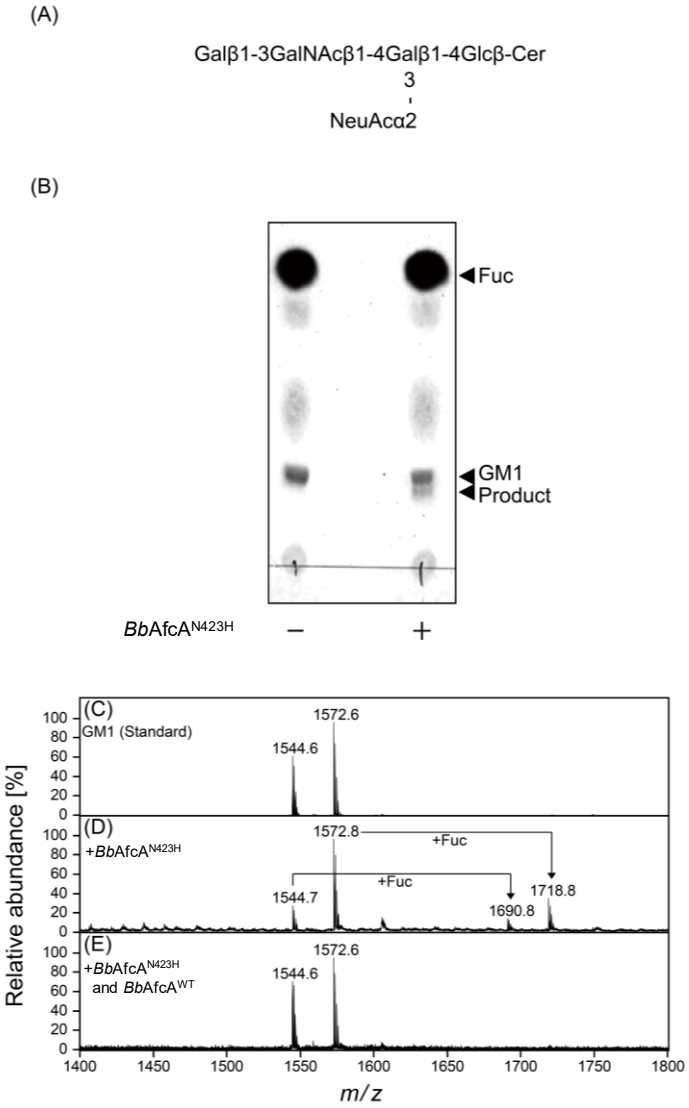

Fig. 5. Fucosynthase reaction using GM1 ganglioside as an acceptor.

Fucosynthase reaction with GM1 ganglioside, the structure of which is indicated in (A), was performed as described in Materials and methods, and then analyzed by TLC (B) and MALDI-TOF MS (C–E).

Fucosylation of plant-derived xyloglucan oligosaccharide

Xyloglucan is a major constituent of hemicellulosic polysaccharide in cell walls of higher plants. XLLG has a β-(1→4) linked glucosyl backbone (β-1,4-glucan) with side chains of α-linked Xyl and Galβ1-2Xyl residues, which are attached to the C-6 position of Glc (Fig. 6A). Fucosyl XLLGs are present in plants and exhibit inhibiting activity for auxin-stimulated growth (19). To examine the ability of the fucosynthase to synthesize the fucosyl XLLGs, the fucosylation reaction was carried out with 10 mM XLLG and the reaction mixtures were analyzed by HPAEC-PAD. The product peaks were observed in the *Bb*AfcA^{N423H}-treated sample (Fig. 6C). The reaction efficiency was 57% against XLLG in this condition. MS analysis of the permethylated reaction products of the reaction with 2 mM XLLG revealed that mono- (*m/z* 1948.2), di- (*m/z* 2122.3), and tri-fucosyl XLLG (*m/z* 2296.0) were generated by *Bb*AfcA^{N423H} treatment, although the signal intensity suggested that tri-fucosyl XLLG was a very minor product (Fig. 6D). Fucosylation most likely occurs at C-2 position of Gal, and could also possibly occur at the C-3 position of the reducing-end glucose in α-anomer, as demonstrated in Fig. 16E in SECTION I of CHAPTER I. The fragmentation by MS/MS analysis of these fucosylated XLLGs identified fragment ion peaks corresponding to *m/z* 1175, the presence of which proved that the third fucosyl residue could be added onto the Glc residue at the reducing end to synthesize a tri-fucosylated structure as shown in Fig. 6B. However, the addition of Fuc to the reducing-end Glc of XLLG was observed only when the β-FucF (donor) concentration exceeded that of XLLG (acceptor) considerably. Collectively, these results indicate that *Bb*AfcA^{N423H} is useful for the production of fucosylated xyloglucan oligosaccharide.

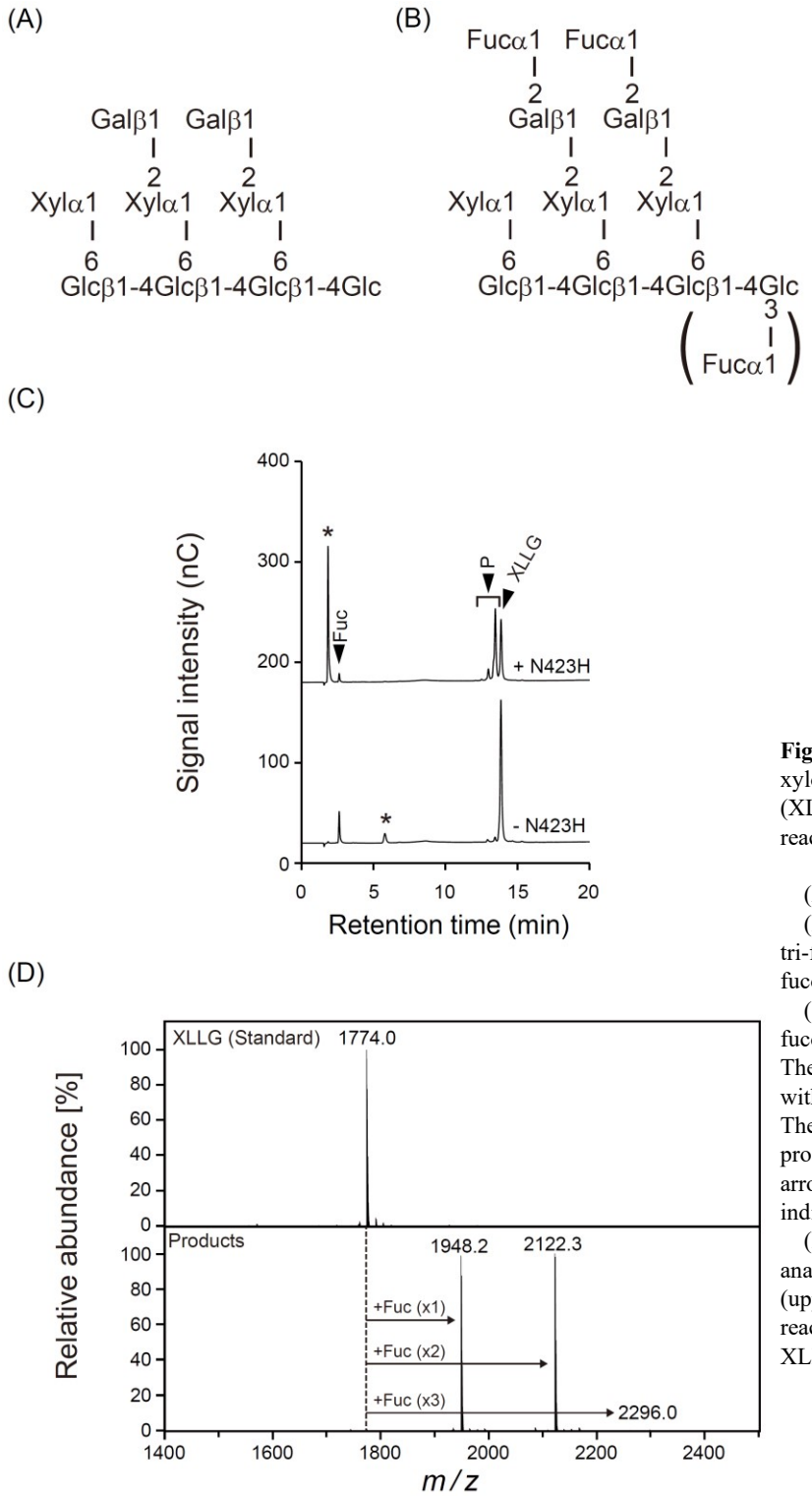

Fig. 6. Synthesis of fucosyl xyloglucan nonasaccharide (XLLG) by fucosynthase reaction.

(A) The structure of XLLG.

(B) An estimated structure of tri-fucosyl XLLG synthesized by fucosynthase reaction.

(C) HPAEC-PAD analysis of fucosynthase reaction product. The reaction was carried out with 10 mM XLLG as acceptor. The peaks of Fuc, XLLG, and product (P) are indicated by arrowheads. Asterisks (*) indicate unidentified peaks.

(D) MALDI-TOF MS analysis of permethylated XLLG (upper panel) and fucosynthase reaction product with 2 mM XLLG as acceptor (lower panel).

REFERENCES

1. Pickard, J. M., and Chervonsky, A. V. (2015) Intestinal fucose as a mediator of host-microbe symbiosis. *J Immunol* **194**, 5588-5593
2. Goto, Y., Obata, T., Kunisawa, J., Sato, S., Ivanov, I. I., Lamichhane, A., Takeyama, N., Kamioka, M., Sakamoto, M., Matsuki, T., Setoyama, H., Imaoka, A., Uematsu, S., Akira, S., Domino, S. E., Kulig, P., Becher, B., Renauld, J. C., Sasakawa, C., Umesaki, Y., Benno, Y., and Kiyono, H. (2014) Innate lymphoid cells regulate intestinal epithelial cell glycosylation. *Science* **345**, 1254009
3. Pham, T. A., Clare, S., Goulding, D., Arasteh, J. M., Stares, M. D., Browne, H. P., Keane, J. A., Page, A. J., Kumasaka, N., Kane, L., Mottram, L., Harcourt, K., Hale, C., Arends, M. J., Gaffney, D. J., Dougan, G., Lawley, T. D., and Project, S. M. G. (2014) Epithelial IL-22RA1-mediated fucosylation promotes intestinal colonization resistance to an opportunistic pathogen. *Cell Host Microbe* **16**, 504-516
4. Ruiz-Palacios, G. M., Cervantes, L. E., Ramos, P., Chavez-Munguia, B., and Newburg, D. S. (2003) *Campylobacter jejuni* binds intestinal H(O) antigen (Fuc alpha 1, 2Gal beta 1, 4GlcNAc), and fucosyloligosaccharides of human milk inhibit its binding and infection. *J Biol Chem* **278**, 14112-14120
5. Matsuki, T., Yahagi, K., Mori, H., Matsumoto, H., Hara, T., Tajima, S., Ogawa, E., Kodama, H., Yamamoto, K., Yamada, T., Matsumoto, S., and Kurokawa, K. (2016) A key genetic factor for fucosyllactose utilization affects infant gut microbiota development. *Nat Commun* **7**, 11939
6. Katayama, T. (2016) Host-derived glycans serve as selected nutrients for the gut microbe: human milk oligosaccharides and bifidobacteria. *Biosci Biotechnol Biochem* **80**, 621-632
7. Bode, L. (2012) Human milk oligosaccharides: every baby needs a sugar mama. *Glycobiology* **22**, 1147-1162
8. Zablackis, E., York, W. S., Pauly, M., Hantus, S., Reiter, W. D., Chapple, C. C., Albersheim, P., and Darvill, A. (1996) Substitution of L-fucose by L-galactose in cell walls of *Arabidopsis mur1*. *Science* **272**, 1808-1810
9. Dumont, M., Lehner, A., Bardor, M., Burel, C., Vauzeilles, B., Lerouxel, O., Anderson, C. T., Mollet, J. C., and Lerouge, P. (2015) Inhibition of fucosylation of cell wall components by 2-fluoro 2-deoxy-L-fucose induces defects in root cell elongation. *Plant J* **84**, 1137-1151
10. Wada, J., Honda, Y., Nagae, M., Kato, R., Wakatsuki, S., Katayama, T., Taniguchi, H., Kumagai, H., Kitaoka, M., and Yamamoto, K. (2008) 1,2-alpha-l-Fucosynthase: a glycosynthase derived from an inverting alpha-glycosidase with an unusual reaction mechanism. *FEBS Lett* **582**, 3739-3743

11. Sakurama, H., Tsutsumi, E., Ashida, H., Katayama, T., Yamamoto, K., and Kumagai, H. (2012) Differences in the substrate specificities and active-site structures of two α-L-fucosidases (glycoside hydrolase family 29) from *Bacteroides thetaiotaomicron*. *Biosci Biotechnol Biochem* **76**, 1022-1024
12. Nagae, M., Tsuchiya, A., Katayama, T., Yamamoto, K., Wakatsuki, S., and Kato, R. (2007) Structural basis of the catalytic reaction mechanism of novel 1,2-alpha-L-fucosidase from *Bifidobacterium bifidum*. *J Biol Chem* **282**, 18497-18509
13. Anderson, K., Li, S. C., and Li, Y. T. (2000) Diphenylamine-aniline-phosphoric acid reagent, a versatile spray reagent for revealing glycoconjugates on thin-layer chromatography plates. *Anal Biochem* **287**, 337-339
14. Ceroni, A., Maass, K., Geyer, H., Geyer, R., Dell, A., and Haslam, S. M. (2008) GlycoWorkbench: a tool for the computer-assisted annotation of mass spectra of glycans. *J Proteome Res* **7**, 1650-1659
15. Takasaki, S., and Kobata, A. (1986) Asparagine-linked sugar chains of fetuin: occurrence of tetrasialyl triantennary sugar chains containing the Gal beta 1→3GlcNAc sequence. *Biochemistry* **25**, 5709-5715
16. Canis, K., McKinnon, T. A., Nowak, A., Haslam, S. M., Panico, M., Morris, H. R., Laffan, M. A., and Dell, A. (2012) Mapping the *N*-glycome of human von Willebrand factor. *Biochem J* **447**, 217-228
17. Lin, B., Hayashi, Y., Saito, M., Sakakibara, Y., Yanagisawa, M., and Iwamori, M. (2000) GDP-fucose: beta-galactoside alpha1,2-fucosyltransferase, MFUT-II, and not MFUT-I or -III, is induced in a restricted region of the digestive tract of germ-free mice by host-microbe interactions and cycloheximide. *Biochim Biophys Acta* **1487**, 275-285
18. Wu, C. S., Yen, C. J., Chou, R. H., Li, S. T., Huang, W. C., Ren, C. T., Wu, C. Y., and Yu, Y. L. (2012) Cancer-associated carbohydrate antigens as potential biomarkers for hepatocellular carcinoma. *PLoS One* **7**, e39466
19. Augur, C., Yu, L., Sakai, K., Ogawa, T., Sinaÿ, P., Darvill, A. G., and Albersheim, P. (1992) Further studies of the ability of xyloglucan oligosaccharides to inhibit auxin-stimulated growth. *Plant Physiol* **99**, 180-185

SUMMARY

In SECTION I of CHAPTER I, the author generated a highly functional 1,2-α-L-fucosynthase (*Bb*AfcA ^{N423H}) by protein engineering of 1,2-α-L-fucosidase from *Bifidobacterium bifidum* JCM 1254. This synthase could specifically introduce H-antigens (Fucα1-2Gal) into the non-reducing ends of oligosaccharides and in *O*-linked glycans in mucin glycoprotein. In this SECTION, the author showed an extended application of the *Bb*AfcA^{N423H} by demonstrating its ability to insert Fuc residues into *N*- and *O*-glycans in fetuin glycoproteins, GM1 ganglioside, and a plant-derived xyloglucan nonasaccharide. This application study broadens the feasibility of this novel H-antigen synthesis technique in functional glycomics.

CHAPTER II
Analysis of polyamine biosynthetic and transport ability of human gut microbes

SECTION I
Analysis of polyamine biosynthetic and transport ability of the dominant human gut microbes and prediction of the presence of novel polyamine biosynthetic and transport proteins

Polyamines (putrescine [Put], spermidine [Spd], spermine [Spm]) are aliphatic amines possessing two or more amino groups. They are widely distributed in eukaryotic (1) and prokaryotic cells (2). In the mammalian colonic lumen, polyamines are present at millimolar concentrations (3), and it was previously reported that these polyamines are derived from gut microbes (4-6). Polyamines in the colonic lumen are transferred into the bloodstream via the colonic mucosa (7), after which they have various effects on the body. For example, high concentrations of polyamines are found in cancer cells because of their role in cell proliferation. The possibility of treating cancer by reducing gut microbial polyamine levels via administration of antibiotics is being investigated (8). However, polyamines in the intestinal tract have various beneficial effects on mammalian health, such as increased longevity (7,9), recovery of injured mucosa (10), and favorable effects on cognitive function (7). As intestinal polyamines are derived from gut microbes, colonic luminal polyamine concentration is determined by microbial polyamine metabolism. The known pathways for microbial polyamine biosynthesis and transport are summarized in Fig.1 (11-14). Kibe *et al.* reported that even though Put increased in the colonic lumen, the abundance of known Put biosynthetic genes (*speB*, *adi*, and *ncpah*; Fig. 1) were unchanged in mice gut microbiota (7). These results suggest that in addition to the previously described polyamine biosynthetic pathway (Fig.1), there is a novel gene or set of genes facilitating Put biosynthesis in the gut microbes. Therefore, identification of new genes for polyamine biosynthesis and transport is indispensable for optimization of polyamine concentrations in human colonic lumen, enabled by regulation of genes facilitating polyamine metabolism in gut microbes.

A "human gut microbial gene catalog" ranking the dominant microbial species/genera in the human gut has been described (15). Recently, Gotoh *et al*. reported that Gifu anaerobic medium (GAM) was useful for the cultivation of 32 species of dominant human gut microbes and for comparison of their metabolite profiles (16). The polyamine concentration in stationary phases of *Alistipes* (17), *Bacteroides* (17,18) and *Parabacteroides* (17) species, which are members of human gut microbes, have been previously reported. However, in some microbes, the polyamine profile in cells and in culture supernatants differ based on their growth phase (19,20): cellular polyamine

concentration is higher in growing phase than that in stationary phase, probably because polyamines are important for cell proliferation. Therefore, the measurement of polyamine concentrations in the cell and culture supernatant in different growth phases is necessary for a better insight into microbial polyamine biosynthetic and transport activity. Furthermore, polyamine biosynthesis and transport should be analyzed in dominant human gut microbial species other than those belonging to the *Alistipes*, *Bacteroides* and *Parabacteroides* genera (Table 1) for a comprehensive understanding of polyamine homeostasis in the human intestinal lumen.

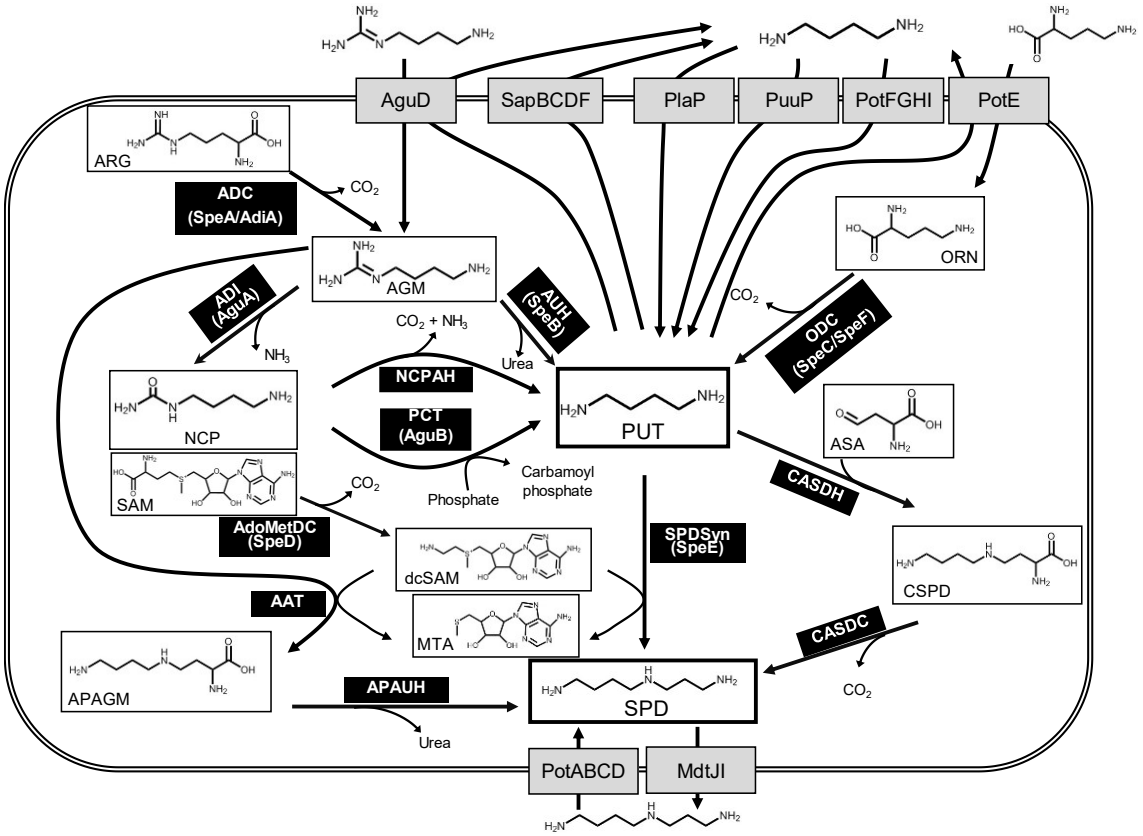

Fig. 1. Polyamine biosynthetic and transport pathways in microbes.

Polyamine biosynthetic and transport pathways previously described in microbes are integrated and illustrated. Gray squares indicate transporters (importer, antiporter, and exporter) that were previously reported in *Escherichia coli* or *Enterococcus faecalis*. Black squares with white letters show abbreviated names of enzymes experimentally identified in *E. coli*, *En. faecalis*, *B. thetaiotaomicron*, *Thermus thermophilus*, *Vibrio cholerae*, or *Pseudomonas aeruginosa*. The abbreviations used are as follows: AAT, agmatine aminopropyltransferase (21); ADC, arginine decarboxylase (22,23); ADI, agmatine deiminase (24); AdoMetDC, *S*-adenosylmethionine decarboxylase (25); AGM, agmatine; AguD, putrescine-agmatine antiporter (26); APAGM, aminopropylagmatine; APAUH, aminopropylagmatine ureohydrolase (21); ARG, arginine; ASA, aspartate-β-semialdehyde; AUH, agmatine ureohydrolase (27); CASDC, carboxyspermidine decarboxylase (19,20,28); CASDH, carboxyspermidine dehydrogenase (19,28); CSPD, carboxyspermidine; dcSAM, decarboxylated *S*-adenosylmethionine; MdtJI, spermidine exporter (29); MTA, 5′-deoxy-5′-methylthioadenosine; NCP, *N*-carbamoylputrescine; NCPAH, *N*-carbamoylputrescine amidohydrolase (30); ODC, ornithine decarboxylase (31,32); ORN, ornithine; PCT, putrescine carbamoyltransferase (24); PlaP, low-affinity putrescine importer (33); PotABCD, ATP-binding cassette type spermidine preferential importer (34); PotE, putrescine-ornithine antiporter (35,36); PotFGHI, ATP-binding cassette type putrescine specific importer (37); PUT, putrescine; PuuP, high-affinity putrescine importer (38); SAM, *S*-adenosylmethionine; SapBCDF, putrescine exporter (see SECTION III of CHAPTER II); SPD, spermidine; SPDSyn, spermidine synthase (39).

In the present study, the author measured polyamine concentration in the cell and culture supernatants of 32 species of dominant human gut microbes cultured in GAM at different growth

phases. Furthermore, by using *in silico* analysis, the author estimated the possibility of gut microbes harboring the novel polyamine biosynthetic and transport proteins.

MATERIALS AND METHODS

Materials

GAM bouillon, putrescine dihydrochloride, spermidine trihydrochloride, and spermine tetrahydrochloride were purchased from Nissui pharmaceuticals (Tokyo, Japan), Wako Pure Chemicals (Osaka, Japan), Nacalai Tesque (Kyoto, Japan), and MP Biomedicals (Solon, OH), respectively.

Strains and growth conditions

Microbial strains were obtained from the Japan Collection of Microorganisms (JCM), the American Type Culture Collection (ATCC), and the German Collection of Microorganisms and Cultures (DSMZ). Microbial strains used in this study are listed in Table 1. The conditions used for their cultivation have been previously described (16).

Analysis of polyamine concentrations in cells and culture supernatants

Polyamine concentrations were measured by high-performance liquid chromatography (HPLC); the analytical conditions were the same as those described previously (20). For analyzing the relationship between the growth stages and polyamine concentrations in cells and culture supernatants, cultures in growing and stationary phases were obtained at an indicated time (Fig. 2). Culture supernatants and cells for the quantification of polyamines were obtained in the previous report (16). Samples for measuring polyamine concentrations in cells and in culture supernatants by HPLC were prepared as described previously (20). To minimize the effect of residual polyamines in GAM in the cell pellet, culture supernatants were completely removed from the cell pellets, resulting in some cells being discarded. Therefore, intracellular polyamine levels were normalized to the amount of cellular protein and expressed as nmol/mg protein.

Search of occurrence of genes by BLAST analysis

Protein BLAST (BlastP) analysis (40) was performed against proteomes of all gut microbial species. Proteins whose functions were demonstrated by experimentation were used as query proteins for BlastP analysis; these query proteins are listed in Table 2. Proteins with more than 100-, 300-, and 500-bit scores were extracted.

Statistics

Values are indicated as mean ± standard deviation (SD). The significant differences were analyzed by using SPSS® software version 21 (IBM, Armonk, NY).

Table 1. Microbial strains used in this study.

Dominance rank[a]	Strain Name	Strain number	Genus
1	*Bacteroides uniformis*	JCM 5828^T	*Bacteroides*
6	*Bacteroides caccae*	JCM 9498^T	*Bacteroides*
8	*Bacteroides thetaiotaomicron*	JCM 5827^T	*Bacteroides*
17	*Bacteroides vulgatus*	JCM 5826^T	*Bacteroides*
23	*Bacteroides ovatus*	JCM 5824^T	*Bacteroides*
27	*Bacteroides xylanisolvens*	JCM 15633^T	*Bacteroides*
32	*Bacteroides dorei*	JCM 13471^T	*Bacteroides*
39	*Bacteroides stercoris*	JCM 9496^T	*Bacteroides*
44	*Bacteroides finegoldii*	JCM 13345^T	*Bacteroides*
51	*Bacteroides intestinalis*	JCM 13265^T	*Bacteroides*
52	*Bacteroides fragilis*	JCM 11019^T	*Bacteroides*
3	*Parabacteroides merdae*	JCM 9497^T	*Parabacteroides*
21	*Parabacteroides distasonis*	JCM 5825^T	*Parabacteroides*
45	*Parabacteroides johnsonii*	JCM 13406^T	*Parabacteroides*
4	*Dorea longicatena*	DSM 13814^T	*Dorea*
16	*Dorea formicigenerans*	ATCC 27755^T	*Dorea*
10	*Ruminococcus torques*	ATCC 27756^T	*Blautia*
33	*Ruminococcus obeum*	DSM 25238^T	*Blautia*
50	*Ruminococcus gnavus*	ATCC 29149^T	*Blautia*
56	*Blautia hansenii*	JCM 14655^T	*Blautia*
18	*Roseburia intestinalis*	DSM 14610^T	*Roseburia*
28	*Coprococcus comes*	ATCC 27758^T	*Coprococcus*
47	*Clostridium nexile*	ATCC 27757^T	*Clostridium*
53	*Clostridium asparagiforme*	DSM 15981^T	*Clostridium*
55	*Clostridium scindens*	JCM 6567^T	*Clostridium*
14	*Ruminococcus lactaris*	ATCC 29176^T	*Ruminococcus*
20	*Eubacterium siraeum*	ATCC 29066^T	*Ruminiclostridium*
49	*Anaerotruncus colihominis*	JCM 15631	*Anaerotruncus*
31	*Eubacterium ventriosum*	ATCC 27560^T	*Eubacterium*
35	*Pseudoflavonifractor capillosus*	ATCC 29799^T	*Pseudoflavonifractor*
54	*Enterococcus faecalis*	ATCC 700802	*Enterococcus*
15	*Collinsella aerofaciens*	JCM 7790	*Collinsella*

[a]The dominance rank indicates the order of occupancy in the human gut (15).

Table 2. Query proteins used for BlastP analysis.

Protein name	Description	Genbank no.	Reference
Query proteins involved in polyamine biosynthesis			
AAT	Agmatine aminopropyltransferase	YP_144090	(21)
ADC (AdiA)	Arginine decarboxylase	NP_418541	(23)
ADI (AguA)	Agmatine deiminase	NP_814483	(24)
PCT (AguB)	Putrescine carbamoyltransferase	EOT48407	(24)
APAUH	Aminopropylagmatine ureohydrolase	YP_144395	(21)
CASDC	Carboxyspermidine decarboxylase	NP_809587	(20)
CASDH	Carboxyspermidine dehydrogenase	WP_000025713	(28)
NCPAH	*N*-Carbamoylputrescine amidohydrolase	NP_248984	(30)
ADC (SpeA)	Arginine decarboxylase	NP_417413	(22)
AUH (SpeB)	Agmatine ureohydrolase	NP_417412	(27)
ODC (SpeC)	Ornithine decarboxylase	NP_417440	(32)
AdoMetDC (SpeD)	*S*-Adenosylmethionine decarboxylase	NP_414662	(25)
SPDsyn (SpeE)	Spermidine synthase	NP_414663	(39)
ODC (SpeF)	Ornithine decarboxylase	NP_415220	(31)
Query proteins involved in polyamine transport			
AguD	Agmatine/putrescine antiporter	NP_814482	(26)
MdtI	Membrane subunit of spermidine efflux transporter MdtJI	NP_416116	(29)
MdtJ	Membrane subunit of spermidine efflux transporter MdtJI	NP_416117	(29)
PlaP	Putrescine/H^+ symporter	NP_416518	(33)
PotA	ATP-binding protein of spermidine ATP-binding cassette transporter PotABCD	NP_415644	(34)
PotB	Permease of spermidine ATP-binding cassette transporter PotABCD	NP_415643	(34)
PotC	Permease of spermidine ATP-binding cassette transporter PotABCD	NP_415642	(34)
PotD	Substrate-binding protein of spermidine ATP-binding cassette transporter PotABCD	NP_415641	(34)
PotE	Ornithine-putrescine antiporter	ALI41513	(35)
PotF	Substrate-binding protein of putrescine ATP-binding cassette transporter PotFGHI	NP_415375	(37)
PotG	ATP-binding protein of putrescine ATP-binding cassette transporter PotFGHI	NP_415376	(37)
PotH	Permease of putrescine ATP-binding cassette transporter PotFGHI	NP_415377	(37)
PotI	Permease of putrescine ATP-binding cassette transporter PotFGHI	NP_415378	(37)
PuuP	Putrescine/H^+ symporter	NP_415812	(38)
SapB	Permease of putrescine ATP-binding cassette exporter SapBCDF	NP_415809	(41)
SapC	Permease of putrescine ATP-binding cassette exporter SapBCDF	NP_415808	(41)
SapD	ATP-binding protein of putrescine ATP-binding cassette exporter SapBCDF	NP_415807	(41)
SapF	ATP-binding protein of putrescine ATP-binding cassette exporter SapBCDF	NP_415806	(41)

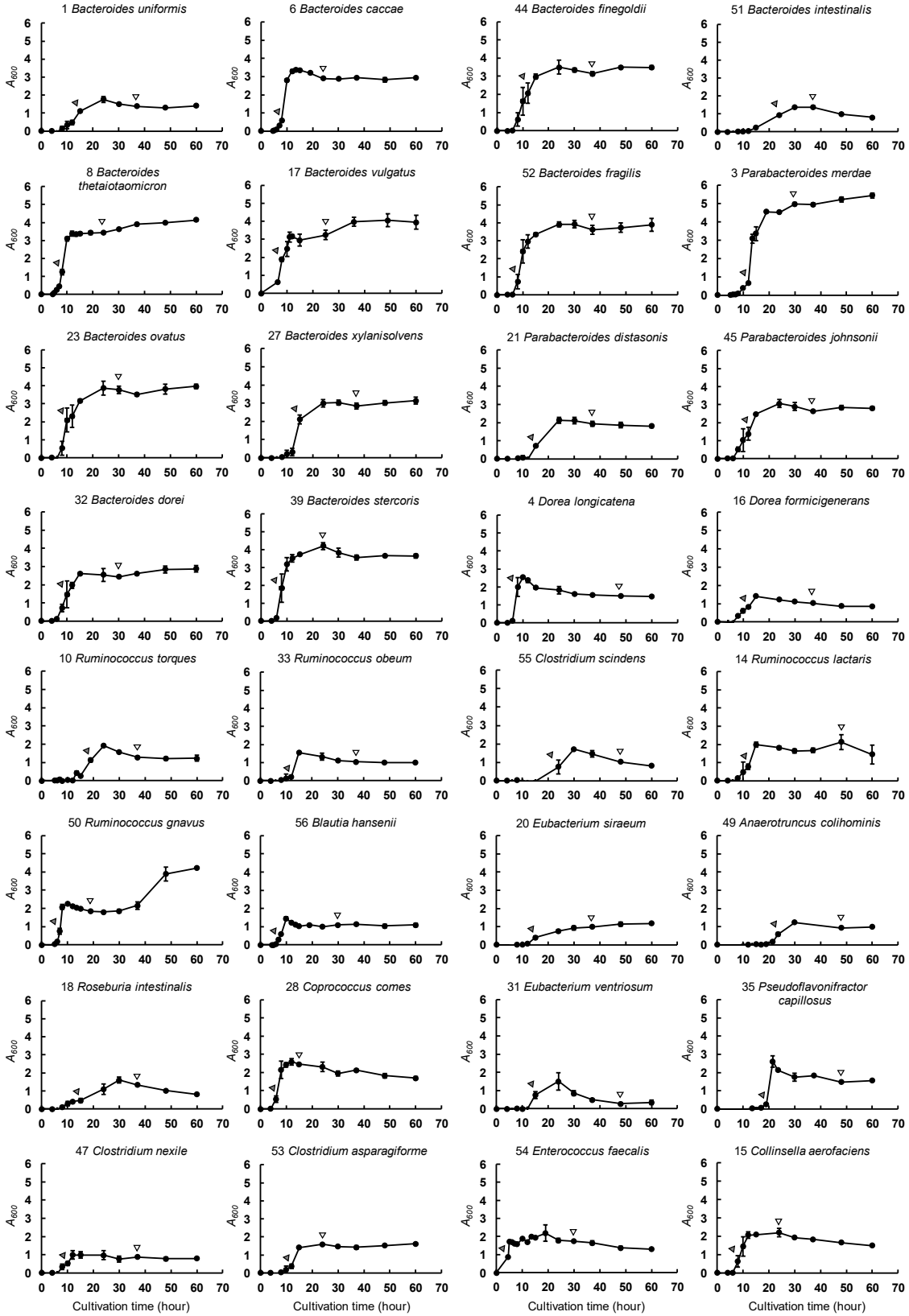

Fig. 2. Growth of dominant human gut microbes.

The sampling time for polyamine analysis is shown by arrowheads on the growth curves of tested dominant human gut microbes; it is obtained by reusing the Supplemental Figure S2 of a previous study (16). The gray arrowheads indicate the sampling point used for the growing phase and the white arrowheads indicate the sampling point used for the stationary phase.

RESULTS

Putrescine biosynthesis and transport in dominant human gut microbes

Put concentrations in dominant human gut microbial cells were normalized to cellular protein levels and are shown as nmol/mg protein. When values (Mean minus SD) of intracellular Put concentration (nmol/mg protein) was greater than zero, it was judged that the microbes possess Put in the cell. Based on this criterion, 5 (16%) (*B. ovatus*, *B. finegoldii*, *B. xylanisolvens*, *Dorea longicatena*, and *Ruminococcus lactaris*) of the 32 tested species of dominant gut microbes contained Put in the growing and/or stationary phase; however, the intracellular Put concentration in *B. xylanisolvens* was very low (0.56 ± 0.39 nmol/mg protein) (Fig. 3A).

The change in Put concentration was calculated by comparing the Put concentration in the culture supernatant with that originally contained in GAM (73.5 ± 3.7 μM, shown as a gray band in Fig. 3B). Because there is no report proving that Put is extracellularly degraded, the decrease in Put levels in the culture supernatant is thought to result from an uptake of Put by the cultured microbes. A decrease in Put concentration was observed in the culture supernatant in the growing and/or stationary phase of 7 (22%) (*B. dorei*, *B. finegoldii*, *P. johnsonii*, *D. formicigenerans*, *Clostridium asparagiforme*, *R. lactaris*, and *Eubacterium ventriosum*) of the 32 tested dominant human gut microbial species (Fig. 3B). In contrast, Put concentrations increased in the culture supernatants of 4 species (13%) (*B. intestinalis*, *R. obeum*, *C. scindens*, and *Enterococcus faecalis*) in the growing or stationary phase (Fig. 3B). Comparing the Put concentrations in the culture supernatant of growing phase to those of stationary phase, the Put concentration in the culture supernatant of 5 species (16%) (*B. dorei*, *B. stercoris*, *R. torques*,

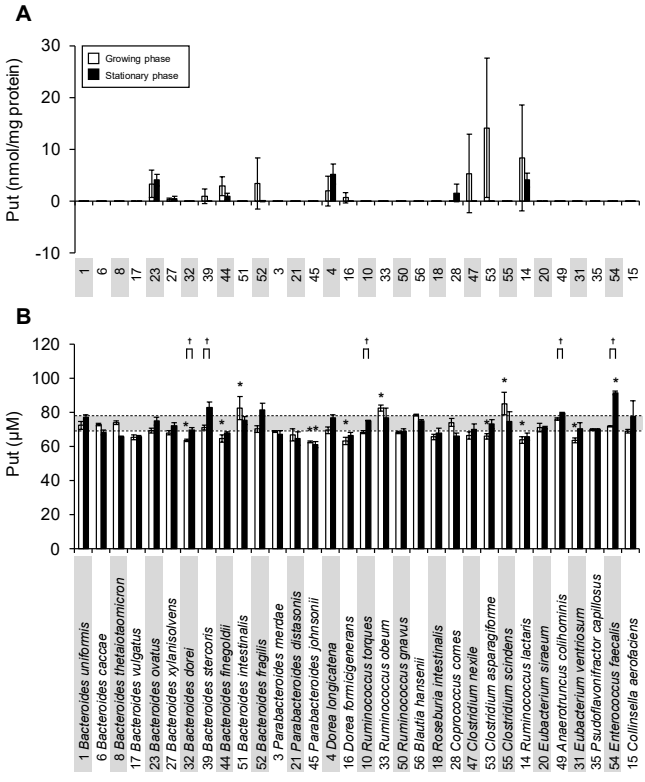

Fig. 3. Putrescine concentration in culture supernatants and cells of dominant human gut microbes.

(A) Intracellular putrescine concentrations in dominant human gut microbes in growing and stationary phases. The amount of putrescine in the cell was quantified by HPLC and normalized to the cellular protein concentration. White bars show putrescine concentrations in the growing phase, black bars show those in the stationary phase. Data are represented as mean ± SD. (n =3).

(B) Putrescine concentration in culture supernatants of gut microbes in the growing and stationary phases. Gray bands indicate the maximum and minimum putrescine concentration values in GAM (n = 3). White bars show the putrescine concentrations in growing phase, and black bars show those in the stationary phase. Data are mean ± SD. (n =3). $^{*}p < 0.01$ (Dunnett's test in comparison with GAM). $^{\dagger}p < 0.01$ (two-tailed unpaired *t*-test).

The number shown before the species name indicates the order of gut microbial occupancy (15).

Anaerotruncus colihominis, and *En. faecalis*), were increased from growing phase to stationary phase (Fig. 3B).

Spermidine biosynthesis and transport in the dominant human gut microbes

The presence of Spd in cells was determined based on the same criterion used for Put. Almost all tested dominant human gut microbial cells contained Spd in the growing or stationary phase (Fig. 4A), except for *D. formicigenerans* and *Collinsella aerofaciens*, which had no Spd in the cell, compared to the other dominant human gut mcirobes (Fig. 4A). *C. nexile* had very low levels of Spd (7.3 ± 5.2 nmol/mg protein).

The change in Spd concentration was calculated by comparing the Spd concentration in the culture supernatant with that originally contained in GAM (24.6 ± 1.0 μM, shown as a gray band in Fig. 4B). As it has not been reported thus far that Spd is extracellularly degraded, the decrease in Spd levels in the culture supernatant is thought to result from the transport of Spd by cultured microbes. The concentrations of Spd decreased in the culture supernatant of 22 (69%) of the 32 tested dominant gut microbial species in the growing or stationary phase. In 4 (13%) species (*B. dorei*, *D. formicigenerans*, *R. torques*, and *Blautia hansenii*), the Spd concentrations in the culture supernatant increased from the growing phase to the stationary phase (Fig. 4B). Furthermore, Spd concentration in the culture supernatant in the stationary phase of *B. vulgatus* was significantly higher than that originally contained in GAM (Fig. 4B). Spd concentrations in the culture supernatants of 10 (31%) species (*B. uniformis*, *B. intestinalis*, *P. merdae*, *P. distasonis*, *R. torques*, *R. obeum*, *Bl. hansenii*, *Eu. siraeum*, *Eu. ventriosum*, and *Co. aerofaciens*) of the 32 tested species did not change in either the growing or stationary phase compared to the Spd concentrations in GAM (Fig.

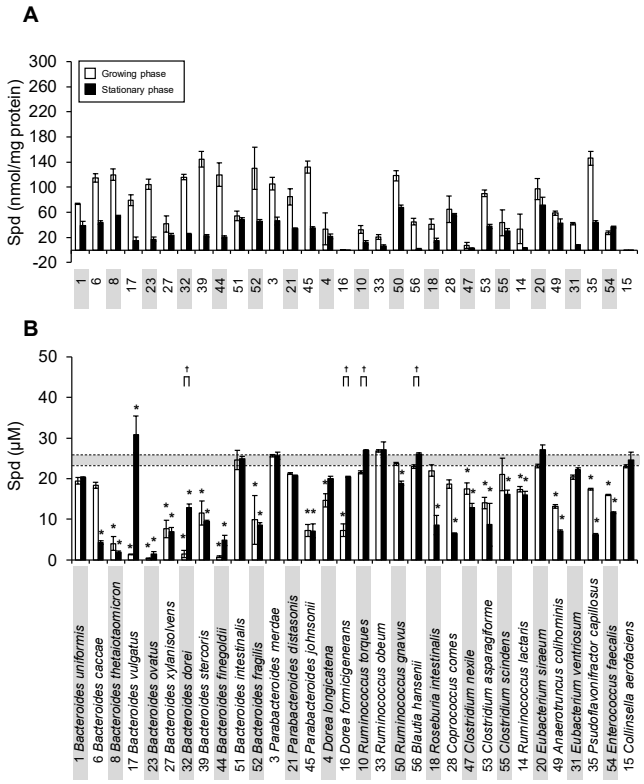

Fig. 4. Spermidine concentration in culture supernatants and cells of dominant human gut microbes.

(A) Intracellular spermidine concentration in the gut microbes in the growing and stationary phases. The amount of spermidine in the cell was quantified by HPLC, and normalized to the cellular protein concentration. White bars indicate spermidine concentrations in the growing phase, black bars indicate those in the stationary phase. Data are represented as mean ± SD. (n =3).

(B) Spermidine concentration in the culture supernatant of the gut microbes in the growing and stationary phases. The gray band indicates the maximum and minimum spermidine concentrations in GAM (n =3). White bars show the spermidine concentrations in the growing phase, black bars show those in the stationary phase. Data are represented mean ± SD. (n =3). $^{*}p < 0.01$ (Dunnett's test in comparison with GAM). $^{\dagger}p < 0.01$ (two-tailed unpaired t-test). The number shown before the species name indicates the order of gut microbial occupancy (15).

4B).

Spermine biosynthesis and transport in the dominant human gut microbes

The presence of Spm in cells was determined based on the same criterion used for Put. Spm was detected in the cells of 13 (41%) species (*B. vulagus*, *B. xylanisolvens, B. intestinalis*, *B. fragilis*, *P. merdae*, *D. longicatena*, *D. formicigenerans*, *R. torques*, *R. obeum*, *R. gnavus*, *Eu. siraeum*, *Eu. ventriosum*, and *Psudoflavonifractor capillosus*) of the 32 tested dominant human gut microbial species in the growing phase and/or stationary phase; however, the Spm concentration in *B. vulgatus*, *B. xylanisolvens*, *B. fragilis*, and *P. merdae* cells was very low (≤ 3.2 nmol/mg protein) (Fig. 5A).

The change in Spm concentration was estimated by comparing the Spm concentration in the culture supernatant of dominant human gut microbes to that in GAM (8.4 ± 0.4 μM, shown as a gray band in Fig. 5B). As with Put and Spd, extracellular Spm degradation has not been reported thus far. Hence, the change in Spm concentrations in the culture supernatant is thought to result from the transport of Spm by the cultured microbes. Spm concentration decreased in the culture supernatants of almost all tested dominant human gut microbes, except for *P. merdae* in the growing or stationary phase (Fig. 5B). In 3 (9%) species (*B. stercoris*, *D. longicatena*, and *R. torques*), Spm concentration in the culture supernatant increased from the growing phase to stationary phase (Fig. 5B).

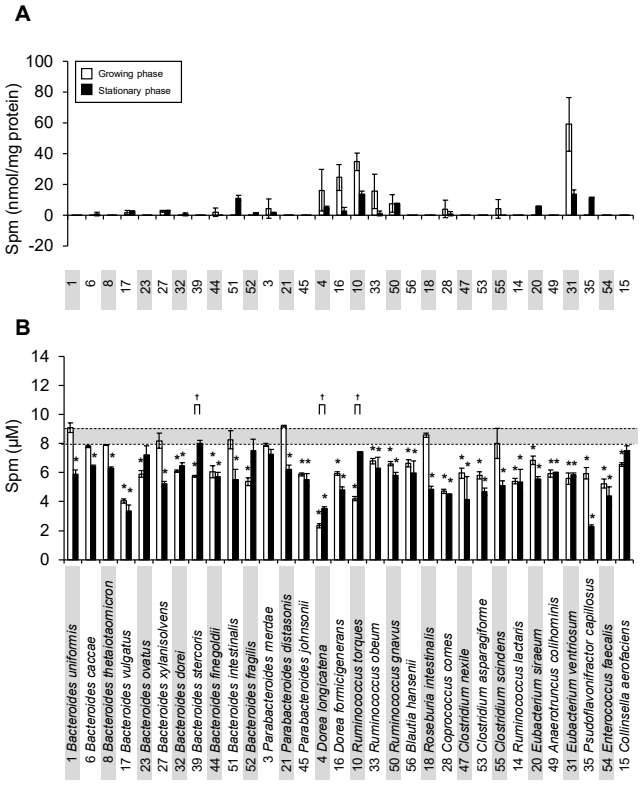

Fig. 5. Spermine concentration in culture supernatants and cells of dominant human gut microbes.

(A) Intracellular spermine concentration in the gut microbes in the growing and stationary phases. The spermine in the cell was quantified by HPLC, and normalized to the cellular protein concentration. White bars show spermine concentrations in the growing phase, black bars show those in the stationary phase. Data are represented as mean ± SD. (n =3).

(B) Spermine concentration in the culture supernatant of the gut microbes in growing and stationary phases. The gray band indicates the maximum and minimum spermine concentrations in GAM (n =3). White bars show the spermine concentrations in the growing phase; black bars show those in the stationary phase. Data are represented as mean ± SD. (n =3). $^{*}p < 0.01$ (Dunnett's test in comparison with GAM). $^{\dagger}p < 0.01$ (two-tailed unpaired t-test). The number shown before the species name indicates the order of gut microbial occupancy (15).

Presence of known polyamine biosynthetic and transport proteins in tested dominant human gut microbes

The results of BlastP analysis that determined the presence or absence of known polyamine biosynthetic or transport proteins in the dominant human gut microbes are shown in Fig. 6. In tested *Bacteroides* and *Parabacteroides* species, homologs of the known Put biosynthetic proteins SpeA, AguA, and NCPAH, which synthesize Put from arginine via *N*-carbamoylputrescine, are highly conserved (Figs. 1 and 6), with the exception of *P. distasonis*, which does not encode a SpeA homolog (Fig. 6). In addition, *B. xylanisolvens* encodes homologs of SpeC and SpeF (Fig. 6). Homologs of PotFGHI are found in all tested *Bacteroides* and *Parabacteroides* species (Fig. 6). Except for *B. uniformis* and *B. dorei*, the tested *Bacteroides* and *Parabacteroides* species possess an AguD homolog. A homolog of PlaP, one of the two Put/proton symporters, is found in *B. uniformis*, *B. vulagatus*, *B. dorei*, *B. fragilis*, *P. merdae*, and *P. johnsonii*. However, a homolog of PuuP, the other Put/proton symporter, is found only in *B. uniformis* (Fig. 6). Among the components of SapBCDF, *B. xylanisolvens* encodes homologs of SapB and SapF, while *B. fragilis* encodes homologs of SapD and SapF (Fig. 6). Homologs of CASDH and CASDC, which are known Spd biosynthetic proteins, are found in all *Bacteroides* and *Parabacteroides* species used in this study (Fig. 6), while only *B. xylanisolvens* encodes a SpeD homolog (Fig. 6). All tested *Bacteroides* and *Parabacteroides* species possess homologs of PotABCD, but do not encode homologs of MdtI and MdtJ (Fig. 6).

Of the known Put biosynthetic proteins, *Dorea* species encodes only the AguB homolog (Fig. 6). Homologs of PotFGHI and SapBCDF are found in *D. longicatena* and *D. formicigenerans* (Fig. 6); additionally, *D. longicatena* encodes an AguD homolog (Fig. 6). Homologs of known Spd biosynthetic proteins are absent from *D. longicatena* and *D. formicigenerans* (Fig. 6); both of these species possess PotABCD homologs (Fig. 6).

A homolog of AguB is possessed by all tested *Blautia* species except in *R. obeum*; additionally, a SpeB homolog is found in all *Blautia* species except in *R. torques* (Fig. 6). *R. torques* and *R. obeum* possess homologs of AguA and NCPAH; in addition, *R. torques* possesses a SpeA homolog (Fig. 6). PotFGHI homologs are found in all tested *Blautia* species (Fig. 6). *R. torques*, *R. obeum*, and *Bl. hansenii* encode SapBCDF homologs, while *R. gnavus* lacks a SapC homolog but encodes SapBDF homologs (Fig. 6). Homologs of APAUH, CASDH, CASDC, and SpeE are found in all tested *Blautia* species (Fig. 6). All *Blautia* species except for *Bl. hansenii* encode an AAT homolog (Fig. 6). A homolog of SpeD is present only in *Bl. hansenii* (Fig. 6). Out of all the known Spd transport proteins, only the PotABCD homologs are found in *Blautia* species (Fig. 6).

C. nexlile, *C. asparagiforme*, and *C. scindens* encode an AguB homolog (Fig. 6); in addition, *C. asparagiforme* and *C. nexile* possess a SpeB homolog (Fig. 6). Out of all the known Put transport proteins, only homologs of PotFGHI and SapBCDF are found in the *Clostridium* species used in this study (Fig. 6). Out of all the known Spd biosynthetic proteins, homologs of AAT, CASDC, CASDH,

and SpeE are found only in *C. nexile* (Fig. 6). An APAUH homolog is found in *C. nexile* and *C. asparagiforme* (Fig. 6). Of the known Spd transport proteins, PotABCD homologs are found in the tested *Clostridium* species (Fig. 6).

Microbes belonging to genera other than *Bacteroides*, *Parabacteroides*, *Dorea*, *Blautia*, and *Clostridium* encode an AguB homolog (Fig. 6). *Coprococcus comes*, *R. lactaris*, and *Ps. capillosus* encode a SpeB homolog (Fig. 6). A homolog of AguA is found in *Roseburia intestinalis*, *Eu. siraeum*, *Co. aerofaciens*, and *En. faecalis* (Fig. 6). *Ro. intestinalis*, *R. lactaris*, and *Eu. siraeum* possess an NCPAH homolog (Fig. 6). *Ro. intestinalis*, *Cop. comes*, *R. lactaris*, *A. colihominis*, *Eu. ventriosum*, *Ps. capillosus*, and *En. faecalis* possess PotFGHI homologs, and *Eu. siraeum* and *Co. aerofaciens* possess only the PotG homolog. (Fig. 6). Homologs of SapBCDF are found in *Ro. intestinalis*, *Cop. comes*, *A. colihominis*, *Eu. ventriosum*, *Ps. capillosus*, *En. faecalis*, and *Co. aerofaciens* (Fig. 6). AguD and its homolog are encoded in both *En. faecalis* and *Co. aerofaciens* (Fig. 6). *Eu. siraeum* does not possess homologs of the known Put transport proteins (Fig. 6). Homologs of known Spd biosynthetic proteins are absent in *A. colihominis*, *Eu. ventriosum*, *En. faecalis*, and *Co. aerofaciens* (Fig. 6). In contrast, *Ps. capillosus* encodes homologs of all the known Spd biosynthetic proteins (Fig. 6). Of the known Spd biosynthetic proteins, *Ro. intestinalis* encodes homologs of AAT, CASDH, CASDC, and SpeE (Fig. 6). *Cop. comes* possesses only APAUH and CASDH homologs (Fig. 6). *R. lactaris* encodes homologs of all the known Spd biosynthetic proteins except SpeD (Fig. 6). *Eu. siraeum* possesses homologs of all known Spd biosynthetic proteins except APAUH (Fig. 6). *Ro. intestinalis*, *Cop. comes*, *R. lactaris*, *A. colihominis*, *Eu. ventriosum*, *Ps. capillosus*, and *En. faecalis* possess PotABCD homologs, whereas *Eu. siraeum* and *Co. aerofaciens* enocode only the PotA homolog out of the known Spd transport proteins (Fig. 6).

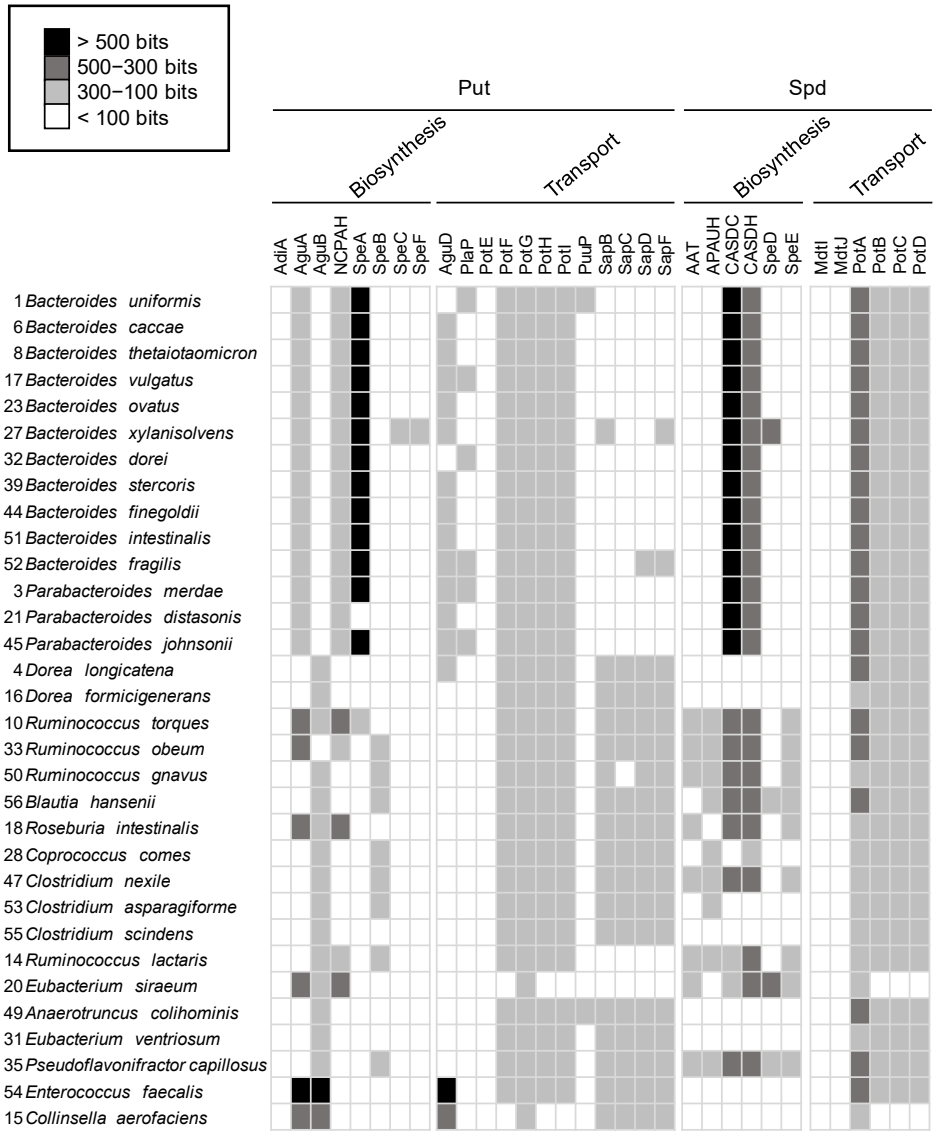

Fig. 6. Occurrence of homologous proteins responsible for synthesis and transport of polyamines in the genomes of dominant human gut microbes.

The BlastP analysis was performed against the genomes of the dominant human gut microbes using query proteins listed in table 2. Black, dark gray, light gray, and white boxes indicate the result of homologs with scores > 500 bits, between 300 and 500 bits, between 100 and 300 bits, and < 100 bits, respectively. The number shown before the species name indicates the order of gut microbial occupancy in a "human gut microbial gene catalog" (15).

DISCUSSION

The presence of novel polyamine biosynthetic/transport proteins in the dominant human gut microbes was determined by integrating biosynthetic and transport activity for each polyamine (Figs. 3-5) and by BlastP analysis (Fig. 6).

First, the presence of novel Put biosynthetic proteins was estimated. Five species (*B. ovatus*, *B. xylanisolvens*, *B. finegoldii*, *D. longicatena*, and *R. lactaris*) contained Put in the cell in the growing or stationary phase (Fig. 3A). A decrease in Put levels in the medium were observed in cultures of *B. finegoldii* and *R. lactrais* (Fig. 3B), suggesting that Put in the cell originates from Put in the medium. Among the remaining three microbial species that appeared not to take up Put from the media (Fig. 3B), *B. ovatus* and *B. xylanisolvens* encode homologs of AdiA, SpeA, AguA, and NCPAH (Fig. 6) and *B. xylanisolvens* encodes a homolog of ODC (Fig. 6). These results suggest that these two species synthesize Put using known Put biosynthetic proteins. In contrast, *D. longicatena* only possesses a PCT homolog with a low score (Fig. 6); its incomplete pathway suggests that *D. longicatena* has novel Put biosynthetic enzyme(s).

All the 7 strains that appeared to take up Put from the media (*B. dorei*, *P. johnsonii*, *D. longicatena*, *D. formicigenerans*, *R. torques*, *R. lactaris*, and *A. colihominis*) (Fig. 3B) contain a PotFGHI homolog (Fig. 6), and *B. dorei* and *P. johnsonii* possess a PlaP homolog in addition to PotFGHI homologs (Fig. 6). These results suggest that these known transporters are involved in the observed uptake of Put. Put concentration in the culture supernatant increased in 5 species (*B. dorei*, *B. stercoris*, *R. torques*, *A. colihominis*, and *En. faecalis*) (Fig. 3B) from the growing phase to stationary phase. The Put-agmatine antiporter AguD and Put exporter SapBCDF have been previously described in *En. faecalis* (26) and *Escherichia coli* (41) (described details in SECTION III of CHAPTER II), respectively. *En. faecalis* possesses homologs of SapBCDF in addition to AguD, suggesting that *En. faecalis* exports Put to the culture supernatant via AguD and/or homologs of SapBCDF. An AguD homolog was found in *B. stercoris* (Fig. 6), and *R. torques* and *A. colihominis* possesses homologs of SapBCDF (Fig. 6). These observations suggest that Put is exported to the culture supernatant from *B. sterocoris* via AguD homolog, and from *R. torques* and *A. colihominis* via SapBCDF homologs. However, *B. dorei* does not possess homologs of AguD, PotE, or SapBCDF (Fig. 6). These results suggest that a novel Put exporter(s) is present in *B. dorei*.

Next, the presence of novel Spd biosynthetic proteins was assessed. Almost all the tested dominant human gut microbes except *D. formicigenerans* and *Co. aerofaciens* contained intracellular Spd (Fig. 4A). A decrease in Spd in the medium of 22 species was observed (Fig. 4B), suggesting that Spd in the cell originates from Spd in the medium. Among the remaining 9 species (*B. uniformis*, *B. intestinalis*, *P. merdae*, *P. distasonis*, *R. torques*, *R. obeum*, *Bl. hansenii*, *Eu. siraeum*, and *Eu. ventriosum*), which appeared not to take up Spd from the medium (Fig. 4B), *B. uniformis*, *B.*

intestinalis, *P. merdae*, *P. distasonis*, *R. torques*, *R. obeum*, *Bl. hansenii*, and *Eu. siraeum* encode CASDC and CASDH homologs (Fig. 6). In addition, *R. torques*, *R. obeum*, *Bl. hansenii*, and *Eu. siraeium* encode a SpeE homolog (Fig. 6). Furthermore, *R. torques* and *R. obeum* possess homologs of AAT and APAUH (Fig. 6), suggesting that these 8 species synthesize Spd using known Spd biosynthetic enzymes. In contrast, *Eu. ventriousm* did not possess any homolog of the known Spd biosynthetic proteins (Fig. 6), suggesting that *Eu. ventriosum* possesses a novel Spd biosynthetic enzyme(s). All 22 strains that appear to take up Spd from the medium (Fig. 4B) possess PotABCD homologs (Fig. 6). These observations suggest that PotABCD homologs are involved in the observed Spd uptake. Although Spd concentration in the culture supernatant of 4 strains (*B. dorei*, *D. formicigenerans*, *R. torques*, and *Bl. hansenii*) increased from the growing to stationary phases (Fig. 4B), homologs of the known Spd exporter MdtJI were not found (Fig. 6). Additionary, Spd concentration in the culture supernatant of *B. vulgatus* was significantly higher than Spd originally contained in GAM, however, *B. vulgatus* does not possess the homologs of MdtJI. These results suggested that a novel Spd exporter(s) is present in these 5 species.

In this study, the author found that cells of 13 species (*B. vulgatus*, *B. xylanisolvens*, *B. intestinalis*, *B. fragilis*, *P. merdae*, *D. longicatena*, *D. formicigenerans*, *R. torques*, *R. obeum*, *R. gnavus*, *Eu. siraeum*, *Eu. ventriosum*, and *Ps. capillosus*) contained Spm (Fig. 5A). A decrease in Spm was observed with all these species except *P. merdae* in the medium (Fig. 5B), suggesting that Spm in the cell originates from Spm in the medium. Since Spm levels in the culture supernatant did not change after cultivation of *P. merdae*, Spm found in the cell of this microbe was not derived from the growth medium (Fig. 5B). Kim *et al*. recently reported that *Agrobacterium tumefaciens* C58 synthesizes Spm from Spd by using CASDH and CASDC (homologs of which are found in *P. merdae*) (Fig. 6) only when ODC activity was partially inhibited using difluoromethylornithine (DFMO, ODC specific inhibitor) (42). Although the possibility of Spm synthesis in *P. merdae* with homologs of CASDH and CASDC cannot be completely excluded, it is possible that *P. merdae* has a novel Spm biosynthetic protein(s) because the condition under which *Ag. tumefaciens* C58 synthesizes Spm is not physiological.

All tested dominant human gut microbes except for *P. merdae* decreased Spm in the culture supernatant in the growing or stationary phase (Fig. 5B). Kashiwagi *et al*. reported that PotABCD in *E. coli* showed a weak Spm uptake activity (43). In addition, Yao *et al*. biochemically showed that PotABCD in *Streptococcus aureus* showed a Spm uptake activity, which was comparable to its Spd uptake activity (44). Therefore, it is possible that almost all dominant human gut microbes take up Spm via a PotABCD homolog. However, because *Eu. siraeum* and *Co. aerofaciens* have only a PotA homolog (Fig. 6), these two species could have a novel Spm transporter(s). Spm concentration in the culture supernatant of 3 species (*B. stercoris*, *D. longicatena*, and *R. torques*) increased from the growing to stationary phase (Fig. 5B). No Spm exporter in these microbes has been previously

described. Therefore, it is conceivable that these 3 species possess a novel Spm exporter(s).

In the present study, the author showed that 32 species of the tested dominant human gut microbes possess different polyamine biosynthetic and transport activities. The potential presence of novel polyamine metabolism and transport genes was shown by combining polyamine concentration analysis in the cells and culture supernatant with analyzing via BlastP. Despite decreased polyamine concentrations in the culture supernatant of some species, intracellular polyamine levels did not increase (e.g., Put concentration in cell and culture supernatant of *B. dorei*, *P. johnsonii*, and *Eu. ventriosum*). These results suggest that these strains (e.g., *B. dorei*, *P. johnsonii*, and *Eu. ventriosum*) rapidly metabolized the polyamines, and/or intracellular polyamine levels of these strains were below the detection limit due to a limited intracellular polyamine pool. On the other hand, some species exhibited increasing polyamine concentrations in the culture supernatant from growing to stationary phases, while intracellular polyamine concentrations did not change (e.g., Put concentration in cell and culture supernatant of *B. dorei*, *B. stercoris*, *R. torques*, *A. colihominis*, and *En. faecalis*). It is possible that these results are due to homeostatic regulation of intracellular polyamine concentration, which is consistent with how *E. coli* exports Put to the culture supernatant, while intracellular Put concentrations remain unchanged (described in SECTION III of CHAPTER II) (41).

The above estimation of the presence of novel polyamine biosynthetic and transport proteins in the tested dominant human gut microbes is summarized in Fig. 7. Thus far, if a microbe synthesizing or transporting polyamines possessed homolog(s) of polyamine biosynthetic proteins or transporters, it was inferred that the microbe did not have novel biosynthetic proteins or transporters for polyamines. However, this criterion is not always appropriate because some microbes have redundant proteins possessing the same functions. For example, *E. coli* has four Put transporters (33,36-38) and two Put biosynthetic pathways (27,32). Therefore, the potential presence of novel polyamine biosynthetic and transport proteins is conceivable even in microbes that do not encode novel proteins involved in polyamine biosynthesis or transport. Furthermore, in BlastP analysis, a bit score cutoff that was ≥ 100 was considered as the threshold for the identification of homologs in the study so far. However, if the threshold value was 200 bits, the number of homologs identified decreased markedly (Fig. 8). As a result, novel polyamine biosynthetic and transport proteins that were predicted to exist in the tested dominant human gut microbes markedly

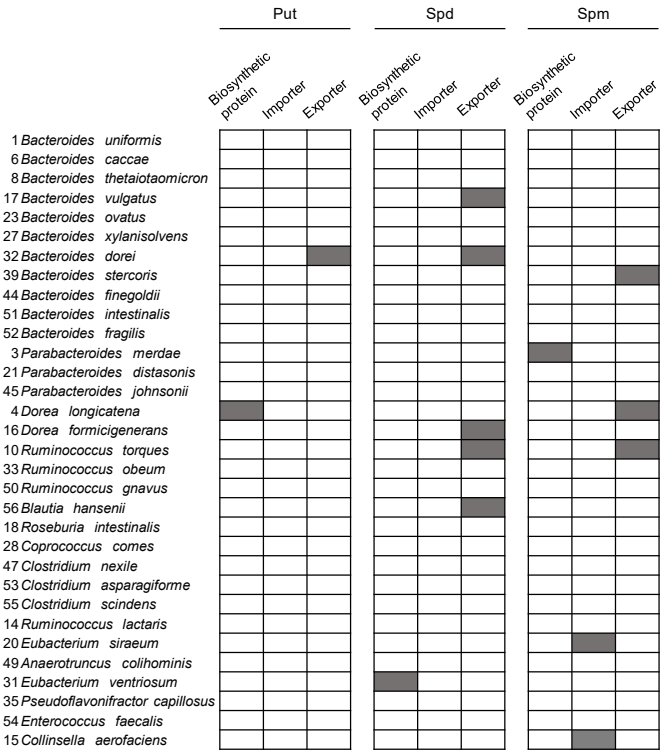

Fig. 7. Novel polyamine biosynthetic proteins and transporters expected to exist in the tested dominant human gut microbes.
The presence of novel polyamine biosynthetic proteins and transporters was predicted from the changes in polyamine concentrations in the culture supernatants and cells and the presence or absence of homologs of known polyamine biosynthetic proteins and transporters. Presence or absence of novel polyamine biosynthetic proteins and transporters is indicated by the color of boxes; gray boxes indicate presence and white boxes indicate absence. The number shown before the species name indicates the order of gut microbial occupancy in a "human gut microbial gene catalog" (15).

increased from 13 to 46 (Fig. 9).

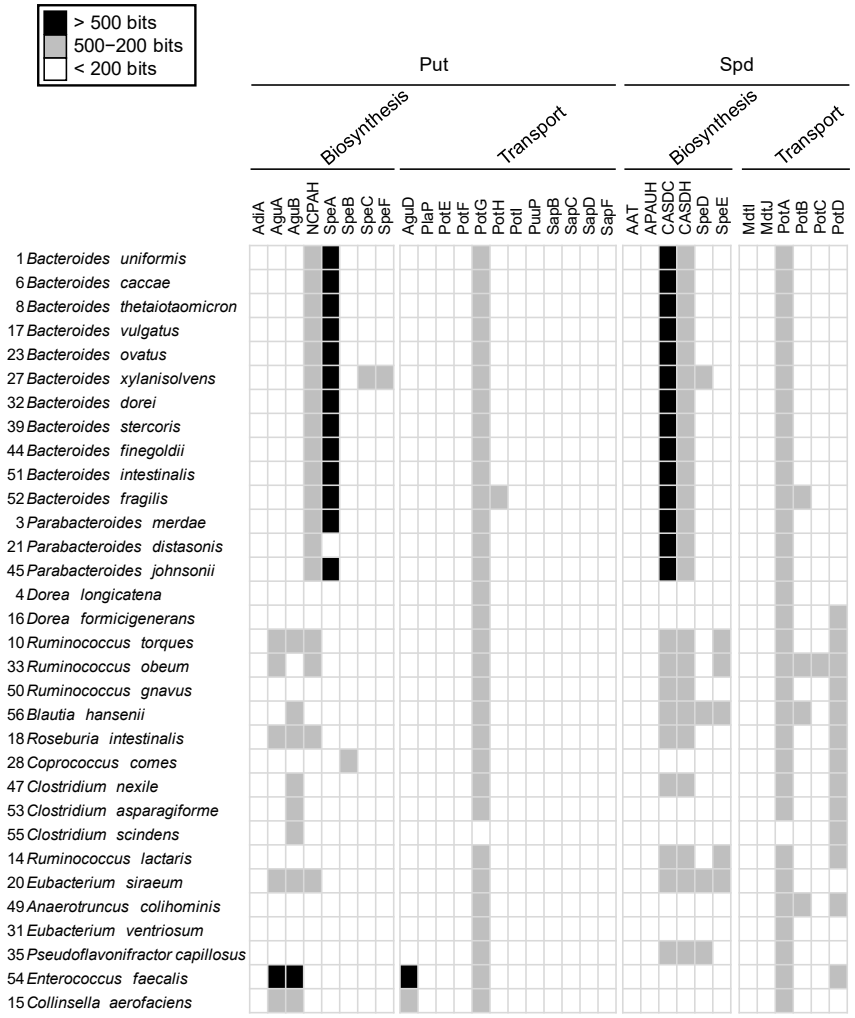

Fig. 8. Occurrence of homologous proteins responsible for synthesis and transport of polyamines in the genomes of dominant human gut microbes. The BlastP analysis was performed against the genomes of the dominant human gut microbes using query proteins listed in table 2. Black, light gray, and white boxes indicate the result of homologs with scores > 500 bits, between 200 and 500 bits, and < 200 bits, respectively. The number shown before the species name indicates the order of gut microbial occupancy in a "human gut microbial gene catalog" (15).

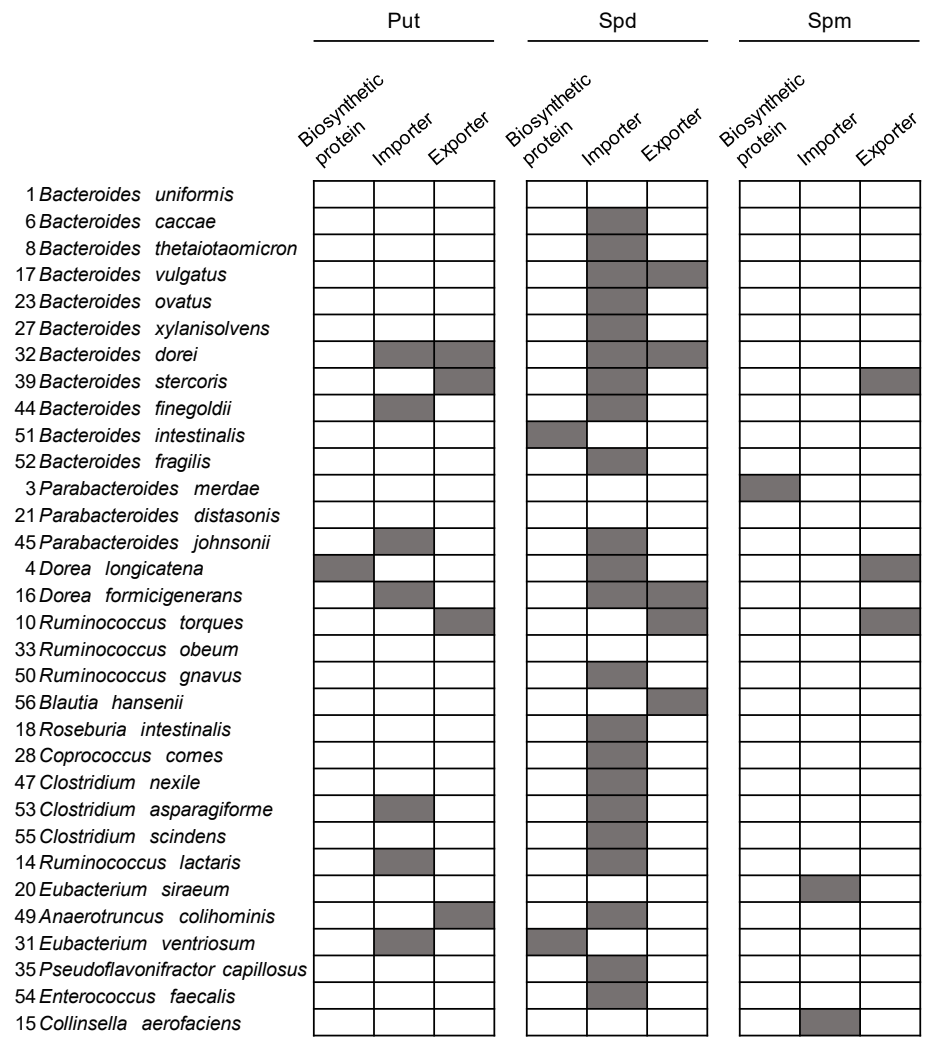

Fig. 9. Novel polyamine biosynthetic proteins and transporters expected to exist in the tested dominant human gut microbes.

The presence of novel polyamine biosynthetic proteins and transporters was predicted from the changes in polyamine concentrations in the culture supernatants and cells and the presence or absence of homologs of known polyamine biosynthetic proteins and transporters (showed in Fig. 8). Presence or absence of novel polyamine biosynthetic proteins and transporters is indicated by the color of boxes; gray boxes indicate presence and white boxes indicate absence. The number shown before the species name indicates the order of gut microbial occupancy in a "human gut microbial gene catalog" (15).

REFERENCES

1. Pegg, A. E. (2009) Mammalian polyamine metabolism and function. *IUBMB Life* **61**, 880-894
2. Tabor, C. W., and Tabor, H. (1985) Polyamines in microorganisms. *Microbiol Rev* **49**, 81-99
3. Matsumoto, M., Kakizoe, K., and Benno, Y. (2007) Comparison of fecal microbiota and polyamine concentration in adult patients with intractable atopic dermatitis and healthy adults. *Microbiol Immunol* **51**, 37-46
4. Matsumoto, M., Kibe, R., Ooga, T., Aiba, Y., Kurihara, S., Sawaki, E., Koga, Y., and Benno, Y. (2012) Impact of intestinal microbiota on intestinal luminal metabolome. *Sci Rep* **2**, 233
5. Noack, J., Kleessen, B., Proll, J., Dongowski, G., and Blaut, M. (1998) Dietary guar gum and pectin stimulate intestinal microbial polyamine synthesis in rats. *J Nutr* **128**, 1385-1391
6. Noack, J., Dongowski, G., Hartmann, L., and Blaut, M. (2000) The human gut bacteria *Bacteroides thetaiotaomicron* and *Fusobacterium varium* produce putrescine and spermidine in cecum of pectin-fed gnotobiotic rats. *J Nutr* **130**, 1225-1231
7. Kibe, R., Kurihara, S., Sakai, Y., Suzuki, H., Ooga, T., Sawaki, E., Muramatsu, K., Nakamura, A., Yamashita, A., Kitada, Y., Kakeyama, M., Benno, Y., and Matsumoto, M. (2014) Upregulation of colonic luminal polyamines produced by intestinal microbiota delays senescence in mice. *Sci Rep* **4**, 4548
8. Johnson, C. H., Dejea, C. M., Edler, D., Hoang, L. T., Santidrian, A. F., Felding, B. H., Ivanisevic, J., Cho, K., Wick, E. C., Hechenbleikner, E. M., Uritboonthai, W., Goetz, L., Casero, R. A., Pardoll, D. M., White, J. R., Patti, G. J., Sears, C. L., and Siuzdak, G. (2015) Metabolism links bacterial biofilms and colon carcinogenesis. *Cell Metab* **21**, 891-897
9. Matsumoto, M., Kurihara, S., Kibe, R., Ashida, H., and Benno, Y. (2011) Longevity in mice is promoted by probiotic-induced suppression of colonic senescence dependent on upregulation of gut bacterial polyamine production. *PLoS One* **6**, e23652
10. Lux, G. D., Marton, L. J., and Baylin, S. B. (1980) Ornithine decarboxylase is important in intestinal mucosal maturation and recovery from injury in rats. *Science* **210**, 195-198
11. Kurihara, S., Oda, S., Kato, K., Kim, H. G., Koyanagi, T., Kumagai, H., and Suzuki, H. (2005) A novel putrescine utilization pathway involves gamma-glutamylated intermediates of *Escherichia coli* K-12. *J Biol Chem* **280**, 4602-4608
12. Michael, A. J. (2016) Biosynthesis of polyamines and polyamine-containing molecules. *Biochem J* **473**, 2315-2329
13. Michael, A. J. (2016) Polyamines in Eukaryotes, Bacteria, and Archaea. *J Biol Chem* **291**, 14896-14903
14. Michael, A. J. (2015) Biosynthesis of Polyamines in Eukaryotes, Archaea,and Bacteria. in

Polyamines, Springer. pp 3-14

15. Qin, J., Li, R., Raes, J., Arumugam, M., Burgdorf, K. S., Manichanh, C., Nielsen, T., Pons, N., Levenez, F., Yamada, T., Mende, D. R., Li, J., Xu, J., Li, S., Li, D., Cao, J., Wang, B., Liang, H., Zheng, H., Xie, Y., Tap, J., Lepage, P., Bertalan, M., Batto, J. M., Hansen, T., Le Paslier, D., Linneberg, A., Nielsen, H. B., Pelletier, E., Renault, P., Sicheritz-Ponten, T., Turner, K., Zhu, H., Yu, C., Jian, M., Zhou, Y., Li, Y., Zhang, X., Qin, N., Yang, H., Wang, J., Brunak, S., Doré, J., Guarner, F., Kristiansen, K., Pedersen, O., Parkhill, J., Weissenbach, J., Bork, P., Ehrlich, S. D., and Consortium, M. (2010) A human gut microbial gene catalogue established by metagenomic sequencing. *Nature* **464**, 59-65
16. Gotoh, A., Nara, M., Sugiyama, Y., Sakanaka, M., Yachi, H., Kitakata, A., Nakagawa, A., Minami, H., Okuda, S., Katoh, T., Katayama, T., and Kurihara, S. (2017) Use of Gifu Anaerobic Medium for culturing 32 dominant species of human gut microbes and its evaluation based on short-chain fatty acids fermentation profiles. *Biosci Biotechnol Biochem* **81**, 2009-2017
17. Hamana, K., Itoh, T., Benno, Y., and Hayashi, H. (2008) Polyamine distribution profiles of new members of the phylum Bacteroidetes. *J Gen Appl Microbiol* **54**, 229-236
18. Hosoya, R., and Hamana, K. (2004) Distribution of two triamines, spermidine and homospermidine, and an aromatic amine, 2-phenylethylamine, within the phylum Bacteroidetes. *J Gen Appl Microbiol* **50**, 255-260
19. Hanfrey, C. C., Pearson, B. M., Hazeldine, S., Lee, J., Gaskin, D. J., Woster, P. M., Phillips, M. A., and Michael, A. J. (2011) Alternative spermidine biosynthetic route is critical for growth of *Campylobacter jejuni* and is the dominant polyamine pathway in human gut microbiota. *J Biol Chem* **286**, 43301-43312
20. Sakanaka, M., Sugiyama, Y., Kitakata, A., Katayama, T., and Kurihara, S. (2016) Carboxyspermidine decarboxylase of the prominent intestinal microbiota species *Bacteroides thetaiotaomicron* is required for spermidine biosynthesis and contributes to normal growth. *Amino Acids* **48**, 2443-2451
21. Ohnuma, M., Terui, Y., Tamakoshi, M., Mitome, H., Niitsu, M., Samejima, K., Kawashima, E., and Oshima, T. (2005) N^1-aminopropylagmatine, a new polyamine produced as a key intermediate in polyamine biosynthesis of an extreme thermophile, *Thermus thermophilus*. *J Biol Chem* **280**, 30073-30082
22. Moore, R. C., and Boyle, S. M. (1990) Nucleotide sequence and analysis of the *speA* gene encoding biosynthetic arginine decarboxylase in *Escherichia coli*. *J Bacteriol* **172**, 4631-4640
23. Stim, K. P., and Bennett, G. N. (1993) Nucleotide sequence of the *adi* gene, which encodes the biodegradative acid-induced arginine decarboxylase of *Escherichia coli*. *J Bacteriol*

175, 1221-1234

24. Llácer, J. L., Polo, L. M., Tavárez, S., Alarcón, B., Hilario, R., and Rubio, V. (2007) The gene cluster for agmatine catabolism of *Enterococcus faecalis*: study of recombinant putrescine transcarbamylase and agmatine deiminase and a snapshot of agmatine deiminase catalyzing its reaction. *J Bacteriol* **189**, 1254-1265
25. Tabor, C. W., and Tabor, H. (1987) The *speEspeD* operon of *Escherichia coli*. Formation and processing of a proenzyme form of *S*-adenosylmethionine decarboxylase. *J Biol Chem* **262**, 16037-16040
26. Suárez, C., Espariz, M., Blancato, V. S., and Magni, C. (2013) Expression of the agmatine deiminase pathway in *Enterococcus faecalis* is activated by the AguR regulator and repressed by CcpA and PTS(Man) systems. *PLoS One* **8**, e76170
27. Satishchandran, C., and Boyle, S. M. (1986) Purification and properties of agmatine ureohydrolyase, a putrescine biosynthetic enzyme in *Escherichia coli*. *J Bacteriol* **165**, 843-848
28. Lee, J., Sperandio, V., Frantz, D. E., Longgood, J., Camilli, A., Phillips, M. A., and Michael, A. J. (2009) An alternative polyamine biosynthetic pathway is widespread in bacteria and essential for biofilm formation in *Vibrio cholerae*. *J Biol Chem* **284**, 9899-9907
29. Higashi, K., Ishigure, H., Demizu, R., Uemura, T., Nishino, K., Yamaguchi, A., Kashiwagi, K., and Igarashi, K. (2008) Identification of a spermidine excretion protein complex (MdtJI) in *Escherichia coli*. *J Bacteriol* **190**, 872-878
30. Nakada, Y., and Itoh, Y. (2003) Identification of the putrescine biosynthetic genes in *Pseudomonas aeruginosa* and characterization of agmatine deiminase and *N*-carbamoylputrescine amidohydrolase of the arginine decarboxylase pathway. *Microbiology* **149**, 707-714
31. Kashiwagi, K., Suzuki, T., Suzuki, F., Furuchi, T., Kobayashi, H., and Igarashi, K. (1991) Coexistence of the genes for putrescine transport protein and ornithine decarboxylase at 16 min on *Escherichia coli* chromosome. *J Biol Chem* **266**, 20922-20927
32. Morris, D. R., and Pardee, A. B. (1965) A biosynthetic ornithine decarboxylase in *Escherichia coli*. *Biochem Biophys Res Commun* **20**, 697-702
33. Kurihara, S., Suzuki, H., Oshida, M., and Benno, Y. (2011) A novel putrescine importer required for type 1 pili-driven surface motility induced by extracellular putrescine in *Escherichia coli* K-12. *J Biol Chem* **286**, 10185-10192
34. Furuchi, T., Kashiwagi, K., Kobayashi, H., and Igarashi, K. (1991) Characteristics of the gene for a spermidine and putrescine transport system that maps at 15 min on the *Escherichia coli* chromosome. *J Biol Chem* **266**, 20928-20933
35. Kashiwagi, K., Miyamoto, S., Suzuki, F., Kobayashi, H., and Igarashi, K. (1992) Excretion

of putrescine by the putrescine-ornithine antiporter encoded by the *potE* gene of *Escherichia coli*. *Proc Natl Acad Sci U S A* **89**, 4529-4533

36. Kashiwagi, K., Shibuya, S., Tomitori, H., Kuraishi, A., and Igarashi, K. (1997) Excretion and uptake of putrescine by the PotE protein in *Escherichia coli*. *J Biol Chem* **272**, 6318-6323
37. Pistocchi, R., Kashiwagi, K., Miyamoto, S., Nukui, E., Sadakata, Y., Kobayashi, H., and Igarashi, K. (1993) Characteristics of the operon for a putrescine transport system that maps at 19 minutes on the *Escherichia coli* chromosome. *J Biol Chem* **268**, 146-152
38. Kurihara, S., Tsuboi, Y., Oda, S., Kim, H. G., Kumagai, H., and Suzuki, H. (2009) The putrescine Importer PuuP of *Escherichia coli* K-12. *J Bacteriol* **191**, 2776-2782
39. Tabor, C. W., Tabor, H., and Xie, Q. W. (1986) Spermidine synthase of *Escherichia coli*: localization of the *speE* gene. *Proc Natl Acad Sci U S A* **83**, 6040-6044
40. Camacho, C., Coulouris, G., Avagyan, V., Ma, N., Papadopoulos, J., Bealer, K., and Madden, T. L. (2009) BLAST+: architecture and applications. *BMC Bioinformatics* **10**, 421
41. Sugiyama, Y., Nakamura, A., Matsumoto, M., Kanbe, A., Sakanaka, M., Higashi, K., Igarashi, K., Katayama, T., Suzuki, H., and Kurihara, S. (2016) A Novel Putrescine Exporter SapBCDF of *Escherichia coli*. *J Biol Chem* **291**, 26343-26351
42. Kim, S. H., Wang, Y., Khomutov, M., Khomutov, A., Fuqua, C., and Michael, A. J. (2016) The Essential Role of Spermidine in Growth of *Agrobacterium tumefaciens* Is Determined by the 1,3-Diaminopropane Moiety. *ACS Chem Biol* **11**, 491-499
43. Kashiwagi, K., Hosokawa, N., Furuchi, T., Kobayashi, H., Sasakawa, C., Yoshikawa, M., and Igarashi, K. (1990) Isolation of polyamine transport-deficient mutants of *Escherichia coli* and cloning of the genes for polyamine transport proteins. *J Biol Chem* **265**, 20893-20897
44. Yao, X., and Lu, C. D. (2014) Functional characterization of the *potRABCD* operon for spermine and spermidine uptake and regulation in *Staphylococcus aureus*. *Curr Microbiol* **69**, 75-81

SUMMARY

Recent studies have reported that polyamines in the colonic lumen might affect animal health and these polyamines are thought to be produced by gut microbes. In this SECTION, the author measured the concentrations of three polyamines (putrescine, spermidine, and spermine) in cells and culture supernatants of 32 dominant human gut microbial species in their growing and stationary phases. Combining polyamine concentration analysis in culture supernatant and cells with available genomic information showed that novel polyamine biosynthetic proteins and transporters were present in dominant human gut microbes. Based on these findings, the author suggested strategies for optimizing polyamine concentrations in the human colonic lumen via regulation of genes responsible for polyamine biosynthesis and transport in the dominant human gut microbes.

SECTION II
Polyamine biosynthetic and transport ability of human indigenous *Bifidobacterium* species

In animal species that have been analyzed, polyamines are also found in the colonic lumen at concentrations ranging from hundreds of micromolar to several millimolar (1,2). These colonic luminal polyamines have been derived from gut bacteria (3-5). In SECTION I of CHAPTER II, the author evaluated polyamine biosynthetic and transport ability of 32 species of dominant human gut microbes.

Bifidobacteria are one of the major human indigenous commensal microbes, which are highly abundant in the healthy adult Japanese gut microbiome (6) and the relative abundance in the gut microbiome of Asian children reaches several tens of percent (7). It was reported that bifidobacteria exert beneficial influences on animals, such as allergy suppression (8), cancer prevention (9,10), and inhibition of pathogen colonization (11). Therefore, several *Bifidobacterium* species are used in probiotics which are a live microbial food supplement that beneficially affects the host animal by modulating its intestinal balance.

Matsumoto *et al*. reported that oral administration of probiotic *Bifidobacterium animalis* subsp. *lactis* significantly increases intestinal spermine (Spm) concentration in mice (12). Two possible mechanisms could explain why intestinal Spm concentration is increased by bifidobacteria administration: (1) bifidobacteria biosynthesize and produce polyamines; (2) polyamines are produced by enterocytes and/or gut microbes stimulated by bifidobacteria. However, there are no reports describing polyamine biosynthetic and transport ability of *Bifidobacterium* species except for one by Hamana in 1997 that quantified the intracellular polyamine concentrations of stationary phase cells of *Bifidobacterium bifidum*, *Bifidobacterium breve*, *Bifidobacterium longum* subsp. *longum*, and *B. longum* subsp. *infantis* (13). It was concluded that these *Bifidobacterium* species do not have polyamine biosynthetic ability (13). However, to understand the influence of bifidobacteria on the environment, i.e., the colonic lumen of their host, the polyamine transport ability of bifidobacteria needs to be analyzed. Additionally, because polyamine concentrations in cells and culture supernatant of microbes are different in growing and stationary phase (SECTION I of CHAPTER II), the analysis should be performed at the different growth phases. Furthermore, recent studies have reported several novel species of *Bifidobacterium* isolated from human hosts (14,15). Therefore, detailed re-analysis is currently required to update our understanding of polyamine biosynthesis and transport by *Bifidobacterium* species.

In this SECTION, the author determined polyamine (putrescine [Put], spermidine [Spd], and Spm) concentrations of both cells and culture supernatants in growing and stationary phases obtained

from the culture of 13 species of human indigenous *Bifidobacterium* (14-16). Furthermore, the author estimated the possibility of the novel polyamine biosynthetic and transport proteins present in *Bifidobacterium* species by using basic local alignment search tool (BLAST) analysis.

MATERIALS AND METHODS

Strains and culture condition

Human indigenous *Bifidobacterium* species used in this study were obtained from the Japan Collection of Microorganisms (JCM) and are listed in Table 1. It should be noted that there are reports that *Bifidobacterium animalis* subsp. *lactis* was isolated from human samples (16,17). Brain-heart infusion (BHI) medium and 199 medium were purchased from Sigma-Aldrich (St. Louis, MO, USA).

Preparation of GAM (Nissui Pharmaceutical, Tokyo, Japan) broth and cultivation of *Bifidobacterium* species in GAM was performed as described previously (18). Briefly, *Bifidobacterium* species were anaerobically pre-cultured in 500 μL of GAM in 96-deep well plates for 24 – 48 h at 37 °C in an anaerobic chamber (INVIVO2 400 [Ruskinn Technologies, UK]). Pre-cultures were inoculated in 500 μL of GAM in 96-deep well plates using a copy plate stand (Tokken, Chiba, Japan), and anaerobically cultured for 60 – 96 h. Growth was monitored by measuring optical density at 600 nm (OD_{600}) on 96 well plate using Multiskan GO (Thermo fisher scientific, Waltham, MA, USA). Confirmation of the purity of the culture of bacteria other than *Bifidobacterium faecale* JCM19861^T was performed as described previously (18) using V1-V3 region of 16S rRNA gene (16S rDNA) sequence. Because V1-V3 region of 16S rDNA of *B. faecale* JCM19861^T is identical to that of *Bifidobacterium adolescentis* BBMN23, *hsp60* was amplified using primer pair hsp60_1F (5'-gaagaccgatgacgtcgcag-3')/hsp60_587R (5'-gtcgccgaagcccggagccttaac-3') and amplified product was sequenced using hsp60_68F (5'-gagggtctgaagaacgtcac-3') for confirmation of the purity of culture of *B. faecale* JCM19861^T.

Dissolved oxygen in 199 medium was eliminated by incubation of the medium in the AnaeroPack jar system (Mitsubishi gas chemical, Tokyo, Japan) at 4 °C for 24 h. *Bifidobacterium* species were pre-cultured in GAM for 24 - 48 h at 37 °C in the anaerobic chamber, and pre-cultured cells were washed with 199 medium. Washed cells were inoculated to 500 μL of 199 medium in 96-deep well plate at initial OD_{600} 0.03. Growth was monitored by measuring OD_{600} on 96 well plate using Multiskan GO.

BHI medium and BHI medium containing 0.03 % biogenic amines were prepared as previously reported by Pugin *et al*. (19). The final concentration of each biogenic amine in the BHI medium containing 0.03 % biogenic amines was 2.7 mM histamine, 2.2 mM tyramine, 2.9 mM cadaverine, 3.4 mM Put, 2.1 mM Spd, and 1.5 mM Spm. Before cultivation, dissolved oxygen in BHI medium and BHI medium containing 0.03 % biogenic amines was eliminated by incubation of the medium in the AnaeroPack jar system for 48 h at room temperature. *B. adolescentis* JCM1275^T was pre-cultured in BHI medium for 24 h at 37 °C in an anaerobic chamber. 2.5 μL of pre-cultured *B. adolescentis* JCM1275^T was inoculated in 500 μL of each medium in 96-deep well plate, and cultured for 48 h in an anaerobic chamber at 37 °C.

Polyamine quantification

Polyamine content was measured by high-performance liquid chromatography (HPLC). Polyamines were separated by cation exchange column (#2619PH, 4.6 × 50 mm, Hitachi Co., Ltd., Tokyo, Japan) in normal-phase mode. The detailed conditions of HPLC were the same as those described previously (20). For analyzing the relationship between the growth stages and polyamine concentrations in cells and culture supernatants, cultures in growing and stationary phases were obtained at indicated times (Figs. 1 and 6A).

Five hundred μL of cultures were centrifuged (18,700 ×*g*, 5 min, 4 °C) to separate the cells and culture supernatant. When GAM was used for culture, cell pellets were washed twice with 500 μL of phosphate-buffered saline to completely remove polyamines derived from the medium.

HPLC sample preparation and cellular protein quantification were performed as described previously (20) and intracellular polyamine concentrations were normalized to the amount of cellular protein and expressed as nmol/mg of cellular protein.

Basic local alignment search tool (BLAST) analysis

Protein BLAST (21) analysis (BlastP) was performed against proteins obtained from National Center for Biotechnology Information (NCBI) protein database. Query proteins involving polyamine biosynthesis and transport were the same as described in Table 2 in SECTION I of CHAPTER II. Additionally, polyamine degradation proteins listed in Table 2 were also analyzed by BlastP. Because insufficient genomic information of *B. faecale* JCM19861^T was available in the NCBI database (only nucleotide and/or protein sequence of 16S rDNA, Hsp60, and DnaJ were available in NCBI database), *B. faecale* JCM19861^T was excluded from BlastP analysis.

Statistics

Values are indicated as mean ± standard deviation (SD). The significant differences were analyzed by using SPSS software version 21 (IBM, Armonk, NY).

Table 1. The *Bifidobacterium* species used in this study.

Name	Strain number	Isolated source[a]
Bifidobacterium adolescentis	JCM1275^T	Adult feces
Bifidobacterium angulatum	JCM7096^T	Adult feces
Bifidobacterium animalis subsp. *lactis*	JCM10602^T	Fermented milk
Bifidobacterium bifidum	JCM1254	Infant feces
Bifidobacterium breve	JCM1192^T	Infant feces
Bifidobacterium catenulatum	JCM1194^T	Adult feces
Bifidobacterium faecale	JCM19861^T	Human feces
Bifiodbacterium gallicum	JCM8224^T	Human feces
Bifidobacterium kashiwanohense	JCM15439^T	Infant feces
Bifidobacterium longum subsp. *infantis*	JCM1222^T	Infant feces
Bifidobacterium longum subsp. *longum*	JCM1217^T	Adult feces
Bifiodbacterium pseudocatenulatum	JCM1200^T	Infant feces
Bifidobacterium scardovii	JCM12489^T	Human sources

[a] Isolated source was quoted the information described in Japan Collection of Microorganisms (http://jcm.brc.riken.jp/ja/).

Table 2. Putrescine, spermidine, and spermine degradation proteins used for BlastP analysis.

Protein name	Description	GenBank accession No.	Ref
Query protein involved in putrescine degradation			
GabD	Succinate-semialdehyde dehydrogenase	NP_417147	(22)
GabT	4-aminobutyrate aminotransferase	NP_417148	(22)
PatA	Putrescine aminotransferase	NP_417544	(22)
PatD	Gamma-aminobutyraldehyde dehydrogenase	NP_415961	(22)
PuO	Putrescine oxidase	ABY74497	(23)
PuuA	Gamma-glutamylputrescine synthetase	NP_415813	(24)
PuuB	Gamma-glutamylputrescine oxidoreductase	NP_415817	(24)
PuuC	$NADP^+$/NAD^+-dependent aldehyde dehydrogenase	NP_415816	(24)
PuuD	Gamma-glutamyl-gamma-aminobutyrate hydrolase	NP_415814	(24)
PuuE	4-aminobutyrate aminotransferase	NP_415818	(24)
Query protein involved in spermidine and spermine degradation			
BltD	Spermine/spermidine acetyltransferase	NP_390537	(25)
PaiA	Spermidine/spermine N^1-acetyltransferase	NP_391095	(26)

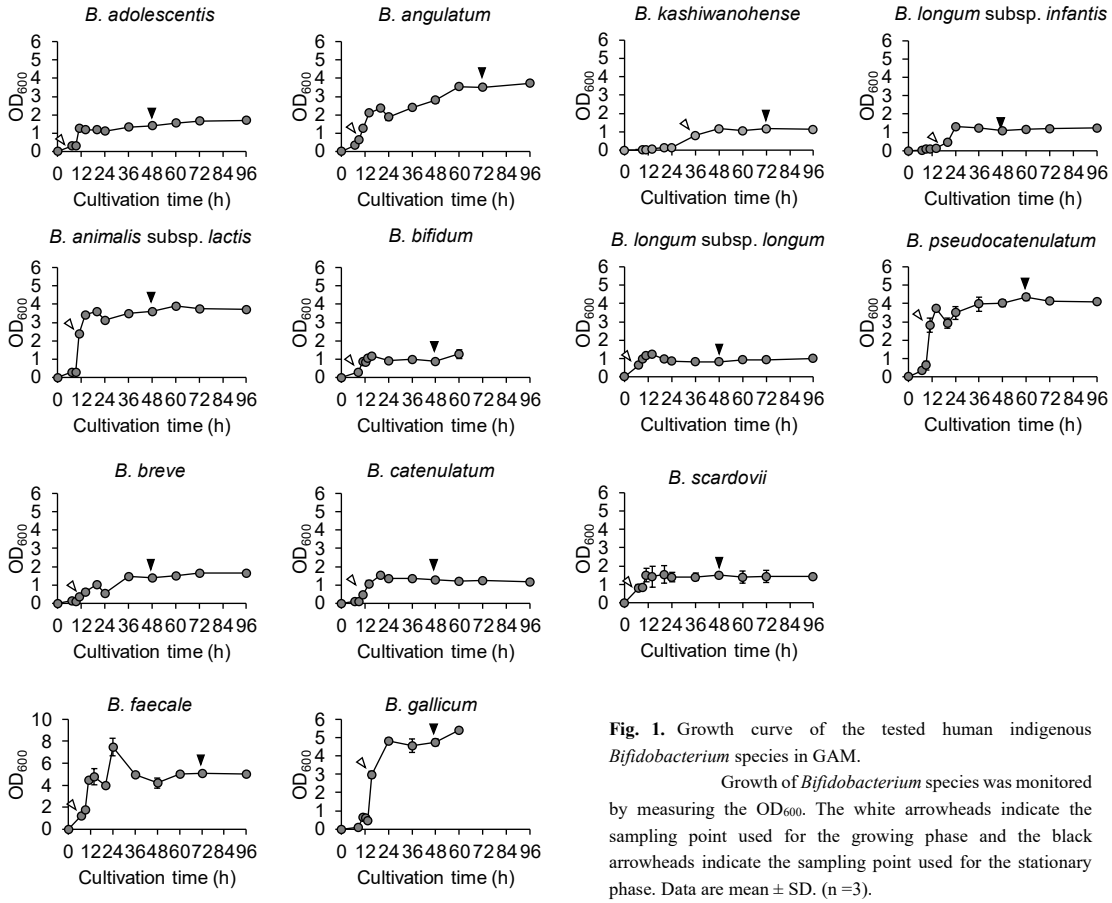

Fig. 1. Growth curve of the tested human indigenous *Bifidobacterium* species in GAM.

Growth of *Bifidobacterium* species was monitored by measuring the OD_{600}. The white arrowheads indicate the sampling point used for the growing phase and the black arrowheads indicate the sampling point used for the stationary phase. Data are mean ± SD. (n =3).

RESULTS

Evaluation criteria of polyamine biosynthetic and transport ability of bifidobacteria

When values (mean minus SD) of intracellular polyamine concentration (nmol/mg of cellular protein) were greater than zero, it was judged that the bacteria contain cellular polyamines. If polyamine was detected in the cells and furthermore polyamine concentration in the culture supernatant was not decreased compared with originally contained in the medium, it was judged that intracellular polyamine was biosynthesized by bifidobacteria and not derived from the medium.

Change in polyamine concentration was calculated by comparing the polyamine concentration in the culture supernatant with that originally contained in medium, or by comparing the concentration in the different growth stages. Because there is no report proving that polyamine is extracellularly degraded, the decrease in polyamine concentration in the culture supernatant is thought to result from an uptake of polyamine by the cultured bifidobacteria. If polyamine concentration in the culture supernatant increased compared with originally contained in the medium or was increasing from growing to stationary phase, the author judged polyamine was excreted by bifidobacteria.

Putrescine biosynthesis and transport of Bifidobacterium *grown in GAM*

Based on above criterion, the tested *Bifidobacterium* species contained no cellular Put when cultivated in GAM (Fig. 2A).

Put concentration in the culture supernatant with that originally contained in GAM (26.5 ± 0.25 μM) was shown as a gray band in Fig. 2B. A decrease in Put concentration was observed in the culture supernatant in the growing and/or stationary phase of 8 species (*B. adolescentis*, *Bifidobacterium angulatum*, *B. breve*, *Bifidobacterium catenulatum*, *B. faecale*, *Bifidobacterium kashiwanohense*, *B. longum* subsp. *longum*, and *Bifidobacterium scardovii*) in the tested 13 species

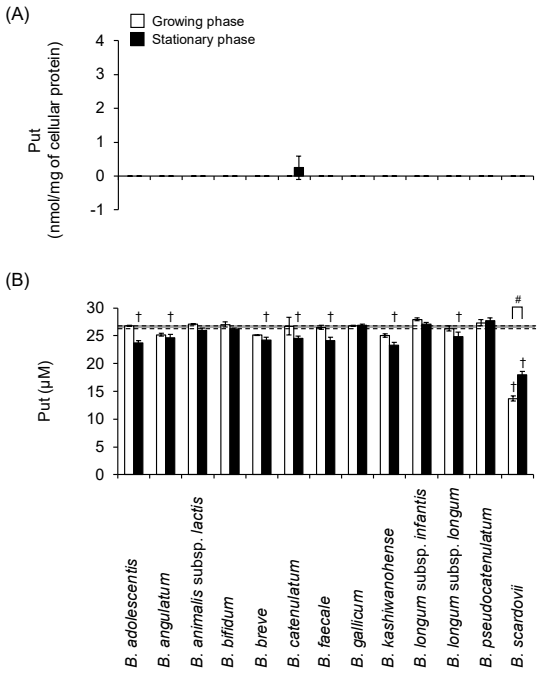

Fig. 2. Putrescine concentrations in cells and culture supernatant of tested *Bifidobacterium* species grown in GAM.

(A) Intracellular putrescine concentrations in tested human indigenous *Bifidobacterium* species in the growing and stationary phases. The amount of putrescine in the cell was quantified by HPLC and normalized to the cellular protein concentration. White bars show putrescine concentrations in the growing phase, black bars show those in the stationary phase. Data are represented as mean ± SD. (n =3).

(B) Putrescine concentration in culture supernatants of tested human indigenous *Bifidobacterium* species in the growing and stationary phases. Gray bands indicate the maximum and minimum putrescine concentration values in GAM (n = 3).

White bars show the putrescine concentrations in growing phase, and black bars show those in the stationary phase. Data are represented as mean ± SD. (n =3). $^{\dagger}p < 0.01$ (Dunnett's test in comparison with GAM). $^{\#}p < 0.01$ (two-tailed unpaired t-test).

(Fig. 2B). Comparing the Put concentrations in the culture supernatant of growing phase to those of stationary phase, the Put concentration in the culture supernatant of *B. scardovii* was increased from growing phase to stationary phase (Fig. 2B).

Spermidine concentrations of **Bifidobacterium** *grown in GAM*

Of the 13 tested species, 11 species contained Spd: in particular, Spd concentration in the cells of *B. animalis* subsp. *lactis* (2.5 ± 0.12 nmol/mg of cellular protein), *B. kashiwanohense* (1.2 ± 0.8 nmol/mg of cellular protein), and *Bifidobacterium pseudocatenulatum* (1.4 ± 0.18 nmol/mg of cellular protein) was relatively high (Fig. 3A). No Spd was detected in the cells in both growing and stationary phase of *B. bifidum* and *Bifidobacterium gallicum* (Fig. 3A).

The Spd concentration in the culture supernatant with that originally contained in GAM (19.4 ± 0.5 μM) was shown as a gray band in Fig. 2B. The concentrations of Spd decreased in the culture supernatant of 5 species (*B. adolescentis*, *B. breve*, *B. catenulatum*, *B. kashiwanohense*, and *B. scardovii*) of the tested 13 species in the growing and/or stationary phase (Fig. 3B).

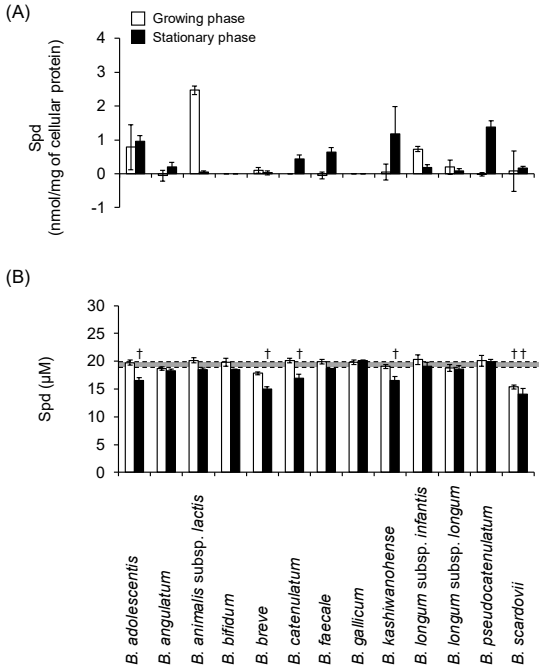

Fig. 3. Spermidine concentrations in the cells and culture supernatant of tested *Bifidobacterium* species grown in GAM.

(A) Intracellular spermidine concentrations in tested human indigenous *Bifidobacterium* species in the growing and stationary phases. The amount of spermidine in the cell was quantified by HPLC and normalized to the cellular protein concentration. White bars show spermidine concentrations in the growing phase, black bars show those in the stationary phase. Data are represented as mean ± SD. (n =3).

(B) Spermidine concentration in culture supernatants of tested human indigenous *Bifidobacterium* species in the growing and stationary phases. Gray bands indicate the maximum and minimum spermidine concentration values in GAM (n = 3).

White bars show the spermidine concentrations in growing phase, and black bars show those in the stationary phase. Data are represented as mean ± SD. (n =3). $^{\dagger}p < 0.01$ (Dunnett's test in comparison with GAM). $^{\#}p < 0.01$ (two-tailed unpaired t-test).

Spermine concentrations of **Bifidobacterium** *grown in GAM*

Of the tested 13 species, 5 species *(B. adolescentis*, *B. angulatum*, *B. animalis* subsp. *lactis*, *B. faecale*, and *B. pseudocatenulatum*) contained Spm in the cells: in particular, *B. animalis* subsp. *lactis* (1.5 ± 0.03 nmol/mg of cellular protein) and *B. pseudocatenulatum* (2.8 ± 0.47 nmol/mg) contained relatively high concentration of Spm in the cells (Fig. 4A).

The Spm concentration in the culture supernatant with that originally contained in GAM (6.3 ± 0.28 μM) was shown as a gray band in Fig. 4B. Spm concentration decreased in the culture supernatants of 5 species (*B. adolescentis*, *B. breve*, *B. kashiwanohense*, *B. longum* subsp. *longum*, and *B. scardovii*) in the growing and/or stationary phase (Fig. 4B). On the other hand, compared with

GAM, Spm concentration in the culture supernatants in the growing phase of *B. animalis* subsp. *lactis* and *B. longum* subsp. *infantis* was increased (Fig. 4B). In *B. longum* subsp. *longum*, Spm concentration in the culture supernatant increased from the growing phase to stationary phase (Fig. 4B).

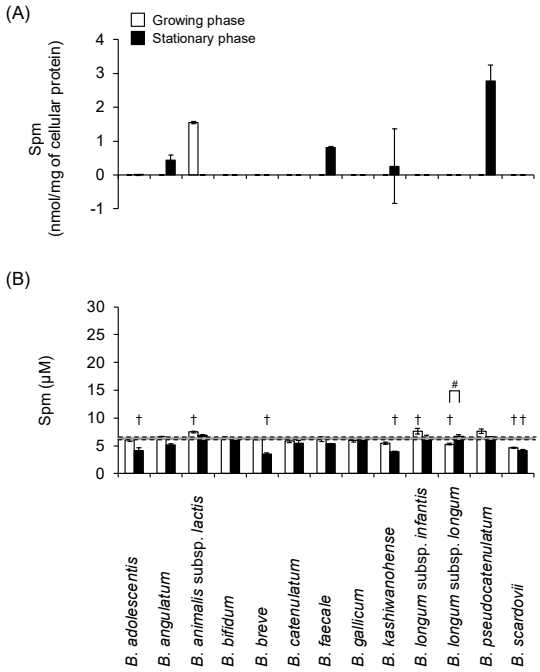

Fig. 4. Spermine concentrations in the cells and culture supernatant of tested *Bifidobacterium* species grown in GAM.

(A) Intracellular spermine concentrations in tested human indigenous *Bifidobacterium* species in the growing and stationary phases. The amount of spermine in the cell was quantified by HPLC and normalized to the cellular protein concentration. White bars show spermine concentrations in the growing phase, black bars show those in the stationary phase. Data are represented as mean ± SD. (n =3).

(B) Spermine concentration in culture supernatants of tested human indigenous *Bifidobacterium* species in the growing and stationary phases. Gray bands indicate the maximum and minimum spermine concentration values in GAM (n = 3).

White bars show the spermine concentrations in growing phase, and black bars show those in the stationary phase. Data are represented as mean ± SD. (n =3). $^{\dagger}p < 0.01$ (Dunnett's test in comparison with GAM). $^{\#}p < 0.01$ (two-tailed unpaired t-test).

Intracellular polyamine profile of Bifidobacterium *grown in 199 medium*

To investigate whether intracellular Spd and Spm was biosynthesized or imported from medium, *Bifidobacterium* species were cultured in 199 medium (polyamine-free synthetic medium). Of the tested *Bifidobacterium* species, 2 species (*B. longum* subsp. *infantis* and *B. scardovii*), which presented relatively good growth (Figs. 5 and 6A), were subjected to the polyamine analyses. No polyamine was observed in the cells of *B. longum* subsp. *infantis* and *B. scardovii* in the growing or stationary phase when 199 medium was used for culture (Figs. 7B and 7C).

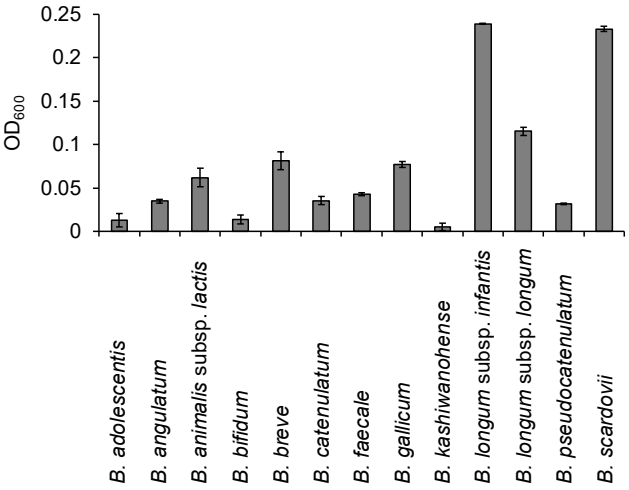

Fig. 5. Growth of the tested human indigenous *Bifidobacterium* species cultured in 199 medium.

Growth of *Bifidobacterium* was monitored by measuring the OD_{600}. OD_{600} value of the tested *Bifidobacterium* species grown in 199 medium for 72 hours is shown. Data are mean ± SD. (n =3).

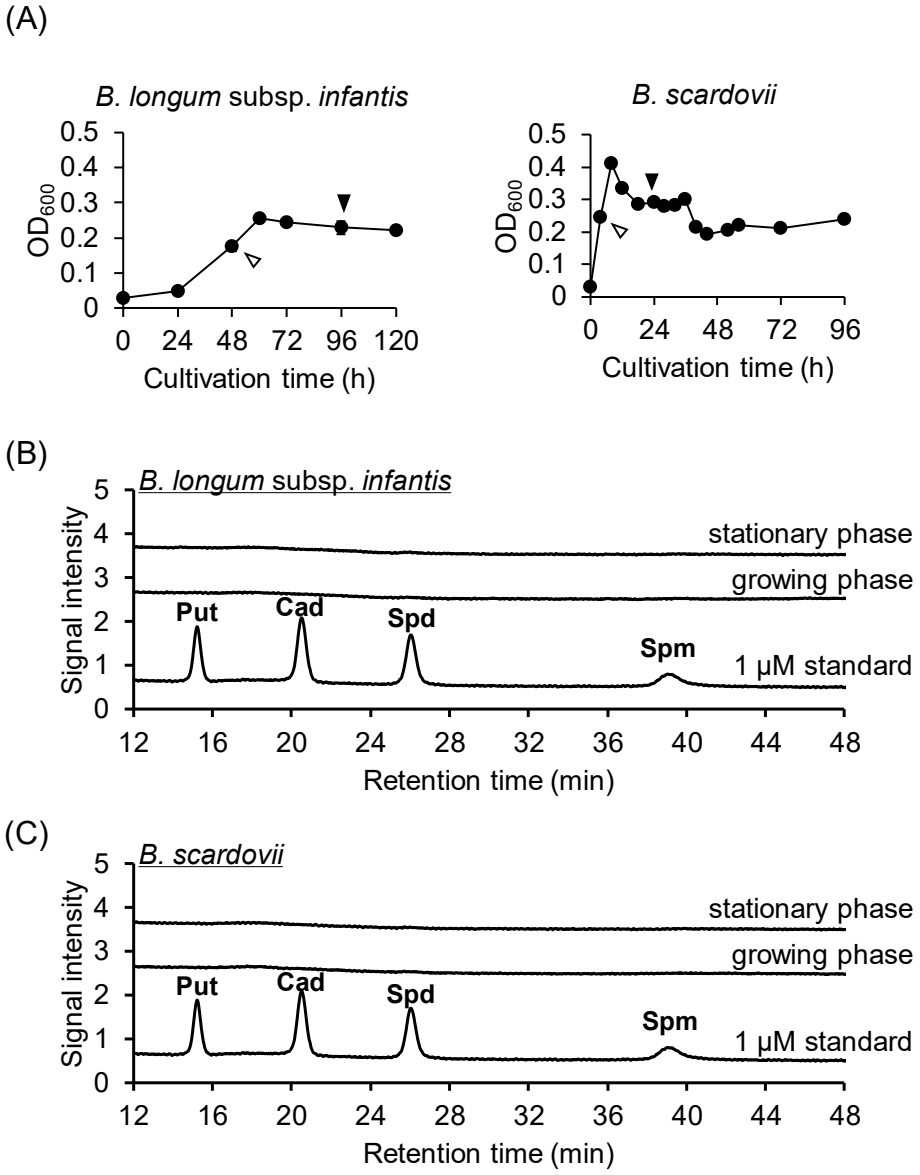

Fig. 6. HPLC chromatogram of cell extract of *B. longum* subsp. *infantis* and *B. scardovii* cultured in 199 medium.
(A) Growth curve of *B. longum* subsp. *infantis* and *B. scardovii* cultured in 199 medium. The white arrowheads indicate the sampling point used for the growing phase and the black arrowheads indicate the sampling point used for the stationary phase. Data are mean ± SD. (n =3).
(B) HPLC chromatogram of cell extract of *B. longum* subsp. *infantis* cultured in 199 medium and 1 μM standard (Put, putrescine; Cad, cadaverine; Spd, spermidine; Spm, spermine).
(C) HPLC chromatogram of cell extract of *B. scardovii* cultured in 199 medium and 1 μM standard (Put, putrescine; Cad, cadaverine; Spd, spermidine; Spm, spermine).

Polyamine biosynthetic activity of **B. adolescentis** *JCM1275^T*

Recently, Pugin *et al*. reported that *B. adolescentis* strain A.1, which was isolated from adult human fecal sample, produced approximately 400 μM of Spd and 900 μM of Spm into the culture supernatant when grown in BHI medium containing 0.03 % biogenic amine cocktail (tyramine, histamine, cadaverine, Put, Spd, and Spm) (19).

Because *B. adolescentis* A.1 is not currently available in any culture collections, the author measured polyamine concentration in the culture supernatant of type strain (JCM1275^T) of *B. adolescentis* grown in BHI medium containing 0.03 % biogenic amine cocktail for comparison of the values of *B. adolescentis* A.1 in the literature. The concentrations of Put, Spd, and Spm in the culture supernatant of *B. adolescentis* JCM1275^T in BHI medium were 101 ± 1.1 μM, 16 ± 0.3 μM, and 7.5 ± 0.3 μM, respectively. These values were not significantly different from the concentrations of polyamines originally found in the BHI medium (Fig. 7A). Moreover, in the BHI medium containing 0.03 % biogenic amine cocktail (Fig. 7B), *B. adolescentis* JCM1275^T did not export Spd or Spm. The growth of *B. adolescentis* JCM1275^T was not changed by biogenic amine cocktail supplementation (Fig. 8).

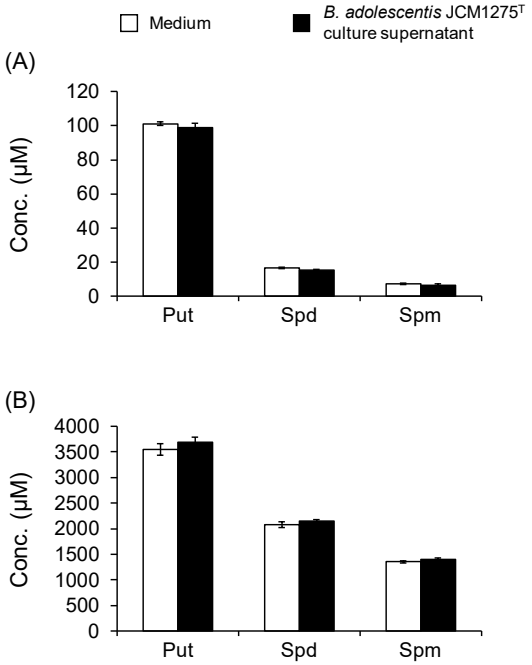

Fig. 7. Polyamine concentrations in the culture supernatant of *B. adolescentis* JCM1275^T grown in BHI medium and BHI medium containing biogenic amines.
(A) Polyamine concentrations in the culture supernatant of *B. adolescentis* JCM1275^T grown in BHI medium.
(B) Polyamine concentrations in the culture supernatant of *B. adolescentis* JCM1275^T grown in BHI medium containing 0.03 % biogenic amine cocktail.
The white bars indicate the polyamine concentrations of the medium after incubation for 48 h at 37 °C in an anaerobic chamber. The black bars indicate the polyamine concentrations of the *B. adolescentis* JCM1275^T culture supernatant grown in BHI medium and in BHI medium containing biogenic amine cocktail for 48 h at 37 °C in an anaerobic chamber. Data are represented as mean ± SD (n = 3).

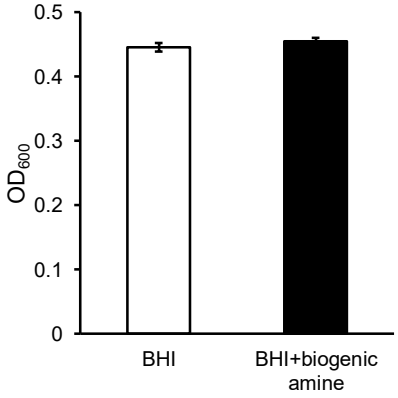

Fig. 8. Growth of *B. adolescentis* JCM1275^T on BHI medium and BHI medium containing 0.03 % biogenic amine cocktail.
Growth of *B. adolescentis* JCM1275^T was monitored by measuring the OD_{600}. OD_{600} value of *B. adolescentis* JCM1275^T grown in BHI medium and BHI medium containing 0.03 % biogenic amine cocktail for 48 hours is shown. Data are mean ± SD. (n =3).

Known polyamine biosynthetic, degradation, and transport proteins in tested* Bifidobacterium *species

Homologs of AguB (putrescine carbamoyl transferase), PlaP (low-affinity putrescine importer) and PuuP (high-affinity putrescine importer) were found in all tested *Bifidobacterium* species (Fig. 9A) by BlastP analysis. *B. adolescentis* encodes an AguD (putrescine-agmatine antiporter) homolog (Fig. 9A). *B. breve* and *B. longum* subsp. *longum* encode a homolog of NCPAH (*N*-carbamoylputrescine amidohydrolase) (Fig. 9A). *B. catenulatum*, *B. kashiwanohense*, and *B. pseudocatenulatum* encode an AguA (agmatine deiminase) homolog (Fig. 9A). Homologs of PuO (putrescine oxidase) and PuuB (gamma-

glutamylputrescine oxidoreductase) were not found in the tested *Bifidobacterium* species (Fig. 9A). Except for *B. bifidum*, tested bifidobacteria possess homologs of GabT (4-aminobutyrate aminotransferase), PatA (putrescine aminotransferase), PuuA (gamma-glutamylputrescine synthetase), and PuuE (4-aminobutyrate aminotransferase) (Fig. 9A). Homologs of GabD (succinate-semialdehyde dehydrogenase) and PuuC (NADP/NAD-dependent aldehyde dehydrogenase) were found in 5 species (*B. breve*, *B. catenulatum*, *B. gallicum*, *B. pseudocatenulatum*, and *B. scardovii*) (Fig. 9A). A homolog of PatD (gamma-aminobutyraldehyde dehydrogenase) was found in 6 species (*B. breve*, *B. catenulatum*, *B. gallicum*, *B. longum* subsp. *longum*, *B. pseudocatenulatum*, and *B. scardovii*). *B. gallicum* and *B. scardovii* encode a PuuD (gamma-glutamyl-gamma-aminobutyrate hydrolase) homolog (Fig. 9A). There is no known Spd biosynthetic and transport protein homolog in analyzed *Bifidobacterium* species (Fig. 9B). Only in *B. animalis* subsp. *lactis*, a PaiA (spermidine/spermine N^1-acetyltransferase) homolog was found (Fig. 9B).

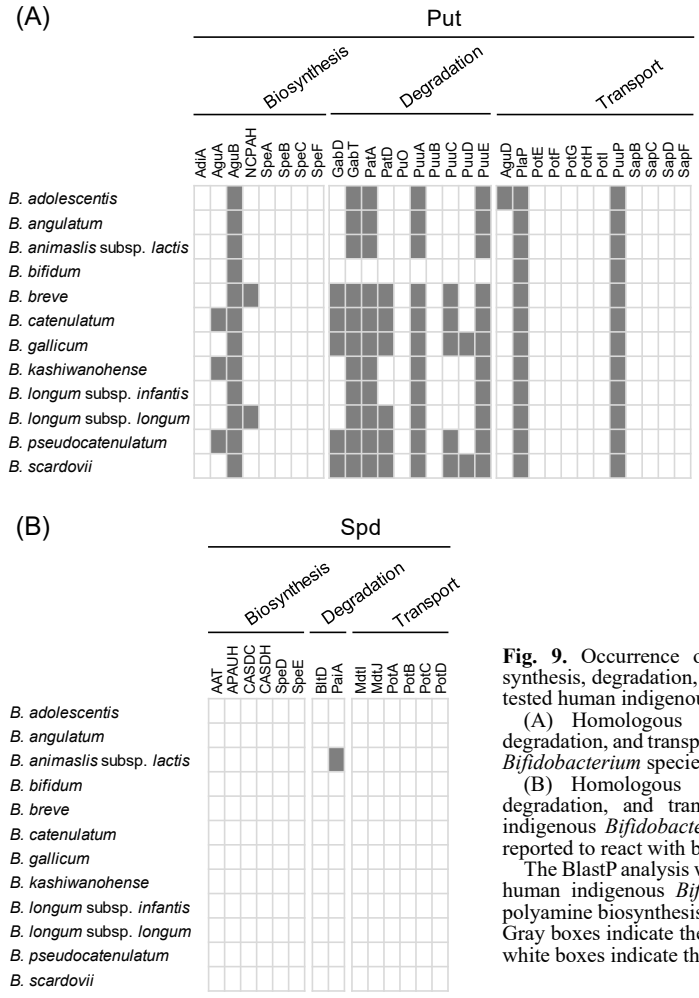

Fig. 9. Occurrence of homologous proteins responsible for the synthesis, degradation, and transport of polyamines in the genomes of tested human indigenous *Bifidobacterium* species.

(A) Homologous proteins responsible for the biosynthesis, degradation, and transport of putrescine in the tested human indigenous *Bifidobacterium* species.

(B) Homologous proteins responsible for the biosynthesis, degradation, and tranasport of spermidine in the tested human indigenous *Bifidobacterium* species. Note that BltD and PaiA were reported to react with both Spd and Spm.

The BlastP analysis was performed against the genomes of the tested human indigenous *Bifidobacterium* using query proteins involving polyamine biosynthesis, transport, and degradation pathways.
Gray boxes indicate the result of homologs with scores > 100 bits and white boxes indicate that there were no homologs.

DISCUSSION

Of the tested *Bifidobacterium* species, Put concentration in the culture supernatant of 8 species (*B. adolescentis*, *B. angulatum*, *B. breve*, *B. catenulatum*, *B. faecale*, *B. kashiwanohense*, *B. longum* subsp. *longum*, and *B. scardovii*) was significantly decreased (Fig. 2B). All 8 species that appeared to take up Put from the medium encode a PlaP homolog and a PuuP homolog (Fig. 9A). Therefore, these results suggest that PlaP and PuuP homologs are involved in the observed Put uptake. However, the other 5 species (*B. animalis* subsp. *lactis*, *B. bifidum*, *B. gallicum*, *B. longum* subsp. *infantis*, and *B. pseudocatenulatum*) possessing the PuuP and PlaP homologs did not show Put uptake (Figs 2B and 9A). These results suggest that these PuuP and PlaP homologs are not functional or were not expressed in the culture conditions used in this study. Although 8 species appeared to take up Put from the media, intracellular Put was not detected in them (Fig. 2A). These 8 species possess the PuuA and PuuE homologs (Fig. 9A), but the protein homologs to produce gamma-aminobutyric acid from gamma-glutamylputrescine (PuuB, PuuC, and PuuD) were not completely conserved within the tested Bifidobacterium species (Fig. 9A). On the other hand, 3 species (*B. breve*, *B. catenulatum*, and *B. scardovii*), which appeared to take up Put from the medium but did not contain Put in the cell, possess all the homologs of GabD, GabT, PatA, and PatD, which are responsible for the transaminase pathway of putrescine degradation (22) (Fig. 9A). This suggests that these 3 species degrade Put via the transaminase pathway. The other 5 species (*B. adolescentis*, *B. angulatum*, *B. faecale*, *B. kashiwanohense*, *B. longum* subsp. *longum*) appear to possess a novel putrescine degradation pathway because these strains possess neither a complete protein set of the transaminase pathway nor the gamma-glutamylation pathway. Put concentration in the *B. scardovii* culture supernatant was found to increase from the growing phase to the stationary phase (Fig. 2B). However, *B. scardovii* does not possess homologs of AguD, PotE, or SapBCDF (Fig. 9A). These results suggest that *B. scardovii* contains novel Put exporter(s).

Known Spd transporter homologs were not found in the tested *Bifidobacterium* species (Fig. 9B). Nevertheless, 5 species (*B. adolescentis*, *B. breve*, *B. catenulatum*, *B. kashiwanohense*, and *B. scardovii*) appeared to take up Spd from the medium (Fig. 3B). These observations suggest that an unknown Spd importer is present in these 5 species. Also, a known Spd biosynthetic protein homolog was not found in the tested *Bifidobacterium* species (Fig. 3B). However, 11 species (*B. adolescentis*, *B. angulatum*, *B. animalis* subsp. *lactis*, *B. breve*, *B. catenulatum*, *B. faecale*, *B. kashiwanohense*, *B. longum* subsp. *infantis*, *B. longum* subsp. *longum*, *B. pseudocatenulatum*, and *B. scardovii*) contained Spd in the cell when grown in GAM (Fig. 3A). Spd concentrations in the medium were decreased in the culture supernatant of *B. adolescentis*, *B. breve*, *B. catenulatum*, *B. kashiwanohense*, and *B. scardovii* (Fig. 3B). Furthermore, *B. scardovii* grown in the 199 medium contains no Spd (Fig. 6C). These results suggest that intracellular Spd of *B. adolescentis*, *B. breve*, *B. catenulatum*, *B.*

kashiwanohense, and *B. scardovii* originates from the medium. Although *B. scardovii* showed the highest Spd uptake activity in the tested bifidobacteria (Fig. 3B), the Spd concentration in the cells was low (Fig. 3A). This suggests the presence of the Spd metabolism in the cells of *B. scardovii*. However, homologs of BltD and PaiA, which are involved in the Spd metabolism, were not found in *B. scardovii* (Fig. 9B). These results suggest that *B. scardovii* degrades Spd by unknown Spd degradation protein(s). On the other hand, Spd concentrations in the culture supernatant of 6 species (*B. angulatum*, *B. animalis* subsp. *lactis*, *B. faecale*, *B. longum* subsp. *infantis*, *B. longum* subsp. *longum*, and *B. pseudocatenulatum*) were not decreased (Fig. 3B). These observations suggest that these 6 species biosynthesize Spd using unknown Spd biosynthetic enzymes. However, intracellular Spd of *B. longum* subsp. *infantis* grown in 199 medium was not observed (Fig. 6B). GAM is nutrition rich medium containing crude extract of animal tissue and plant (18). It was considered that the Spd biosynthetic pathway of *B. longum* subsp. *infantis* was activated by unknown compound(s) contained in GAM.

Spm concentration in the culture supernatant of 5 species significantly decreased (Fig. 4B). In bacteria, Spm uptake via PotABCD has been reported (27). However, these 5 species, which appeared to take up Spm, have no PotABCD homolog (Fig. 9B). These results suggest that a novel Spm importer(s) is present in these 5 species. On the other hand, compared to medium, Spm concentration in the culture supernatant of growing phase of *B. animalis* subsp. *lactis* and *B. longum* subsp. *infantis* were increased (Fig. 4B). In addition, Spm concentration in the culture supernatant of *B. longum* subsp. *longum* increased from growing phase to stationary phase (Fig. 4B). No Spm exporter has been reported so far. Therefore, it is conceivable that these 3 species possess a novel Spm exporter(s). In this study, the author found that 4 species (*B. angulatum*, *B. animalis* subsp. *lactis*, *B. faecale*, and *B. pseudocatenulatum*) contained Spm in the cell (Fig. 4A). A decrease in Spm concentration in the culture supernatant was not observed with all these species (Fig. 4B), suggesting that these 4 species biosynthesize Spm using unknown Spm biosynthetic enzymes. However, *B. scardovii* did not contain Spm in its cells (Fig. 4A), although the concentration of Spm in the culture supernatant of *B. scardovii* was found to decrease (Fig. 4B). Therefore, the possibility of the Spm metabolism was considered in *B. scardovii* cells but homologs of BltD and PaiA, which are involved in Spd metabolism, were not found in *B. scardovii* (Fig. 9B). These results suggest that *B. scardovii* degrades Spm by novel Spm degradation protein(s).

Pugin *et al.* reported that *B. adolescentis* A.1, which was isolated by them, exports a large amount of polyamine into the culture supernatant (19). However, the author could not reproduce this using *B. adolescentis* JCM1275^{T} grown in the same medium (BHI medium containing 0.03 % biogenic amines) used in their study (Fig. 7B). Moreover, *B. adolescentis* JCM1275^{T} did not produce Spd and Spm when grown in BHI medium without biogenic amines (Fig. 7A).

To date, it has been thought that *Bifidobacterium* species have no polyamine biosynthetic

ability (13). In the present study, the author suggested that 6 species (*B. angulatum*, *B. animalis* subsp. *lactis*, *B. faecale*, *B. longum* subsp. *infantis*, *B. longum* subsp. *longum*, and *B. pseudocatenulatum*) of human indigenous *Bifidobacterium* has Spd and/or Spm biosynthetic ability. Furthermore, to the best of my knowledge, polyamine transport ability of human indigenous *Bifidobacterium* species has not been reported. My results indicate that 10 species of human indigenous *Bifidobacterium* possess polyamine transport ability. In the future, identification of the polyamine biosynthetic and transport proteins of *Bifidobacterium* species at the genetic level is necessary for understanding the polyamine metabolism of *Bifidobacterium*.

REFERENCES

1. Kibe, R., Kurihara, S., Sakai, Y., Suzuki, H., Ooga, T., Sawaki, E., Muramatsu, K., Nakamura, A., Yamashita, A., Kitada, Y., Kakeyama, M., Benno, Y., and Matsumoto, M. (2014) Upregulation of colonic luminal polyamines produced by intestinal microbiota delays senescence in mice. *Sci Rep* **4**, 4548
2. Matsumoto, M., Kakizoe, K., and Benno, Y. (2007) Comparison of fecal microbiota and polyamine concentration in adult patients with intractable atopic dermatitis and healthy adults. *Microbiol Immunol* **51**, 37-46
3. Matsumoto, M., Kibe, R., Ooga, T., Aiba, Y., Kurihara, S., Sawaki, E., Koga, Y., and Benno, Y. (2012) Impact of intestinal microbiota on intestinal luminal metabolome. *Sci Rep* **2**, 233
4. Noack, J., Kleessen, B., Proll, J., Dongowski, G., and Blaut, M. (1998) Dietary guar gum and pectin stimulate intestinal microbial polyamine synthesis in rats. *J Nutr* **128**, 1385-1391
5. Noack, J., Dongowski, G., Hartmann, L., and Blaut, M. (2000) The human gut bacteria *Bacteroides thetaiotaomicron* and *Fusobacterium varium* produce putrescine and spermidine in cecum of pectin-fed gnotobiotic rats. *J Nutr* **130**, 1225-1231
6. Nishijima, S., Suda, W., Oshima, K., Kim, S. W., Hirose, Y., Morita, H., and Hattori, M. (2016) The gut microbiome of healthy Japanese and its microbial and functional uniqueness. *DNA Res* **23**, 125-133
7. Nakayama, J., Watanabe, K., Jiang, J., Matsuda, K., Chao, S. H., Haryono, P., La-Ongkham, O., Sarwoko, M. A., Sujaya, I. N., Zhao, L., Chen, K. T., Chen, Y. P., Chiu, H. H., Hidaka, T., Huang, N. X., Kiyohara, C., Kurakawa, T., Sakamoto, N., Sonomoto, K., Tashiro, K., Tsuji, H., Chen, M. J., Leelavatcharamas, V., Liao, C. C., Nitisinprasert, S., Rahayu, E. S., Ren, F. Z., Tsai, Y. C., and Lee, Y. K. (2015) Diversity in gut bacterial community of school-age children in Asia. *Sci Rep* **5**, 8397
8. Iwabuchi, N., Takahashi, N., Xiao, J. Z., Miyaji, K., and Iwatsuki, K. (2007) In vitro Th1 cytokine-independent Th2 suppressive effects of bifidobacteria. *Microbiol Immunol* **51**, 649-660
9. Sivan, A., Corrales, L., Hubert, N., Williams, J. B., Aquino-Michaels, K., Earley, Z. M., Benyamin, F. W., Lei, Y. M., Jabri, B., Alegre, M. L., Chang, E. B., and Gajewski, T. F. (2015) Commensal *Bifidobacterium* promotes antitumor immunity and facilitates anti-PD-L1 efficacy. *Science* **350**, 1084-1089
10. Kim, S. W., Kim, H. M., Yang, K. M., Kim, S. A., Kim, S. K., An, M. J., Park, J. J., Lee, S. K., Kim, T. I., Kim, W. H., and Cheon, J. H. (2010) *Bifidobacterium lactis* inhibits NF-kappaB in intestinal epithelial cells and prevents acute colitis and colitis-associated colon cancer in mice. *Inflamm Bowel Dis* **16**, 1514-1525

11. Fukuda, S., Toh, H., Hase, K., Oshima, K., Nakanishi, Y., Yoshimura, K., Tobe, T., Clarke, J. M., Topping, D. L., Suzuki, T., Taylor, T. D., Itoh, K., Kikuchi, J., Morita, H., Hattori, M., and Ohno, H. (2011) Bifidobacteria can protect from enteropathogenic infection through production of acetate. *Nature* **469**, 543-547
12. Matsumoto, M., Kurihara, S., Kibe, R., Ashida, H., and Benno, Y. (2011) Longevity in mice is promoted by probiotic-induced suppression of colonic senescence dependent on upregulation of gut bacterial polyamine production. *PLoS One* **6**, e23652
13. Hamana, K. (1997) Polyamine Distribution Patterns in Gram-Positive Eubacteria : The Absence of Cellular Polyamine Synthesis. *Ann. Rep. Coo. Med. Care Technol. Gunma Univ.* **17**, 137-144
14. Bottacini, F., Ventura, M., van Sinderen, D., and O'Connell Motherway, M. (2014) Diversity, ecology and intestinal function of bifidobacteria. *Microb Cell Fact* **13 Suppl 1**, S4
15. Choi, J. H., Lee, K. M., Lee, M. K., Cha, C. J., and Kim, G. B. (2014) *Bifidobacterium faecale* sp. nov., isolated from human faeces. *Int J Syst Evol Microbiol* **64**, 3134-3139
16. Yatsunenko, T., Rey, F. E., Manary, M. J., Trehan, I., Dominguez-Bello, M. G., Contreras, M., Magris, M., Hidalgo, G., Baldassano, R. N., Anokhin, A. P., Heath, A. C., Warner, B., Reeder, J., Kuczynski, J., Caporaso, J. G., Lozupone, C. A., Lauber, C., Clemente, J. C., Knights, D., Knight, R., and Gordon, J. I. (2012) Human gut microbiome viewed across age and geography. *Nature* **486**, 222-227
17. Milani, C., Duranti, S., Lugli, G. A., Bottacini, F., Strati, F., Arioli, S., Foroni, E., Turroni, F., van Sinderen, D., and Ventura, M. (2013) Comparative genomics of *Bifidobacterium animalis* subsp. *lactis* reveals a strict monophyletic bifidobacterial taxon. *Appl Environ Microbiol* **79**, 4304-4315
18. Gotoh, A., Nara, M., Sugiyama, Y., Sakanaka, M., Yachi, H., Kitakata, A., Nakagawa, A., Minami, H., Okuda, S., Katoh, T., Katayama, T., and Kurihara, S. (2017) Use of Gifu Anaerobic Medium for culturing 32 dominant species of human gut microbes and its evaluation based on short-chain fatty acids fermentation profiles. *Biosci Biotechnol Biochem* **81**, 2009-2017
19. Pugin, B., Barcik, W., Westermann, P., Heider, A., Wawrzyniak, M., Hellings, P., Akdis, C. A., and O'Mahony, L. (2017) A wide diversity of bacteria from the human gut produces and degrades biogenic amines. *Microb Ecol Health Dis* **28**, 1353881
20. Sakanaka, M., Sugiyama, Y., Kitakata, A., Katayama, T., and Kurihara, S. (2016) Carboxyspermidine decarboxylase of the prominent intestinal microbiota species *Bacteroides thetaiotaomicron* is required for spermidine biosynthesis and contributes to normal growth. *Amino Acids* **48**, 2443-2451

21. Camacho, C., Coulouris, G., Avagyan, V., Ma, N., Papadopoulos, J., Bealer, K., and Madden, T. L. (2009) BLAST+: architecture and applications. *BMC Bioinformatics* **10**, 421
22. Schneider, B. L., Hernandez, V. J., and Reitzer, L. (2013) Putrescine catabolism is a metabolic response to several stresses in *Escherichia coli*. *Mol Microbiol* **88**, 537-550
23. van Hellemond, E. W., van Dijk, M., Heuts, D. P., Janssen, D. B., and Fraaije, M. W. (2008) Discovery and characterization of a putrescine oxidase from *Rhodococcus erythropolis* NCIMB 11540. *Appl Microbiol Biotechnol* **78**, 455-463
24. Kurihara, S., Oda, S., Kato, K., Kim, H. G., Koyanagi, T., Kumagai, H., and Suzuki, H. (2005) A novel putrescine utilization pathway involves gamma-glutamylated intermediates of *Escherichia coli* K-12. *J Biol Chem* **280**, 4602-4608
25. Woolridge, D. P., Martinez, J. D., Stringer, D. E., and Gerner, E. W. (1999) Characterization of a novel spermidine/spermine acetyltransferase, BltD, from *Bacillus subtilis*. *Biochem J* **340 (Pt 3)**, 753-758
26. Forouhar, F., Lee, I. S., Vujcic, J., Vujcic, S., Shen, J., Vorobiev, S. M., Xiao, R., Acton, T. B., Montelione, G. T., Porter, C. W., and Tong, L. (2005) Structural and functional evidence for *Bacillus subtilis* PaiA as a novel N^1-spermidine/spermine acetyltransferase. *J Biol Chem* **280**, 40328-40336
27. Yao, X., and Lu, C. D. (2014) Functional characterization of the *potRABCD* operon for spermine and spermidine uptake and regulation in *Staphylococcus aureus*. *Curr Microbiol* **69**, 75-81

SUMMARY

Bifidobacteria are members of the human intestinal microbiota, being numerically dominant in the colon of infants, and also being prevalent in the large intestine of adults. In this study, the author measured the concentrations of major polyamines (putrescine, spermidine, and spermine) in cells and culture supernatant of 13 species of human indigenous *Bifidobacterium* at growing and stationary phase. Except for *Bifidobacterium bifidum* and *Bifidobacterium gallicum*, 11 species contained spermidine and/or spermine when grown in Gifu anaerobic medium (GAM). However, *Bifidobacterium scardovii* and *Bifidobacterium longum* subsp. *infantis*, which contain spermidine when grown in GAM, did not contain spermidine when grown in polyamine-free 199 medium. Of the tested 13 *Bifidobacterium* species, 10 species showed polyamine transport ability. Combining polyamine concentration analysis in culture supernatant and in cells, with basic local alignment search tool analysis suggested that 11 species of tested human indigenous *Bifidobacterium*, except for *B. bifidum* and *B. gallicum* may possess novel polyamine biosynthetic proteins and/or transporters

SECTION III
Analysis of a novel putrescine exporter SapBCDF of *Escherichia coli*

Polyamines in the colonic lumen are derived from gut microbes and impact the health of animals either negatively (1-3) or positively (4-6). Briefly, polyamine catabolism contributes to enterotoxigenic *Bacteroides fragilis*-induced colon tumorigenesis (1), and levels of rectal mucosal polyamines are increased colorectal adenoma (3). On the other hand, upregulation of colonic luminal polyamines produced by the gut microbes delays senescence in mice (4,5). At physiological pH polyamines are positively charged and hydrophilic, and therefore cannot pass through hydrophobic cytoplasmic membranes. Consequently, polyamine transporters are required for their uptake and export in the gut microbes, and the concentration of polyamines in the intestinal tract results from the balance of uptake by polyamine importers and export by polyamine exporters of the gut microbes.

In *Escherichia coli* which is a model organism of the gut microbes, putrescine is synthesized from ornithine by ornithine decarboxylase (SpeC/SpeF) (7,8) or from arginine by the sequential actions of arginine decarboxylase (SpeA) (9) and agmatine ureohydrolase (SpeB) (10). Putrescine is converted to spermidine, another polyamine, by the addition of an aminopropyl group derived from decarboxylated *S*-adenosylmethionine by spermidine synthase (SpeE) (11).

Five putrescine importers in *E. coli* have been experimentally identified. PotFGHI has been identified as an ATP-dependent putrescine transporter of the ATP-binding cassette (ABC) transporter family (12). PotABCD is a spermidine transporter of the ABC transporter family that takes up putrescine with lower affinity (13). PuuP was discovered as a putrescine importer dependent on proton motive force (14) and is indispensable when *E. coli* grows on putrescine as a sole carbon or nitrogen source (14). PlaP is a proton-dependent putrescine importer that is important when *E. coli* exhibits surface motility (15). PotE is responsible for both excretion and uptake of putrescine (16,17). PotE is a proton-dependent putrescine importer at neutral pH, but at acidic pH PotE is a putrescine-ornithine antiporter (17). An acid-inducible ornithine decarboxylase is encoded by *speF*, which is located in the same operon as *potE* (8). SpeF converts ornithine to putrescine with consumption of a proton, and PotE exports putrescine with uptake of ornithine (16). Through this process *E. coli* adapts to the acidic environment. In addition, at neutral pH, *E. coli* excretes putrescine into environment independently of PotE (18), suggesting that there are other unidentified putrescine exporters in *E. coli*.

Considering the importance of gut microbes as the source of polyamines in colon, obtaining a better understanding of polyamine export is clearly of interest. In this SECTION, the author performed a genome-wide screening for novel putrescine exporters of *E. coli* and biochemically demonstrated that the *sapBCDF* operon contributes to putrescine export from the cell to the environment.

MATERIALS AND METHODS

Strains and plasmids

Strains used in the present study are listed in Table 1 except that the Keio gene knockout collection (19) used for initial screening for the putrescine exporter. Strains used for initial screening for the putrescine exporter are listed in Table 2. P1 transduction (20) was used to transfer the chromosomal deletion of genes: Δ*puuP* (JW1289) in the Keio collection (19), into MG1655 (wild-type background), generating SK614 (Δ*puuP*::FRT-*kan*+-FRT). Plasmid pCP20 (21) was introduced to eliminate the kanamycin resistance gene (*kan*+), generating SK623 (Δ*puuP*::FRT). Gene disruptions of *speB*, *speC*, and *sapBCDF* were performed employing a previously described method using pKD3 or pKD13 (21). pSK607 (pACYC184-$sapB^{+}C^{+}D^{+}F^{+}$) was constructed as follows. The 4,142 bp DNA fragment including *sapBCDF* and 500-bp of the upstream region of *sapB* on the chromosome of *E. coli* MG1655 was amplified by PCR using KOD-plus- polymerase (Toyobo, Osaka, Japan), "TTT_HindIII_sapBCDF_start_side" and "AAA_SphI_sapBCDF_term_side" as primers, and genomic DNA of *E. coli* MG1655 as template. The amplified fragment was cloned into pACYC184 digested by HindIII and SphI, and the cloned region was sequenced to confirm there was no mutation.

Media and Growth conditions

M9 + tryptone medium (M9 minimal medium, except that 1 % Bacto-tryptone was used instead of 0.2 % glucose) (22) was employed for the bactericidal assay (23) and for analysis of putrescine concentration of the culture supernatant of strains with a deletion of *puuP* encoding a putrescine importer previously described (14). Because *puuP* is negatively regulated by succinate (24), 0.2 % of sodium succinate was supplemented to the M9 + tryptone in analysis of putrescine concentration of culture supernatant of strains with $puuP^{+}$ backgrounds. One millimolar stable isotope-labeled arginine was supplemented to the M9 + tryptone medium in analysis of stable isotope-labeled putrescine concentration of the culture supernatant of strains. In screening for putrescine exporters, strains were grown in 5 mL of M9 + tryptone + succinate medium in 20 mL test tubes at 37 °C, with reciprocal shaking at 140 rpm for 6 hours. In the other experiments, strains were grown at 37 °C with reciprocal shaking at 140 rpm in 60 mL of media in a 300 mL Erlenmeyer flask.

Bactericidal assay

To assess the susceptibility of *E. coli* MG1655 and YS40 (MG1655 except Δ*sapBCDF*) strains to an antimicrobial peptide LL-37, the experiment was performed according to Harwig *et al.* (23) with some modifications. Briefly, *E. coli* MG1655 and YS40 (MG1655 except Δ*sapBCDF*) were grown in M9 + tryptone medium with 140 rpm at 37 °C for 4 hours. An assay medium was prepared by adding 100 μL of Luria-Bertani (LB) medium to 6.9 mL of 10 mM sodium phosphate buffer (pH

7.4) and warmed to 37 °C prior to use. Cells were washed with ice-cold 10 mM sodium phosphate buffer (pH 7.4), and resuspended in the same buffer to a concentration of 5×10^6 cells/mL. A reaction mixture containing 10 μL of cell suspension, 5 μL of LL-37, and 35 μL of assay medium, was incubated for 2 hours at 37 °C. The reaction was stopped by adding 450 μL of ice-cold 150 mM sodium chloride to the reaction mixture. After the reaction, the reaction mixture was serially diluted with ice-cold 10 mM sodium phosphate buffer (pH 7.4) and plated on LB medium. Plates were incubated at 37 °C for 22 hours and the numbers of colonies were counted to quantify cell viability in the reaction mixture. Cell viability in the reaction mixture was quantified by counting colony formations. Survival ratios were calculated by dividing the colony forming units of the cells treated with LL-37 by those of the cells without LL-37 treatment.

Quantification of polyamines

Polyamines concentrations were quantified by high-performance liquid chromatography (HPLC). HPLC analysis and sample preparation was performed as described previously (25). Briefly, a normal-phase HPLC system (Chromaster, Hitachi Co., Ltd., Tokyo, Japan) equipped with a cation-exchange column (#2619PH, 4.6 × 50 mm; Hitachi) was used for separation of polyamines. Eluted polyamines were derivatized with *o*-phthalaldehyde using the post-column method and were detected using a fluorescence detector (λ_{ex} 340 nm, λ_{em} 435 nm). The concentration of each polyamine was calculated based on a standard curve created using standards of known concentrations. In the preparation of culture supernatant samples, 500 μL of culture was centrifuged (18,700 ×*g*, 4 °C, 5 min) and the supernatant was collected. To remove proteins, 1/10 volume of 100 % (*w*/*v*) trichloroacetic acid was added and mixed using a Vortex machine followed by a centrifugation (18,700 × *g*, 4 °C, 30 min). After the centrifugation, polyamines in the supernatant were analyzed by HPLC. In the preparation of whole-cell samples, 500 μL of OD_{600} = 0.5 (samples cultured for 2 hours) or OD_{600} = 1 (samples cultured for 4 to 24 hours) culture was centrifuged and the pellet was washed with 1 mL of ice-cold M9 minimal medium without glucose. The washed pellet was resuspended in 300 μL of 5 % (*w*/*v*) trichloroacetic acid and boiled for 15 min to rupture the cells. The suspension was centrifuged (21,500 ×*g*, 4 °C, 15 min), the supernatant was applied to the HPLC column after filtration using Cosmonice filter W (Nacalai Tesque, Kyoto, Japan), and the precipitated protein was dissolved in 300 μL of 0.1 *N* NaOH. Protein concentration of the solution was quantified by the Bradford method using a Bio-Rad protein assay kit (Bio-Rad Laboratories, Hercules, CA, USA). The resulting concentration of putrescine was expressed as nmol/mg of total cell protein.

Detection of stable isotope-labeled putrescine by gas chromatography-mass spectrometry

The amount of stable isotope-labeled putrescine was determined by gas chromatography-mass spectrometry (GC-MS) using a modified version of the methods described in Chen *et al* (26).

E. coli strains were cultured for 8 hours in M9 + tryptone medium supplemented with stable isotope-labeled L-[$^{13}C_6$, $^{15}N_4$]-arginine (S.I.Arg, Wako Pure Chemicals, Osaka, Japan) at a final concentration of 1 mM. Culture supernatant of the strain grown in S.I.Arg was mixed with 10 % (*v*/*v*) of 100 % (*w*/*v*) trichloroacetic acid to precipitate proteins. The sample was then clarified by centrifugation at 18,700 ×*g* for 35 min at 4 °C, and 600 µL of the supernatant was extracted by vortexing for 1 min in 2 mL diethyl ether. The emulsion was then separated by centrifugation at 15,000 ×*g* for 5 min at 4 °C, and the ether layer containing lipids, carbohydrates, and other potential contaminants was discarded, and the aqueous layer was extracted in the same manner once more. A 500 µL aliquot was supplemented with 10 µL 0.01 % (*w*/*v*) 1, 6-hexanediamine (Kanto Chemical, Tokyo, Japan) as internal standard, and adjusted to pH 11.5 ± 0.5 with 5 M NaOH. To carry out the *N*-ethoxycarbonylation of the amines, 1 mL of diethyl ether containing 50 µL of ethylchloroformate (Kanto Chemical) was added to the sample solution. The reaction mixture was shaken at room temperature for 30 min, and then centrifuged at 15,000 ×*g* for 5 min at 4 °C. The ether layer containing the polyamine *N*- ethoxycarbonyl derivatives was transferred to a glass tube with screw cap. This derivatization reaction was repeated by re-extracting the aqueous phase with 1 mL of diethyl ether containing 50 µL ethylchloroformate. The ether layers from the two extractions were combined and dried under a dry nitrogen stream. Dried *N*-ethoxylcarbonyl polyamine derivatives were taken up in 100 µL of ethyl acetate to which 200 µL of trifluoroacetic acid anhydride (Sigma-Aldrich, St. Louis, MO, USA) was added. The mixture in sealed glass tubes were placed on a 75 °C heating block for 60 min to complete the trifluoroacetylation reaction, and then completely dried under a dry nitrogen stream. Derivatives were reconstituted in 200 µL of ethyl acetate and 2 µL of derivatized samples were injected into a GC-MS. Analysis were carried on an Equity-5 capillary column (30 m × 0.25 mm, 0.25 µm film thickness, Sigma-Aldrich) using helium as a carrier gas. Temperatures of injector and source were 260 °C and 150 °C, respectively. The GC oven was programmed from 140 °C to 190 °C at 8 °C /min followed by a 4-min hold, then to 300 °C at 20 °C /min, followed by a 4 min hold. A final temperature increased to 320 °C at 20 °C /min was held as bake out for 4 min. Fragment ions were monitored in selected ion monitoring mode, and the ion with *m/z* +355 was used as basis fragment for putrescine. Extraction and derivatization rates were standardized using 1,6-hexanediamine, and putrescine was quantified using external calibration curves.

Table 1. Strains, plasmids, and oligonucleotides used in the present study.

Strain, plasmid, or oligonucleotide	Characteristic or sequence	Source or Reference
Strain		
BW25113	*rrnB3* Δ*lacZ4787 hsdR514* Δ(*araBAD*)*567* Δ(*rhaBAD*)*568 rph*-1	(19,27)
MG1655	F^- prototrophic	Laboratory stock
SK614	MG1655 but Δ*puuP*::*kan*$^+$FRT	This study
SK623	MG1655 but Δ*puuP*::FRT	This study
SK626	MG1655 but Δ*puuP*::FRT Δ*sapBCDF*::*kan*$^+$ FRT	This study
SK627	pACYC184/SK623	This study
SK628	pACYC184/SK626	This study
SK634	pSK607/ SK626	This study
YS40	MG1655 but Δ*sapBCDF*::*kan*$^+$ FRT	This study
YS111	pACYC184/MG1655	This study
YS112	pACYC184/YS40	This study
YS113	pSK607/YS40	This study
YS226	MG1655 but Δ*puuP*::FRT Δ*speB*::FRT Δ*speC*::FRT	This study
YS227	MG1655 but Δ*puuP*::FRT Δ*speB*::FRT Δ*speC*::FRT Δ*sapBCDF*::FRT	This study
YS233	pACYC184/YS226	This study
YS234	pACYC184/YS227	This study
YS235	pSK607/YS227	This study
Plasmid		
pACYC184	p15A replicon *cat*$^+$ *tet*$^+$	New England Biolabs
pCP20	*oriR101 bla*$^+$ *cat*$^+$ *cI857* λPR	(21)
pKD3	*oriRγ bla*$^+$ FRT-*cat*$^+$-FRT	(21)
pKD13	*oriRγ bla*$^+$ FRT-*kan*$^+$-FRT	(21)
pSK607	p15A replicon *cat*$^+$ *sapB*$^+$*C*$^+$*D*$^+$*F*$^+$	This study
Oligonucleotide		
TTT_HindIII_sapBCDF_start_side	TTTAAGCTTTGGGTGCCCACACGTTCGCA	This study
AAA_SphI_sapBCDF_term_side	AAAGCATGCTTAGCGATCTTTACGCCACG	This study

Table 2. Strains from Keio collection used for putrescine exporter screening and the concentration of putrescine (Put) in the culture supernatant.

Keio collection No.	Deleted gene	Put conc. (μM)	Keio collection No.	Deleted gene	Put conc. (μM)
JW0699	*ybgH*	75.5	JW0779	*ybhG*	53.8
JW1787	*leuE*	72.0	JW3236	*yhdW*	53.5
JW2562	*eamB*	69.9	JW3313	*kefB*	53.5
JW0798	*rhtA*	68.6	JW3423	*livK*	53.4
JW1052	*mdtH*	68.5	JW1322	*mppA*	53.0
JW2062	*mdtD*	66.7	JW0454	*kefA*	53.0
JW3209	*aaeB*	66.3	JW3333	*frlA*	52.4
JW3087	*tdcC*	66.2	JW3239	*yhdZ*	52.1
JW0531	*emrE*	65.0	JW3434	*zntA*	51.9
JW2061	*mdtC*	64.7	JW0563	*cusB*	51.7
JW1110	*potC*	64.2	JW0795	*glnP*	51.6
JW3469	*arsB*	62.5	JW0753	*ybhI*	51.5
JW2369	*yfdV*	62.1	JW0863	*macB*	51.5
JW1235	*oppA*	61.8	JW0794	*glnQ*	51.1
JW0066	*thiP*	61.2	JW3482	*mdtF*	50.7
JW3422	*livH*	60.1	JW2304	*hisM*	50.6
JW0562	*cusF*	60.1	JW0046	*kefC*	50.3
JW3035	*ttdT*	60.1	JW1111	*potB*	50.2
JW3508	*yhjV*	59.5	JW0564	*cusA*	50.1
JW0565	*pheP*	58.5	JW3633	*setC*	49.9
JW1469	*yddG*	58.1	JW0148	*fhuD*	49.9
JW3420	*livG*	56.5	JW3419	*livF*	49.6
JW0451	*acrB*	56.3	JW0108	*aroP*	49.4
JW3210	*aaeA*	56.3	JW1592	*mdtJ*	49.4
JW1591	*mdtI*	56.0	JW2060	*mdtB*	49.1
JW1109	*potD*	55.9	JW1902	*yecC*	49.1
JW0320	*yahN*	55.9	JW1903	*yecS*	49.1
JW3421	*livM*	55.8	JW0561	*cusC*	49.1
JW3425	*livJ*	55.4	JW0065	*thiQ*	49.0
JW0452	*acrA*	54.6	JW0069	*setA*	48.5
JW3481	*mdtE*	54.6	JW0391	*brnQ*	48.5
JW1487	*gadC*	54.4	JW1112	*potA*	48.4

Table 2 *continued.*

Keio collection No.	Deleted gene	Put conc. (μM)	Keio collection No.	Deleted gene	Put conc. (μM)
JW1287	*sapA*	48.3	JW2661	*emrB*	40.4
JW0604	*citT*	48.3	JW0679	*potE*	40.4
JW1521	*ydeA*	47.8	JW0841	*potI*	40.4
JW3509	*dppF*	47.4	JW1597	*ydgI*	40.3
JW0149	*fhuB*	47.1	JW0796	*glnH*	40.2
JW1289	*puuP*	46.9	JW3558	*yiaV*	39.9
JW0735	*zitB*	46.8	JW2621	*yfjV*	39.8
JW2305	*hisQ*	46.8	JW0359	*tauC*	39.6
JW3234	*acrF*	46.2	JW2813	*yqeG*	39.4
JW2143	*lysP*	45.2	JW0067	*tbpA*	39.2
JW3193	*nanT*	44.9	JW2436	*eutH*	39.1
JW1088	*fhuE*	44.8	JW0358	*tauB*	38.9
JW0357	*tauA*	44.5	JW2364	*emrY*	38.8
JW0840	*potH*	44.5	JW0473	*copA*	38.6
JW3130	*mtr*	44.0	JW0475	*ybaT*	38.1
JW5802	*ydbA*	43.9	JW0826	*cmr*	37.7
JW2638	*gabP*	43.8	JW1965	*yeeO*	37.6
JW0468	*fsr*	43.7	JW0845	*artM*	37.6
JW3513	*dppA*	43.7	JW0862	*macA*	37.4
JW2307	*argT*	43.4	JW0847	*artI*	37.3
JW0548	*ybcW*	43.0	JW2454	*acrD*	36.7
JW3212	*aaeR*	42.9	JW1040	*mdtG*	36.5
JW2157	*setB*	42.9	JW1464	*narU*	36.5
JW1780	*yeaN*	42.7	JW0476	*cueR*	35.6
JW3510	*dppD*	42.7	JW1895	*tyrP*	34.1
JW1655	*mdtK*	42.6	JW2767	*sdaC*	33.1
JW2365	*emrK*	42.4	JW2660	*emrA*	31.2
JW2303	*hisP*	42.2	JW1284	*sapD*	25.5
JW0049	*apaG*	41.8	JW1283	*sapF*	18.6
JW0838	*potF*	41.1			

RESULTS

Screening for a putrescine exporter

Based on the hypothesis that the putrescine concentration in the culture supernatant of strains with a deletion of the gene encoding a putrescine exporter is lower than that of the parental strain, the putrescine concentration was measured in the culture supernatant of 123 strains with deletions of genes involved in or annotated as transport systems (Fig. 1A and Table 2). The deletion strains were obtained from the Keio collection, which is an *E. coli* single gene deletion mutant library that has been previously described (19). The screening indicated that the putrescine concentration of culture supernatant of *E. coli* Δ*sapF* strain (JW1283) was the lowest (18.6 μM) of the tested strains, and the second lowest putrescine concentration of the culture supernatant was 25.5 μM observed in Δ*sapD* strain (JW1284). These values were significantly lower than those of the parental strain (BW25113, 48.8 μM) or the median (48.7 μM) of the strains tested (Fig. 1A). These results suggested that *sapD* and *sapF* contribute to putrescine export from the cell.

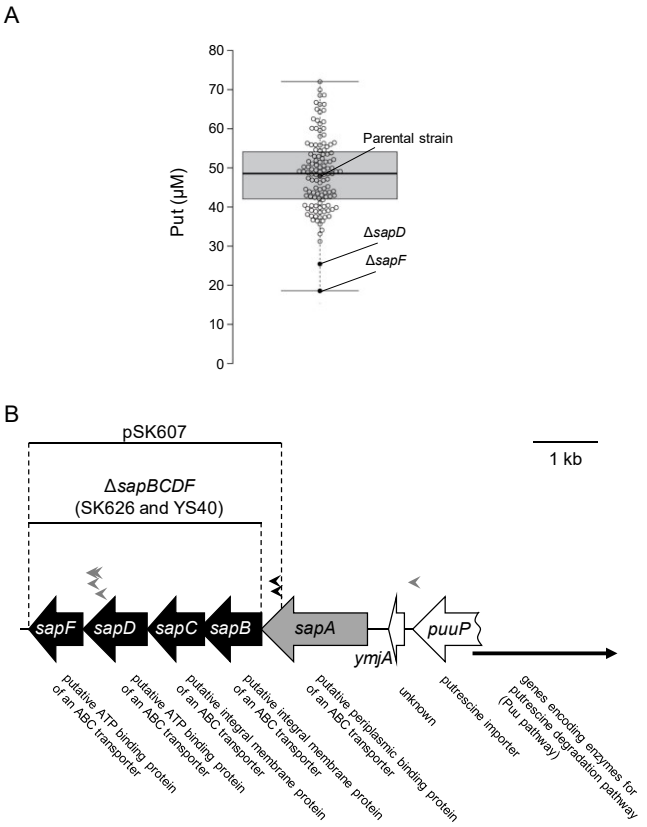

Fig. 1. Putrescine concentrations of culture supernatant of screened strains and depiction of putative *sapABCDF* operon.

(A) Putrescine concentrations of the culture supernatant of the screened strains. Bacterial strains were grown for 6 hours at 37 ºC with reciprocal shaking at 140 rpm in 5 mL of M9 + tryptone + succinate medium in a 20 mL test tube. Culture supernatant was harvested and subjected to HPLC analysis. Dots in the box plot indicate putrescine concentration of culture supernatant of tested mutants. The concentration of putrescine of culture supernatant of parental strain (BW25113), Δ*sapD* (JW1284), and Δ*sapF* (JW1283) are indicated as solid dots.

(B) The putative *sapABCDF* operon and its deleted or subcloned regions in this study. Locations and directions of genes are indicated by arrows and the annotations of genes are indicated below the arrows. Locations of predicted promoters are shown by arrowheads: Gray arrowheads indicate σ54, black arrowheads indicate σ70. The deleted region of the chromosome in the Δ*sapBCDF* strains and cloned regions in the pACYC184 vector are shown in the illustration.

*Putrescine concentration of the culture supernatant is not influenced by Δ***sapA** *but is affect by Δ***sapBCDF**

An *in silico* analysis predicts that *sapD* and *sapF* are located in the *sapABCDF* operon (Fig.

1B) but the function of *sapABCDF* has not been experimentally determined. From *in silico* annotation, SapA is predicted as a periplasmic binding protein of an ABC transporter, and SapB and SapC are predicted as integral membrane proteins of an ABC transporter, furthermore SapD and SapF are predicted to be ATP binding proteins of an ABC transporter (Fig. 1B). Based on the hypothesis that *sapABCDF* encodes a novel putrescine exporter, putrescine concentrations of culture supernatants of Δ*sapA* (JW1287), Δ*sapB* (JW1286), and Δ*sapC* (JW1285) strains were measured. Unexpectedly, the concentration of putrescine in the culture supernatant of Δ*sapA* (48.3 μM) was almost equivalent to that of the parental strain BW25113. In contrast, the putrescine concentration of culture supernatant of Δ*sapB* and Δ*sapC* strains were 37 % (18.2 μM) and 47 % (23.4 μM) of that of the parental strain BW25113, respectively. These results indicate that the decrease of putrescine concentration of culture supernatant came from the deletion of *sapB*, *sapC*, *sapD*, and *sapF* genes, but that *sapA* was not involved in the decrease of putrescine.

SapBCDF does not contribute to resistance against antimicrobial peptide LL-37

Previous studies have reported that SapABCDF proteins of *Salmonella enterica* sv. Typhimurium (28) and *Haemophillus influenzae* (29) contribute to resistance against antimicrobial peptides by uptake of these peptides followed by intracellular degradation of the peptide bonds. To examine the contribution of *sapBCDF* of *E. coli* to resistance against an antimicrobial peptide, the susceptibility of the *E. coli* MG1655 (wild type) and YS40 (MG1655 Δ*sapBCDF*) to the antimicrobial peptide LL-37 was analyzed (Fig. 2). *E. coli* was killed by LL-37 in a manner dependent on the concentration of the antimicrobial peptide, however, susceptibility to the LL-37 was not significantly different in MG1655 and YS40 (Δ*sapBCDF*) (Fig. 2). These results demonstrate that SapBCDF do not contribute to resistance against the antimicrobial peptide LL-37.

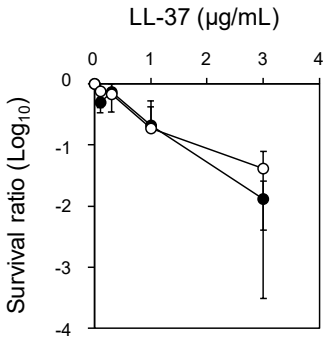

Fig. 2. Effect of the deletion of *sapBCDF* on resistance against LL-37, an antimicrobial peptide.
Strains were incubated with different concentrations of LL-37. After incubation, the cells were plated, and the numbers of colonies were counted after incubation. Survival ratios were calculated by dividing the colony forming units of strains incubated with LL-37 by those without LL-37. Closed and open circles indicate the mean survival ratio of MG1655 (parental strain) and YS40 (*sapBCDF* deleted strain), respectively. Data are expressed as the mean ± standard deviation (SD) of three separated experiments.

sapBCDF *increases the concentration of putrescine in culture supernatant*

To elucidate the role of *sapBCDF* in the regulation of putrescine concentration in culture supernatant, YS111 (pACYC184/wild type), YS112 (pACYC184/Δ*sapBCDF*), and YS113 (pACYC184-*sapB*$^+$*C*$^+$*D*$^+$*F*$^+$/Δ*sapBCDF*) were constructed, and the cell density (OD_{600}), putrescine concentrations of culture supernatant normalized by the cell density (μM/OD_{600}), and putrescine

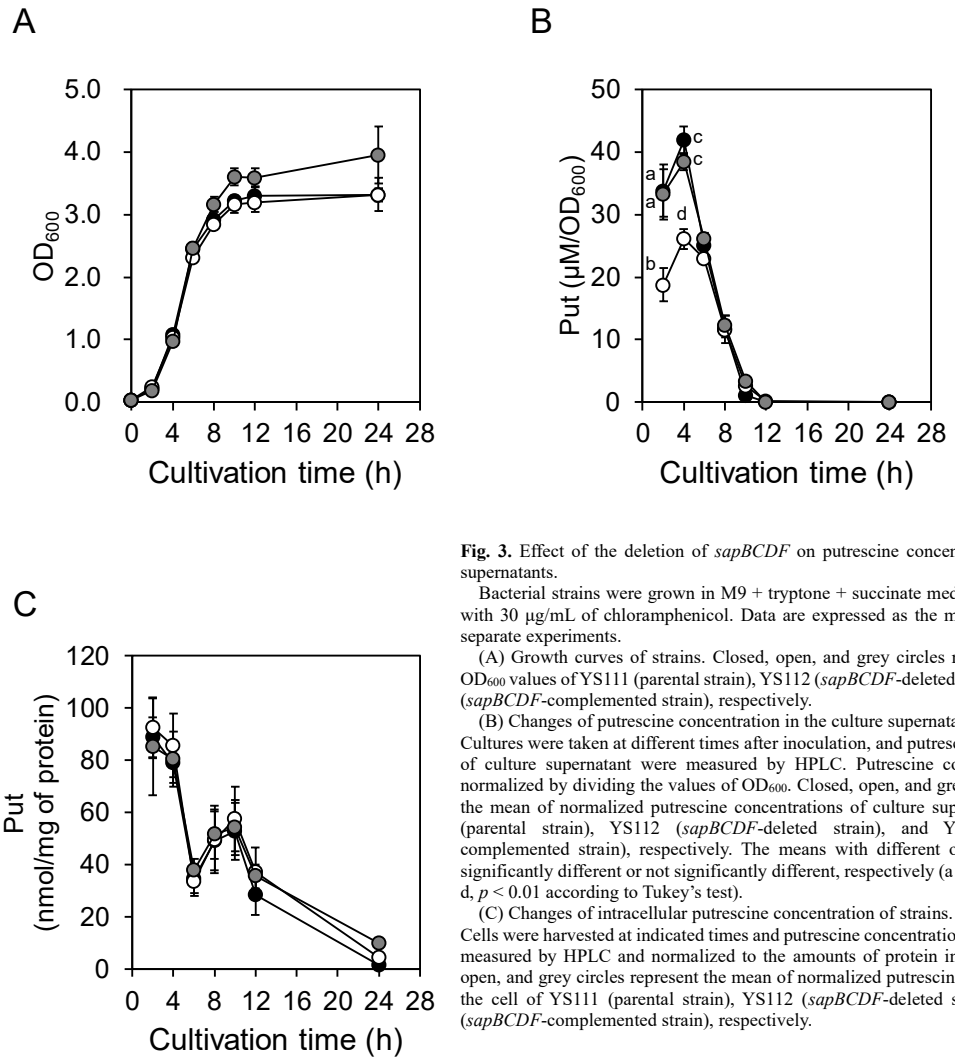

Fig. 3. Effect of the deletion of *sapBCDF* on putrescine concentrations of culture supernatants.

Bacterial strains were grown in M9 + tryptone + succinate medium supplemented with 30 μg/mL of chloramphenicol. Data are expressed as the mean ± SD of three separate experiments.

(A) Growth curves of strains. Closed, open, and grey circles represent the mean OD_{600} values of YS111 (parental strain), YS112 (*sapBCDF*-deleted strain), and YS113 (*sapBCDF*-complemented strain), respectively.

(B) Changes of putrescine concentration in the culture supernatant of strains. Cultures were taken at different times after inoculation, and putrescine concentrations of culture supernatant were measured by HPLC. Putrescine concentrations were normalized by dividing the values of OD_{600}. Closed, open, and grey circles represent the mean of normalized putrescine concentrations of culture supernatant of YS111 (parental strain), YS112 (*sapBCDF*-deleted strain), and YS113 *(sapBCDF*-complemented strain), respectively. The means with different or same letters are significantly different or not significantly different, respectively (a vs b, $p < 0.01$; c vs d, $p < 0.01$ according to Tukey's test).

(C) Changes of intracellular putrescine concentration of strains. Cells were harvested at indicated times and putrescine concentrations in the cells were measured by HPLC and normalized to the amounts of protein in the cells. Closed, open, and grey circles represent the mean of normalized putrescine concentrations in the cell of YS111 (parental strain), YS112 (*sapBCDF*-deleted strain), and YS113 (*sapBCDF*-complemented strain), respectively.

concentration in the cells (nmol/mg of protein) were measured (Fig. 3). Cell growth of YS111 (parental strain) and YS112 (*sapBCDF*-deleted strain) were not significantly different although that of YS113 (*sapBCDF*-complemented strain) was slightly increased compared to the YS111 and YS112 (Fig. 3A). Putrescine concentrations of culture supernatants of YS111 (parental strain) and YS113 (*sapBCDF*-complemented strain) peaked at 4 hours after inoculation and reached 41.9 μM/OD_{600} and 38.4 μM/OD_{600}, respectively (Fig. 3B) and decreased to zero at 12 hours. In contrast, the peak putrescine concentration of culture supernatant of YS112 (*sapBCDF* deleted strain) was 26.2 μM/OD_{600} (63 % of parental strain) at 4 hours after inoculation (Fig. 3B). The difference in the putrescine concentration of culture supernatant between $sapB^+C^+D^+F^+$ strains (YS111 and YS113) and Δ*sapBCDF* (YS112) was highly statistically significant ($p < 0.01$, Tukey's test) at 2 and 4 hours after inoculation (Fig. 3B). In contrast, putrescine concentration in the cell was not influenced by deletion and complementation of *sapBCDF* (Fig. 3C), suggesting that the decrease in putrescine concentration of the culture supernatant by the deletion of *sapBCDF* (Fig. 3B) was not caused by decreased production of

putrescine in *E. coli* cells. The putrescine concentrations of culture supernatant started to decrease rapidly at 4 hours after inoculation (Fig. 3B). Kurihara *et al*. previously reported that the decrease of putrescine in culture supernatant was caused by putrescine uptake by a putrescine importer PuuP (14). To emphasize the increase of putrescine in culture supernatant by *sapBCDF*, strains SK627 (pACYC184/Δ*puuP*, parental strain), SK628 (*sapBCDF*-deleted strain), and SK634 *(sapBCDF*-complemented strain) were constructed in the *puuP* deletion background. Cell growth of SK627 (parental strain) and SK634 (*sapBCDF*-complemented strain) were almost identical, however, cell growth of SK628 (*sapBCDF*-deleted strain) was inhibited compared to SK627 and SK634 (Fig. 4A). Putrescine concentrations of culture supernatant of SK627 (parental strain) and SK634 (*sapBCDF*-complemented strain) peaked at 8 to 10 hours, respectively, after inoculation, and reached 103.4 μM and 83.6 μM, respectively (Fig. 4B). In contrast, the maximum putrescine concentration of culture supernatant of SK628 (*sapBCDF*-deleted strain) was only 33.6 μM (32 % of parental strain) at 12 hours after inoculation (Fig. 4B). Putrescine concentration of culture supernatant normalized by cell growth (μM/OD_{600}) showed a similar trend where putrescine concentration of the culture supernatant depended on the presence of *sapBCDF* (Fig. 4C). These results demonstrate that *sapBCDF* plays an important role in increasing putrescine concentration of the culture supernatant.

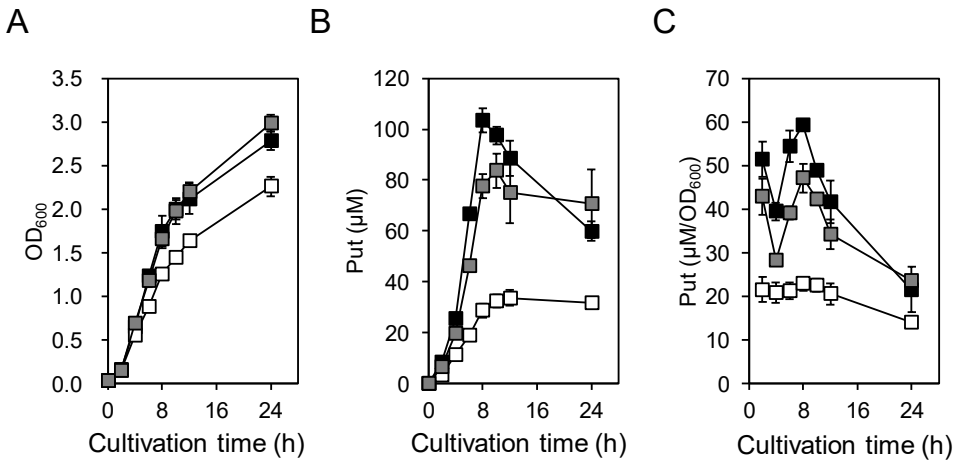

Fig. 4. Effect of the deletion of *sapBCDF* in Δ*puuP* background on putrescine concentrations of culture supernatant.
Bacterial strains were grown in M9 + tryptone medium supplemented with 30 μg/mL of chloramphenicol. Data are expressed as the mean ± SD of three separate experiments.
(A) Growth curves of strains. Closed, open, and grey squares represent the mean of OD_{600} values of SK627 (pACYC184/Δ*puuP*, parental strain), SK628 (*sapBCDF*-deleted strain), SK634 (*sapBCDF*-complemented strain), respectively.
(B and C) Changes of putrescine concentration of the culture supernatant of strains.
Cultures were taken at different times after inoculation, and putrescine concentrations of culture supernatant were measured by HPLC (B). The putrescine concentrations were normalized by dividing the values of OD_{600} (C). Closed, open, and grey squares represent the mean of normalized putrescine concentrations of culture supernatant of SK627 (pACYC184/Δ*puuP*, parental strain), SK628 (*sapBCDF*-deleted strain), SK634 (*sapBCDF*-complemented strain), respectively.

*Δ*sapBCDF *does not stimulate putrescine uptake*

To eliminate the possibility that putrescine uptake was facilitated by the deletion of *sapBCDF*, YS233 (pACYC184/Δ*puuP* Δ*speB* Δ*speC*, parental strain), YS234 (*sapBCDF*-deleted strain), and YS235 (*sapBCDF*-complemented strain) were grown in M9 + tryptone medium supplemented with 100 μM putrescine and the concentration of putrescine of the culture supernatant was measured. In this experiment, to facilitate comparison of decreases of putrescine in the culture supernatant, export of putrescine from *E. coli* cell was abolished by deletion of *speB* and *speC* genes encoding enzymes for putrescine biosynthesis. Cell growth of YS235 (*sapBCDF*-complemented strain) was considerably inhibited compared to that of YS233 (parental strain), furthermore, cell growth of YS234 (*sapBCDF*-deleted strain) was considerably decreased compared to that of YS235 (*sapBCDF*-complemented strain) (Fig. 5A). Putrescine concentrations of the culture supernatant of tested strains were decreased gradually, but no significant differences of the putrescine concentration of culture supernatants were observed (Fig. 5B). Decrease of the concentration of putrescine normalized by the cell growth (μM/OD_{600}) was not significantly different at 8 hours after inoculation of the tested strains (Fig. 5C), suggesting that deletion and complementation of *sapBCDF* did not influence uptake of putrescine from the medium. Taken together, the decrease of putrescine concentration of culture supernatant by the deletion of *sapBCDF* (Figs. 3 and 4) did not result from increased putrescine uptake but from decreased putrescine export from *E. coli* cells.

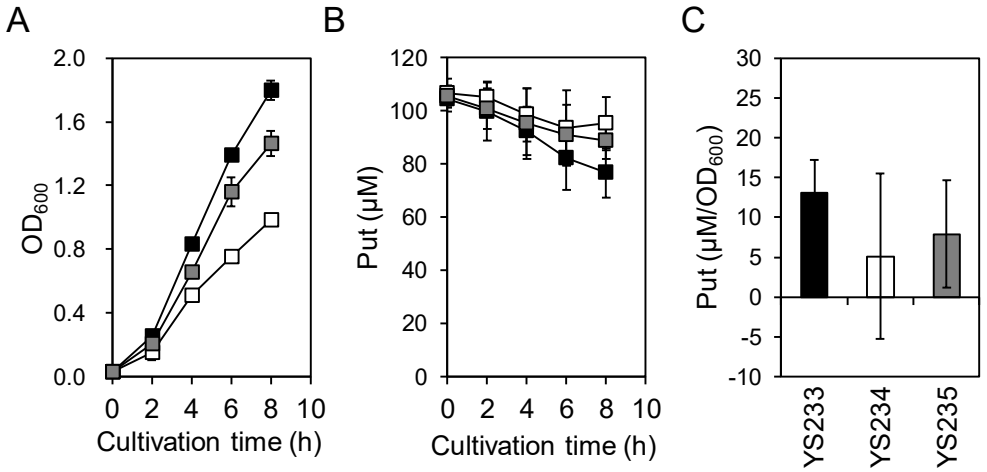

Fig. 5. Effect of the deletion of *sapBCDF* on putrescine uptake from the medium.
Bacterial strains were grown in M9 + tryptone medium supplemented with 30 μg/mL of chloramphenicol and 100 μM putrescine, and growth of strains were measured optical density at 600 nm (OD_{600}). Data are expressed as the mean ± SD of three separate experiments.
(A) Growth curves of strains.
Closed, opens, and grey squares represent the mean of OD_{600} values of YS233 (pACYC184/Δ*speB* Δ*speC* Δ*puuP* parental strain), YS234 (*sapBCDF*-deleted strain), and YS235 (*sapBCDF*-complemented strain), respectively.
(B) Uptake of putrescine from culture by tested strains.
Cultures were taken at different times after inoculation and putrescine concentration of culture supernatant was measured by HPLC. Closed, open, and grey squares represent the mean of putrescine concentration of culture supernatant of YS233 (pACYC184/Δ*speB* Δ*speC* Δ*puuP* parental strain), YS234 (*sapBCDF*-deleted strain), and YS235 (*sapBCDF*-complemented strain), respectively.
(C) Decreases of putrescine in the culture supernatants of tested strains.
First, a decrease of putrescine concentration during the culture was calculated by subtracting putrescine concentration (μM) of culture supernatant at 8 hours after inoculation from 100 μM, which is the original putrescine concentration of the medium used in this experiment. Then, the decreases (μM) were normalized by dividing the values of OD_{600}. Closed, open, and grey bars represent the normalized decrease of putrescine concentration of culture supernatant of YS233 (pACYC184/Δ*speB* Δ*speC* Δ*puuP* parental strain), YS234 (*sapBCDF*-deleted strain), and YS235 (*sapBCDF*-complemented strain), respectively.

Export of putrescine by SapBCDF

To demonstrate clearly that the increase of putrescine in the culture supernatant resulted from transport of putrescine from *E. coli* cells into the environment mediated by SapBCDF, an assay using stable isotope-labeled arginine (S.I.Arg) was performed. In this experiment (Fig. 6A), S.I.Arg is imported into *E. coli* cells by an arginine transporter and metabolized to stable isotope-labeled putrescine (S.I.Put) via stable isotope-labeled agmatine through sequential reactions catalyzed by SpeA (arginine decarboxylase) and SpeB (agmatine ureohydrolase). If the resultant S.I.Put is exported from the *E. coli* cells to the medium by SapBCDF, the concentration of S.I.Put in the culture supernatant will be influenced by deletion and complementation of *sapBCDF*. In the culture supernatant of SK627 (pACYC184/Δ*puuP*, parental strain), concentration of S.I.Put was 21.8 μM/OD_{600}. In contrast, the concentration of S.I.Put in culture supernatant of SK628 (*sapBCDF*-deleted strain) was 8.3 μM/OD_{600} and this value was a 62 % decrease ($p < 0.01$, Tukey's test) from the value of parental strain SK627. In the complementation strain SK634 (*sapBCDF*-complemented strain), the concentration of S.I.Put in culture supernatant was restored to 77 % (16.9 μM/OD_{600}) of the value of the parental strain SK627 (Fig. 6B). Total putrescine concentration (Fig. 5C) showed similar trends to S.I.Put concentration in culture supernatant (Fig. 6B) and the ratio of stable isotope-labeled and unlabeled putrescine was almost same in the three strains used in the study (Fig. 6D), suggesting the stable-isotope-labeling affected neither arginine metabolism nor putrescine export from *E. coli* cells. These results demonstrated that SapBCDF is responsible for putrescine export.

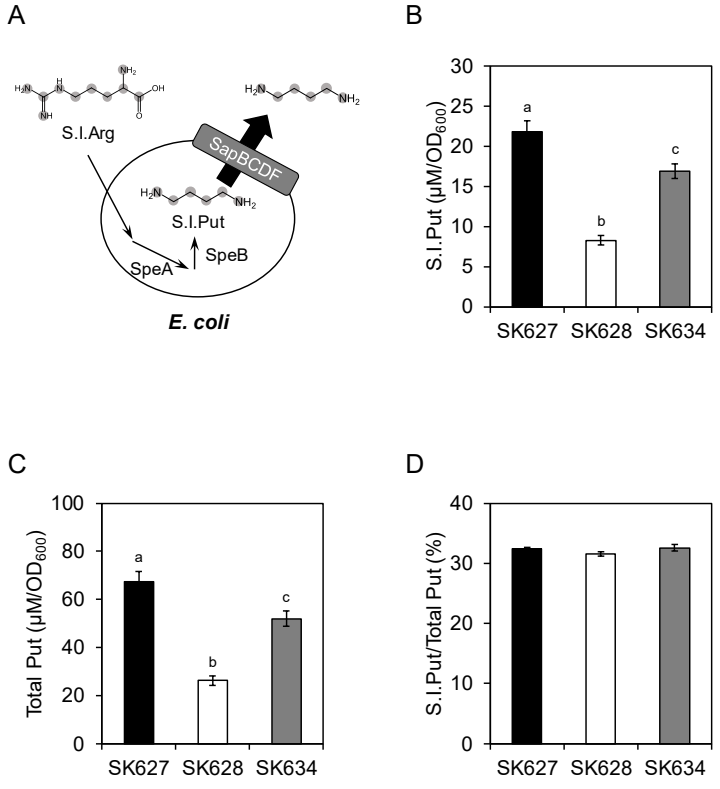

Fig. 6. Effect of the deletion of *sapBCDF* on the concentration of culture supernatant of stable isotope-labeled putrescine derived from stable isotope-labeled arginine supplemented to the medium.

Bacterial cells were grown in M9 + tryptone medium supplemented with 30 μg/mL of chloramphenicol and 1 mM of S.I.Arg. Cultures were harvested at 8 hours after inoculation. Analysis of S.I.Put of the culture supernatant was performed by GC-MS, and putrescine concentration was quantified using a standard curve and internal standard methods. Data are expressed as the mean ± SD of three separated experiments.

(A) Schematic illustration of the experiment. Gray circles indicate stable isotope-labeled atoms.

(B and C) Concentration of S.I.Put (B) and total putrescine, sum of S.I.Put and native putrescine (C) of culture supernatant of SK627 (pACYC184/Δ*puuP*, parental strain), SK628 (*sapBCDF*-deleted strain), and SK634 (*sapBCDF*-complemented strain). The columns with different letters are significantly different (a vs b, $p < 0.01$; a vs c, $p < 0.05$; b vs c, $p < 0.01$ according to Tukey's test).

(D) Ratio of S.I.Put to total putrescine of SK627 (pACYC184/Δ*puuP*, parental strain), SK628 (*sapBCDF*-deleted strain), and SK634 (*sapBCDF*-complemented strain).

DISCUSSION

The present study has revealed that SapBCDF of *E. coli* export putrescine from cells to the extracellular environment. In previous studies, MdtJI of *E. coli* (30) and Blt of *Bacillus subtilis* (31) were reported as spermidine exporters. Additionally, in *Shigella flexneri* it was reported that MdtJI was a putrescine exporter (32). However, in these three reports strains overexpressing genes of polyamine exporters were used for assays of polyamine export. Furthermore, none of these previous studies analyzed the decreased polyamine export activity of the mutant strains with the deletion of genes encoding polyamine exporters, nor measured the polyamine concentration of the culture supernatant (30-32). It was previously reported that PotE is a putrescine-ornithine antiporter at acidic pH (17). Also, it was previously described that at neutral pH, *E. coli* excretes putrescine into the environment independently of PotE (18), suggesting that there are other unidentified putrescine exporters in *E. coli*. The present study demonstrated that SapBCDF plays a major role in this putrescine export (Figs. 3 and 4).

For the characterization of metabolite exporters, inside-out membrane vesicles (16) or the reconstituted proteoliposomes should be used, ideally (33). However, there are many reports where these methods were not used because of the technical difficulty of the procedure (34). In the present study, because inside-out membrane vesicles and the reconstituted proteoliposomes were not used, the kinetic parameters were not determined, however, the present study clearly revealed that S.I.Put metabolized from S.I.Arg in *E. coli* cells was exported from cells to the extracellular environment by SapBCDF (Fig. 6).

SapABCDF is specifically distributed within gamma-proteobacteria. Previous studies reported that SapABCDF contributes to resistance of bacteria against cationic antimicrobial peptides: LL-37, β-defensin, and protamine, produced by mammals (28,35). Parra-Lopez *et al*., reported that *S. enterica* sv. Typhimurium Δ*sapABCDF* strain was more sensitive to protamine than the parental strain and they hypothesized that *S. enterica* sv. Typhimurium took up antimicrobial peptides followed by the degradation in the cell by peptidases (28). This hypothesis was experimentally confirmed in *H. influenzae* using LL-37 and β-defensin (35). Furthermore, *H. influenzae sapA* mutant exhibited attenuated survival in a chinchilla model of otitis media (29). The amino acid identity of SapABCDF in *E. coli* and *S. enterica* sv. Typhimurium is very high (SapA, 90 %; SapB, 92 %; SapC, 95 %; SapD, 96 %; SapF, 98 %). Nonetheless, to date there has been no study showing that SapABCDF of *E. coli* contributes to resistance against antimicrobial peptides. In the present study, it was shown that SapBCDF of *E. coli* did not contribute to resistance against an antimicrobial peptide LL-37 (Fig. 2). In *E. coli*, there is no report describing experimentally the function of SapA, SapB, SapC, or SapF, and there has been only one report that SapD (also known as TrkE) of *E. coli* plays a role as an ATPase for potassium transporters TrkH and TrkG (36). Similarly to *E. coli*, it was reported previously that

the uptake of potassium by a *H. influenzae* Δ*sapD* strain decreased, suggesting that SapD is involved in the uptake of potassium (37). In the previous reports, it was described that in plants and animals, intracellular polyamine inhibited the uptake of potassium from the extracellular environment (38-40). Therefore, it is possible that in *E. coli* potassium uptake by TrkH and TrkG driven by ATPase activity of SapD has some relationship to putrescine export by SapBCDF.

Polyamines are important for cell proliferation and therefore the intracellular concentration of polyamines in bacteria are high at exponential growth phase and lower at stationary phase (41) (Fig. 3C), and both degradation and export of polyamines may consume intracellular pool of polyamines. The Puu pathway is the putrescine degradation pathway (14,22,24,42-44) expressed at early stationary phase. If the regulation of *sapBCDF*, mediating putrescine export, and the *puu* gene cluster, responsible for putrescine degradation, is executed in a co-ordinate manner, putrescine level effectively decreases from exponential growth phase to stationary phase in *E. coli*. Because the *sapBCDF* gene cluster is located immediately adjacent to the *puu* gene cluster on *E. coli* chromosome, it is possible that genes of this region are coordinately regulated. Therefore, it is probable that these two co-localized gene clusters, *sapBCDF* and the *puu* gene cluster function to decrease putrescine levels at the end of the exponential growth phase.

In the present study, export of putrescine was not inhibited by the deletion of *sapA* (Table 2). It is logical that SapA is not involved in the export of putrescine from cytosol to the extracellular environment because SapA is annotated as periplasmic substrate binding protein of an ABC transporter. Furthermore, it was previously reported that *sapABCDF* of *S. enterica* sv. Typhimurium are expressed polycistronically (28) in *E. coli*; however, the predicted promotor of *sapA* is located independently of that of *sapBCDF* (Fig. 1B) and the predicted sigma factor for *sapA* (σ70) is different from that for *sapBCDF* (σ54). Therefore, it is quite possible that *sapA* and *sapBCDF* are expressed separately, suggesting that SapBCDF has a function independent of SapA. In the present study, as the first report identifying the functions of SapB, SapC, and SapF, it was shown that SapBCDF of *E. coli* exported putrescine from cells to the extracellular environment (Figs. 3, 4, and 6) but did not contribute to resistance against an antimicrobial peptide LL-37 (Fig. 2). Therefore, it is very probable that SapBCDF is a novel putrescine exporter functioning in the neutral environmental conditions. However, approximately 30 μM of putrescine was detected in the culture supernatant of a Δ*puuP* Δ*sapBCDF* double mutant (Fig. 4B), suggesting the existence of additional putrescine exporters other than SapBCDF in *E. coli*.

REFERENCES

1. Goodwin, A. C., Destefano Shields, C. E., Wu, S., Huso, D. L., Wu, X., Murray-Stewart, T. R., Hacker-Prietz, A., Rabizadeh, S., Woster, P. M., Sears, C. L., and Casero, R. A. (2011) Polyamine catabolism contributes to enterotoxigenic *Bacteroides fragilis*-induced colon tumorigenesis. *Proc Natl Acad Sci U S A* **108**, 15354-15359
2. Dubin, K., Callahan, M. K., Ren, B., Khanin, R., Viale, A., Ling, L., No, D., Gobourne, A., Littmann, E., Huttenhower, C., Pamer, E. G., and Wolchok, J. D. (2016) Intestinal microbiome analyses identify melanoma patients at risk for checkpoint-blockade-induced colitis. *Nat Commun* **7**, 10391
3. Thompson, P. A., Wertheim, B. C., Zell, J. A., Chen, W. P., McLaren, C. E., LaFleur, B. J., Meyskens, F. L., and Gerner, E. W. (2010) Levels of rectal mucosal polyamines and prostaglandin E2 predict ability of DFMO and sulindac to prevent colorectal adenoma. *Gastroenterology* **139**, 797-805, 805.e791
4. Kibe, R., Kurihara, S., Sakai, Y., Suzuki, H., Ooga, T., Sawaki, E., Muramatsu, K., Nakamura, A., Yamashita, A., Kitada, Y., Kakeyama, M., Benno, Y., and Matsumoto, M. (2014) Upregulation of colonic luminal polyamines produced by intestinal microbiota delays senescence in mice. *Sci Rep* **4**, 4548
5. Matsumoto, M., Kurihara, S., Kibe, R., Ashida, H., and Benno, Y. (2011) Longevity in mice is promoted by probiotic-induced suppression of colonic senescence dependent on upregulation of gut bacterial polyamine production. *PLoS One* **6**, e23652
6. Soda, K., Dobashi, Y., Kano, Y., Tsujinaka, S., and Konishi, F. (2009) Polyamine-rich food decreases age-associated pathology and mortality in aged mice. *Exp Gerontol* **44**, 727-732
7. Morris, D. R., and Pardee, A. B. (1965) A biosynthetic ornithine decarboxylase in *Escherichia coli*. *Biochem Biophys Res Commun* **20**, 697-702
8. Kashiwagi, K., Suzuki, T., Suzuki, F., Furuchi, T., Kobayashi, H., and Igarashi, K. (1991) Coexistence of the genes for putrescine transport protein and ornithine decarboxylase at 16 min on *Escherichia coli* chromosome. *J Biol Chem* **266**, 20922-20927
9. Moore, R. C., and Boyle, S. M. (1990) Nucleotide sequence and analysis of the *speA* gene encoding biosynthetic arginine decarboxylase in *Escherichia coli*. *J Bacteriol* **172**, 4631-4640
10. Satishchandran, C., and Boyle, S. M. (1986) Purification and properties of agmatine ureohydrolyase, a putrescine biosynthetic enzyme in *Escherichia coli*. *J Bacteriol* **165**, 843-848
11. Tabor, C. W., Tabor, H., and Xie, Q. W. (1986) Spermidine synthase of *Escherichia coli*: localization of the *speE* gene. *Proc Natl Acad Sci U S A* **83**, 6040-6044

12. Pistocchi, R., Kashiwagi, K., Miyamoto, S., Nukui, E., Sadakata, Y., Kobayashi, H., and Igarashi, K. (1993) Characteristics of the operon for a putrescine transport system that maps at 19 minutes on the *Escherichia coli* chromosome. *J Biol Chem* **268**, 146-152
13. Furuchi, T., Kashiwagi, K., Kobayashi, H., and Igarashi, K. (1991) Characteristics of the gene for a spermidine and putrescine transport system that maps at 15 min on the *Escherichia coli* chromosome. *J Biol Chem* **266**, 20928-20933
14. Kurihara, S., Tsuboi, Y., Oda, S., Kim, H. G., Kumagai, H., and Suzuki, H. (2009) The putrescine Importer PuuP of *Escherichia coli* K-12. *J Bacteriol* **191**, 2776-2782
15. Kurihara, S., Suzuki, H., Oshida, M., and Benno, Y. (2011) A novel putrescine importer required for type 1 pili-driven surface motility induced by extracellular putrescine in *Escherichia coli* K-12. *J Biol Chem* **286**, 10185-10192
16. Kashiwagi, K., Miyamoto, S., Suzuki, F., Kobayashi, H., and Igarashi, K. (1992) Excretion of putrescine by the putrescine-ornithine antiporter encoded by the *potE* gene of *Escherichia coli*. *Proc Natl Acad Sci U S A* **89**, 4529-4533
17. Kashiwagi, K., Shibuya, S., Tomitori, H., Kuraishi, A., and Igarashi, K. (1997) Excretion and uptake of putrescine by the PotE protein in *Escherichia coli*. *J Biol Chem* **272**, 6318-6323
18. Schiller, D., Kruse, D., Kneifel, H., Krämer, R., and Burkovski, A. (2000) Polyamine transport and role of *potE* in response to osmotic stress in *Escherichia coli*. *J Bacteriol* **182**, 6247-6249
19. Baba, T., Ara, T., Hasegawa, M., Takai, Y., Okumura, Y., Baba, M., Datsenko, K. A., Tomita, M., Wanner, B. L., and Mori, H. (2006) Construction of *Escherichia coli* K-12 in-frame, single-gene knockout mutants: the Keio collection. *Mol Syst Biol* **2**, 2006.0008
20. Miller, J. H. (1972) *A Short Course in Bacterial Genetics.*, Cold Spring Harbor Laboratory Press, Cold Spring Harbor, NY.
21. Datsenko, K. A., and Wanner, B. L. (2000) One-step inactivation of chromosomal genes in *Escherichia coli* K-12 using PCR products. *Proc Natl Acad Sci U S A* **97**, 6640-6645
22. Kurihara, S., Oda, S., Kato, K., Kim, H. G., Koyanagi, T., Kumagai, H., and Suzuki, H. (2005) A novel putrescine utilization pathway involves gamma-glutamylated intermediates of *Escherichia coli* K-12. *J Biol Chem* **280**, 4602-4608
23. Harwig, S. S., Ganz, T., and R.I., L. (1994) Neutrophil defensins: purification, characterization, and antimicrobial testing. in *Methods in Enzymology*. pp 160-172
24. Kurihara, S., Kato, K., Asada, K., Kumagai, H., and Suzuki, H. (2010) A putrescine-inducible pathway comprising PuuE-YneI in which gamma-aminobutyrate is degraded into succinate in *Escherichia coli* K-12. *J Bacteriol* **192**, 4582-4591
25. Sakanaka, M., Sugiyama, Y., Kitakata, A., Katayama, T., and Kurihara, S. (2016)

Carboxyspermidine decarboxylase of the prominent intestinal microbiota species *Bacteroides thetaiotaomicron* is required for spermidine biosynthesis and contributes to normal growth. *Amino Acids* **48**, 2443-2451

26. Chen, G. G., Turecki, G., and Mamer, O. A. (2009) A quantitative GC-MS method for three major polyamines in postmortem brain cortex. *J Mass Spectrom* **44**, 1203-1210
27. Grenier, F., Matteau, D., Baby, V., and Rodrigue, S. (2014) Complete Genome Sequence of *Escherichia coli* BW25113. *Genome Announc* **2**
28. Parra-Lopez, C., Baer, M. T., and Groisman, E. A. (1993) Molecular genetic analysis of a locus required for resistance to antimicrobial peptides in *Salmonella typhimurium*. *EMBO J* **12**, 4053-4062
29. Mason, K. M., Munson, R. S., and Bakaletz, L. O. (2005) A mutation in the *sap* operon attenuates survival of nontypeable *Haemophilus influenzae* in a chinchilla model of otitis media. *Infect Immun* **73**, 599-608
30. Higashi, K., Ishigure, H., Demizu, R., Uemura, T., Nishino, K., Yamaguchi, A., Kashiwagi, K., and Igarashi, K. (2008) Identification of a spermidine excretion protein complex (MdtJI) in *Escherichia coli*. *J Bacteriol* **190**, 872-878
31. Woolridge, D. P., Vazquez-Laslop, N., Markham, P. N., Chevalier, M. S., Gerner, E. W., and Neyfakh, A. A. (1997) Efflux of the natural polyamine spermidine facilitated by the *Bacillus subtilis* multidrug transporter Blt. *J Biol Chem* **272**, 8864-8866
32. Leuzzi, A., Di Martino, M. L., Campilongo, R., Falconi, M., Barbagallo, M., Marcocci, L., Pietrangeli, P., Casalino, M., Grossi, M., Micheli, G., Colonna, B., and Prosseda, G. (2015) Multifactor Regulation of the MdtJI Polyamine Transporter in *Shigella*. *PLoS One* **10**, e0136744
33. Sasahara, A., Nanatani, K., Enomoto, M., Kuwahara, S., and Abe, K. (2011) Substrate specificity of the aspartate:alanine antiporter (AspT) of *Tetragenococcus halophilus* in reconstituted liposomes. *J Biol Chem* **286**, 29044-29052
34. Pathania, A., and Sardesai, A. A. (2015) Distinct Paths for Basic Amino Acid Export in *Escherichia coli*: YbjE (LysO) Mediates Export of L-Lysine. *J Bacteriol* **197**, 2036-2047
35. Shelton, C. L., Raffel, F. K., Beatty, W. L., Johnson, S. M., and Mason, K. M. (2011) Sap transporter mediated import and subsequent degradation of antimicrobial peptides in *Haemophilus*. *PLoS Pathog* **7**, e1002360
36. Harms, C., Domoto, Y., Celik, C., Rahe, E., Stumpe, S., Schmid, R., Nakamura, T., and Bakker, E. P. (2001) Identification of the ABC protein SapD as the subunit that confers ATP dependence to the K^+-uptake systems Trk(H) and Trk(G) from *Escherichia coli* K-12. *Microbiology* **147**, 2991-3003
37. Mason, K. M., Bruggeman, M. E., Munson, R. S., and Bakaletz, L. O. (2006) The non-

typeable *Haemophilus influenzae* Sap transporter provides a mechanism of antimicrobial peptide resistance and SapD-dependent potassium acquisition. *Mol Microbiol* **62**, 1357-1372

38. Liu, K., Fu, H., Bei, Q., and Luan, S. (2000) Inward potassium channel in guard cells as a target for polyamine regulation of stomatal movements. *Plant Physiol* **124**, 1315-1326
39. Lopatin, A. N., Makhina, E. N., and Nichols, C. G. (1994) Potassium channel block by cytoplasmic polyamines as the mechanism of intrinsic rectification. *Nature* **372**, 366-369
40. Vandenberg, C. A. (2008) Integrins step up the pace of cell migration through polyamines and potassium channels. *Proc Natl Acad Sci U S A* **105**, 7109-7110
41. Igarashi, K., and Kashiwagi, K. (2000) Polyamines: mysterious modulators of cellular functions. *Biochem Biophys Res Commun* **271**, 559-564
42. Kurihara, S., Oda, S., Kumagai, H., and Suzuki, H. (2006) Gamma-glutamyl-gamma-aminobutyrate hydrolase in the putrescine utilization pathway of *Escherichia coli* K-12. *FEMS Microbiol Lett* **256**, 318-323
43. Kurihara, S., Oda, S., Tsuboi, Y., Kim, H. G., Oshida, M., Kumagai, H., and Suzuki, H. (2008) gamma-Glutamylputrescine synthetase in the putrescine utilization pathway of *Escherichia coli* K-12. *J Biol Chem* **283**, 19981-19990
44. Nemoto, N., Kurihara, S., Kitahara, Y., Asada, K., Kato, K., and Suzuki, H. (2012) Mechanism for regulation of the putrescine utilization pathway by the transcription factor PuuR in *Escherichia coli* K-12. *J Bacteriol* **194**, 3437-3447

SUMMARY

Recent research has suggested that polyamines (putrescine, spermidine, and spermine) in the intestinal tract impact the health of animals either negatively or positively. The concentration of polyamines in the intestinal tract results from the balance of uptake and export of gut microbes. However, the mechanism of polyamine export from microbial cells to the intestinal lumen is still unclear. In *Escherichia coli*, PotE was previously identified as a transporter responsible for putrescine excretion in an acidic growth environment. The author observed putrescine concentration in the culture supernatant was increased from zero to 50 μM during growth of *E. coli* under a neutral pH environment. Screening for the unidentified putrescine exporter was performed using a gene knockout collection of *E. coli* and deletion of *sapBCDF* significantly decreased putrescine levels in the culture supernatant. Complementation of the deletion mutant with the *sapBCDF* genes restored putrescine levels in the culture supernatant. Additionally, the Δ*sapBCDF* strain did not facilitate uptake of putrescine from the culture supernatant. Taken together, these findings suggested that *sapBCDF* is responsible for the putrescine export. Quantification of stable isotope-labeled putrescine derived from stable isotope-labeled arginine supplemented in the medium revealed that SapBCDF exported putrescine from *E. coli* cells to the culture supernatant. It was previously reported that SapABCDF of *Salmonella enterica* sv. Typhimurium and *Haemophilus influenzae* conferred resistance to antimicrobial peptides; however, the *E. coli* Δ*sapBCDF* strain did not affect resistance to antimicrobial peptide LL-37. These results strongly suggest that the natural function of the SapBCDF proteins is the export of putrescine.

CONCLUSION

As described in "*GENERAL INTRODUCTION*", host and gut microbes interact, and unraveling and understanding this interaction is extremely important in managing the health of the host. To develop a basis for understanding the host-gut microbe interaction from the perspective of compounds, the author focused on glycans, especially the H-antigen structure as a host-derived factor and polyamines as gut microbe-derived factors.

In CHAPTER I, the author focused on H-antigen structure and aimed for the efficient enzymatic synthesis of H-antigen structures. In SECTION I, the author developed highly functional 1,2-α-L-fucosynthase *Bb*AfcA^{N423H} from *Bb*AfcA. *Bb*AfcA^{N423H} synthesized type-1, type-2, type-3, and type-4 H-antigens, Le$^{b/y}$ antigens, and other H-antigen-containing unnatural oligosaccharides. It also introduced H-antigens onto *O*-glycans of porcine gastric mucin. In addition, the author revealed the structural characteristics that *Bb*AfcA^{N423H} requires to recognize as acceptor. In SECTION II, the author applied *Bb*AfcA^{N423H} to introduce H-antigen structures on various glycoconjugates. *Bb*AfcA^{N423H} could introduce H-antigen structures on *O*- and *N*-glycans of glycoproteins, glycolipid, and plant xyloglucan. By virtue of high efficiency, high regio-specificity at the non-reducing end, and mild reaction conditions, *Bb*AfcA^{N423H} not only provided H-antigen-containing glycoconjugates for better understanding the host-gut microbe interaction mediated by H-antigen structures, but also served as a useful tool in the field of glycobiology.

In CHAPTER II, the author focused on polyamine biosynthesis and transport of human gut microbes. In SECTION I, the author evaluated the biosynthesis and transport abilities of the polyamines (putrescine, spermidine, and spermine) of 32 species of GAM culturable human dominant gut microbes. Furthermore, by combining the polyamine concentration determinations in the culture supernatants and cells with the data from BlastP analysis the author showed that 11 species of tested human gut microbes may possess novel polyamine biosynthetic proteins and/or transporters. In SECTION II, the author evaluated the biosynthesis and transport abilities of the polyamines (putrescine, spermidine, and spermine) of 13 species of human indigenous *Bifidobacterium* species. The author showed that 6 species of human indigenous bifidobacteria possessed polyamine biosynthetic ability and 10 species possessed polyamine transport ability. In addition, by combining polyamine concentration determinations in culture supernatant and cells with the data from BlastP analysis the author showed that 11 species of tested human indigenous *Bifidobacterium*, except for *B.*

bifidum and *B. gallicum* may possess novel polyamine biosynthetic proteins and/or transporters. In SECTION III, the author revealed that SapBCDF is a novel putrescine exporter in *Escherichia coli*, a model gut microbe. To date, the putrescine exporter which functions under a neutral growth environment has not been reported in human gut microbes. This is the first report in gut microbes that shows that SapBCDF exports putrescine under a similar neutral growth environment as that of the colonic lumen; thus, it is expected to function in the colonic lumen. These results are important regarding the regulation of polyamine levels in the colonic lumen by controlling gut microbes and their metabolisms.

In conclusion, the author developed a basis for understanding host-gut microbe interactions from the perspective of compounds.

ACKNOWLEDGEMENTS

The author would like to express his deepest appreciation for Dr. Jun Ogawa, Professor of the Graduate School of Agriculture, Kyoto University, for his kind instructions, constructive advice, and warm encouragement.

The author greatly appreciates Dr. Takane Katayama, Professor of the Graduate School of Biostudies, Kyoto University, for his kind encouragement, insightful comments, and invaluable support.

The author is deeply indebted to Dr. Shin Kurihara, Lecturer of the Faculty of Biology-Oriented Science and Technology, Kindai University, for his constructive instructions, warm support, and continuous encouragement.

The author would like to express his sincere gratitude for Dr. Hidehiko Kumagai, Consultant of Ishikawa Prefectural University and Emeritus Professor of Kyoto University and Ishikawa Prefectural University, and Dr. Kenji Yamamoto, Visiting Professor of Wakayama University and Emeritus Professor of Kyoto University and Ishikawa Prefectural University, for their sincere encouragement.

The author would like to express thankful appreciation to Dr. Hisashi Ashida, Professor of the Faculty of Biology-Oriented Science and Technology, Kindai University; Dr. Motomitsu Kitaoka, Professor of the Faculty of Agriculture, Niigata University; Dr. Kazuei Igarashi, Amine Pharma Research Institute and Emeritus Professor of Chiba University; Dr. Hideyuki Suzuki, Professor of the Division of Applied Biology, Kyoto Institute of Technology; Dr. Yuji Honda, Associate Professor of the Faculty of Bioresources and Environmental Science, Ishikawa Prefectural University; Dr. Shujiro Okuda, Associate Professor of the Graduate School of Medical and Dental Sciences, Niigata University; Dr. Mitsuharu Matsumoto, Kyodo Milk Industry Co., Ltd.; Dr. Kyohei Higashi, Lecturer of the Faculty of Pharmaceutical Science, Tokyo University of Science; Dr. Toshihiko Katoh, Assistant Professor of the Graduate School of Biostudies, Kyoto University; and Mr. Atsuo Nakamura, Kyodo Milk Industry Co., Ltd., for their valuable collaboration and insightful comments on this study.

The author is very grateful to Dr. Mikiyasu Sakanaka, National Food Institute of Technical University of Denmark, and Dr. Aina Gotoh, the Graduate School of Biostudies, Kyoto University, for their technical cooperation and valuable comments on this study.

The author thanks Dr. Erina Yoshida, Ms. Misaki Nara, and Mrs. Aya Kitakata from Ishikawa Prefectural University, and Ms. Ayaka Kanbe from Kyoto Institute of Technology, for providing technical assistance for this study.

The author expresses his gratitude to all the members of the Host-Microbe Interaction Research laboratory of Ishikawa Prefectural University for their kind support.

Acknowledgements are also made to Dr. Akira Nakagawa, Lecturer of Ishikawa Prefectural

University, for his helpful comments and moral support.

The author wishes to express his appreciation to Dr. Shigenobu Kishino, Associate Professor of the Graduate School of Agriculture, Kyoto University, for his incisive comments and passionate encouragement.

The author would like to offer special thanks to Dr. Hajime Ohigashi, Emeritus Professor of Kyoto University and Fukui Prefectural University, for his hearty and continued encouragement, and valuable advice.

Last, but not least, the author greatly thanks and acknowledges his family who has been understanding and supporting.

Yuta Sugiyama

LIST OF PUBLICATIONS

[I] **Yuta Sugiyama, Aina Gotoh, Toshihiko Katoh, Yuji Honda, Erina Yoshida, Shin Kurihara, Hisashi Ashida, Hidehiko Kumagai, Kenji Yamamoto, Motomitsu Kitaoka, and Takane Katayama.**

Introduction of H-antigens into oligosaccharides and sugar chains of glycoproteins using highly efficient 1,2-α-L-fucosynthase.

Glycobiology., 26:1235-1247 (2016)

[II] **Yuta Sugiyama, Atsuo Nakamura, Mitsuharu Matsumoto, Ayaka Kanbe, Mikiyasu Sakanaka, Kyohei Higashi, Kazuei Igarashi, Takane Katayama, Hideyuki Suzuki, and Shin Kurihara.**

A Novel Putrescine Exporter SapBCDF of *Escherichia coli*.

Journal of Biological Chemistry., 291:26343-26351 (2016)

[III] **Yuta Sugiyama, Toshihiko Katoh, Yuji Honda, Aina Gotoh, Hisashi Ashida, Shin Kurihara, Kenji Yamamoto, and Takane Katayama.**

Application study of 1,2-α-L-fucosynthase: introduction of Fucα1-2Gal disaccharide structures on *N*-glycan, ganglioside, and xyloglucan oligosaccharide.

Bioscience, Biotechnology, and Biochemistry., 81:283-291 (2017)

[IV] **Yuta Sugiyama, Misaki Nara, Mikiyasu Sakanaka, Aina Gotoh, Aya Kitakata, Shujiro Okuda, and Shin Kurihara.**

Comprehensive analysis of polyamine transport and biosynthesis in the dominant human gut bacteria: Potential presence of novel polyamine metabolism and transport genes.

International Journal of Biochemistry & Cell Biology., 93:52-61 (2017)

[V] **Yuta Sugiyama, Misaki Nara, Mikiyasu Sakanaka, Aya Kitakata, Shujiro Okuda, and Shin Kurihara.**

Analysis of polyamine biosynthetic- and transport ability of human indigenous *Bifidobacterium*.

Bioscience, Biotechnology, and Biochemistry., 82:1606-1614 (2018)

RELATED ARTICLE

1. **Masakazu Takahashi, Yuta Sugiyama, Kyuichi Kawabata, Yu Takahashi, Kazuhiro Irie, Akira Murakami, Yoshito Kubo, Kyoichi Kobayashi, and Hajime Ohigashi.**
   1,2-Di-*O*-α-linolenoyl-3-*O*-β-galactosyl-*sn*-glycerol as a Superoxide Generation Inhibitor from *Perilla frutescens* var. *crispa.*
   Bioscience, Biotechnology, and Biochemistry., 75:2240-2242 (2011)

2. **Kyuichi Kawabata, Yuta Sugiyama, Taiken Sakano, and Hajime Ohigashi.**
   Flavonols enhanced production of anti-inflammatory substance(s) by *Bifidobacterium adolescentis*: prebiotic actions of galangin, quercetin, and fisetin.
   Biofactors., 39:422-429 (2013)

3. **Aina Gotoh, Toshihiko Katoh, Yuta Sugiyama, Shin Kurihara, Yuji Honda, Haruko Sakurama, Taiho Kambe, Hisashi Ashida, Motomitsu Kitaoka, Kenji Yamamoto, and Takane Katayama.**
   Novel substrate specificities of two lacto-*N*-biosidases towards β-linked galacto-*N*-biose-containing oligosaccharides of globo H, Gb5, and GA1.
   Carbohydrate Research., 408:18-24 (2015)

4. **Mikiyasu Sakanaka, Yuta Sugiyama, Aya Kitakata, Takane Katayama, and Shin Kurihara.**
   Carboxyspermidine decarboxylase of the prominent intestinal microbiota species *Bacteroides thetaiotaomicron* is required for spermidine biosynthesis and contributes to normal growth.
   Amino Acids., 48:2443-2451 (2016)

5. **Aina Gotoh, Misaki Nara, Yuta Sugiyama, Mikiyasu Sakanaka, Hiroyuki Yachi, Aya Kitakata, Akira Nakagawa, Hiromichi Minami, Shujiro Okuda, Toshihiko Katoh, Takane Katayama, and Shin Kurihara.**
   Use of Gifu Anaerobic Medium for culturing 32 dominant species of human gut microbes and its evaluation based on short-chain fatty acids fermentation profiles.
   Bioscience, Biotechnology, and Biochemistry., 81:2009-2017 (2017)

6. **Mikiyasu Sakanaka, Yuta Sugiyama, Misaki Nara, Aya Kitakata, and Shin Kurihara.**
   Functional analysis of arginine decarboxylase gene *speA* of *Bacteroides dorei* by markerless gene deletion.
   FEMS Microbiology Letters., 365, fny003 (2018)

7. **Mikiyasu Sakanaka, Morten Ejby Hansen, Aina Gotoh, Toshihiko Katoh, Keisuke Yoshida, Toshitaka Odamaki, Hiroyuki Yachi, Yuta Sugiyama, Shin Kurihara, Junko Hirose, Tadasu Urashima, Jin-zhong Xiao, Motomitsu Kitaoka, Satoru Fukiya, Atsushi Yokota, Leila Lo Leggio, Maher Abou Hachem, and Takane Katayama.**
   Evolutionary adaptation in fucosyllactose uptake systems supports bifidobacteria-infant symbiosis.
   Science Advances., 5, eaaw7696 (2019)

8. **Miki Matsue, Yumiko Mori, Satoshi Nagase, Yuta Sugiyama, Rika Hirano, Kazuhiro Ogai, Kohei Ogura, Shin Kurihara, and Shigefumi Okamoto.**
   Measuring the antimicrobial activity of lauric acid against various bacteria in human gut microbiota by using a new method.
   Cell transplantation., 28:1528-1541 (2019)